DISSERTATION

DEVELOPMENTS IN SEASONAL ATLANTIC BASIN TROPICAL CYCLONE PREDICTION

Submitted by

Philip J. Klotzbach

Department of Atmospheric Science

In partial fulfillment of the requirements

For the Degree of Doctor of Philosophy

Colorado State University

Fort Collins, Colorado

Summer 2007

COLORADO STATE UNIVERSITY

JULY 9, 2007

WE HEREBY RECOMMEND THAT THE DISSERTATION PREPARED UNDER OUR SUPERVISION BY PHILIP J. KLOTBACH ENTITLED DEVELOPMENTS IN SEASONAL ATLANTIC BASIN TROPICAL CYCLONE PREDICTION BE ACCEPTED AS FULFILLING IN PART REQUIREMENTS FOR THE DEGREE OF DOCTOR OF PHILOSOPHY.

Committee on Graduate Work

William Gray

Roger Pielke

Paul Mielke

Adviser Wayne Schubert

Department Head Richard Johnson

ABSTRACT OF DISSERTATION

DEVELOPMENTS IN SEASONAL ATLANTIC BASIN
TROPICAL CYCLONE PREDICTION

Seasonal forecasts of Atlantic basin hurricane activity have been issued since 1984 by the Tropical Meteorology Project at Colorado State University headed by William Gray. Since these initial forecasts were developed, considerable improvements in data and statistical techniques have led to improved amounts of skill in both hindcasting and forecasting of seasonal Atlantic basin hurricane activity. Statistical seasonal forecasts derive their skill from atmospheric and oceanic predictors that span various portions of the globe.

Recent developments in statistical prediction include revised statistical predictions of tropical cyclone activity for seasonal forecasts issued in early December, early April, early June and early August. In addition, individual forecast schemes for predicting activity during the months of August, September and October have been developed. The development of landfall probabilities has been a primary area of interest over the past several years. Landfall probabilities are now available online for all United States coastal counties from Brownsville, Texas to Eastport, Maine.

Atlantic basin tropical cyclone activity has been observed to increase dramatically over the past decade. Potential increases in global tropical cyclone activity as well as Atlantic tropical cyclone activity are investigated, to determine if it is possible to see a

human-induced fingerprint on global or Atlantic tropical cyclone activity trends. A potential linkage between the Atlantic thermohaline circulation and Atlantic basin multi-decadal variability is proposed.

Philip J. Klotzbach
Department of Atmospheric Science
Colorado State University
Fort Collins, CO 80523
Summer 2007

ACKNOWLEDGEMENTS

My Masters thesis advisor and mentor, Dr. William Gray, has been an incredible teacher and friend and has taught me an immense amount about tropical cyclone prediction over the past several years. I deeply appreciate our very close working and personal relationship. I would also like to thank my Ph. D. advisor, Dr. Wayne Schubert, for providing support throughout the project and for helping a struggling first-year graduate student understand the complexities of atmospheric dynamics. I would also like to thank my other graduate committee members, Dr. Paul Mielke and Dr. Roger Pielke, for their advice and assistance.

I would like to thank several members of the Gray and Schubert projects for many informative discussions on hurricanes. These individuals include Eric Blake, Matt Eastin, Brian McNoldy, Stacey Seseske, and Jonathan Vigh. I would also like to thank John Knaff and Ray Zehr for helpful suggestions and advice on seasonal hurricane prediction. Thanks also to the Geo-Graphics Laboratory at Bridgewater State College, and especially Dr. Uma Shama and Larry Harman, for their help in developing the United States Landfalling Hurricane Probability Webpage.

Reanalysis data utilized to develop these prediction schemes was primarily taken from the National Centers for Environmental Prediction/National Center for Atmospheric Research reanalysis project. Tropical cyclone data was obtained from the National Hurricane Center. This research was supported by the National Science Foundation and by AIG - Lexington Insurance Company.

I would like to thank my parents for providing me with an incredible educational experience. The tremendous sacrifices that they made to home school me are immensely appreciated. I certainly would not be where I am today without their efforts to provide me with an outstanding education.

TABLE OF CONTENTS

Chapter 1
Introduction

This report discusses recent developments in seasonal and sub-seasonal prediction of Atlantic basin TC activity. United States landfall probabilities, Atlantic basin multi-decadal variability and trends in global tropical cyclone (TC) activity are also investigated in this manuscript. The focus of this document following this introduction is on recent developments in statistical prediction implemented by the Tropical Meteorology Project (TMP) in the Department of Atmospheric Science at Colorado State University (CSU) since 2003. In the introduction, I examine developments in statistical prediction at CSU prior to 2003 and also discuss developments in seasonal prediction at other institutions. Much of the discussion in the introduction is taken from Klotzbach (2007a).

1.1 Atlantic basin seasonal prediction background

Statistical prediction of seasonal tropical cyclone activity was first conducted in the Atlantic basin using research pioneered by Gray (1984a, 1984b) at CSU. Prior to 1984, there was no knowledge as to how active or inactive the upcoming Atlantic basin tropical cyclone season was likely to be. Seasonal forecasts for the Atlantic basin are considered important since the Atlantic basin has considerable year-to-year variability. For example, when evaluating the coefficients of variation (ratio of standard deviation to mean) for

named storms from 1986-2005, the Atlantic basin's coefficient is nearly twice as large as the coefficient of variation for the East Pacific and almost three times as large as the coefficient of variation for the West Pacific. As an example of this considerable year-to-year variability, the 2005 tropical cyclone season had 27 named tropical cyclones, while 1972 and 1983 only had 4 named tropical cyclones. Eight major or intense hurricanes (category 3-4-5 on the Saffir-Simpson scale) (Simpson 1974) occurred in 1950 while no major hurricanes were observed in 1968, 1972, 1986 and 1994.

Hess and Elsner (1994) provide an excellent discussion of developments in seasonal prediction in the Atlantic basin between 1984-1993. The remainder of this introduction focuses on developments between 1993-2002 at CSU as well as statistical prediction developments at other institutions. Dynamical seasonal prediction of tropical cyclones is also now being attempted; however, it has yet to document skill at comparable levels to statistical techniques (Vitart and Stockdale 2001). This report only discusses advances in statistical prediction for Atlantic basin tropical cyclones.

Initial seasonal predictions were issued in early June and early August beginning in 1984 by Gray and colleagues at CSU. They used statistical relationships between the El Niño – Southern Oscillation (ENSO), the Quasi-Biennial Oscillation (QBO) and Caribbean basin sea level pressures with tropical cyclone activity in the Atlantic basin. When ENSO was cooler than normal, the QBO was in the west phase, and Caribbean basin sea level pressures were below normal, more tropical cyclones were predicted. The original early June and early August forecasts used a rules-based formula where correction factors were added or subtracted depending on ENSO, QBO and Caribbean basin sea level pressure conditions. Initially, forecasts for the total number of named

storms, named storm days, hurricanes and hurricane days were issued. It was a surprising discovery that the atmosphere/ocean had a long-period memory that enabled a skillful prediction of meso- to synoptic scale events such as tropical cyclones several months in advance.

The use of a Poisson regression model was suggested as a way to improve seasonal forecasting skill in the Atlantic basin for major hurricanes (Elsner and Schmertmann 1993). They argued that since major hurricanes are a non-linear phenomena, a Poisson regression model was more appropriate. They demonstrated improvement in hindcast skill utilizing the Poisson technique. Additionally, it was suggested that prediction of tropical-only storms, that is, those that form purely from tropical waves, has greater skill than for all tropical cyclones (Hess et al. 1995).

1.2 Atlantic basin seasonal prediction developments at CSU from 1994-2002

Seasonal hurricane predictions have continued to develop since the middle 1990s. Additional physical relationships were discovered which improved the hindcast skill of seasonal forecasts including the relationship between the Azores high and the upcoming season's hurricane activity. When the springtime Azores high was stronger than normal, it created a self-enhancing feedback that increased trade wind strength and evaporation. This tended to cool sea surface temperatures in the upcoming summer (Knaff 1998). The strength of this ridge in the previous October-November and the current March had a strong correlation (~0.5) with Net Tropical Cyclone (NTC) activity during the upcoming Atlantic basin tropical cyclone season. NTC activity is calculated by summing the following six parameters normalized by their 1950-2000 climatological averages and dividing by six: named storms, named storm days, hurricanes, hurricane days, intense

hurricanes and intense hurricane days (Gray et al. 1994). An average season accumulates 100 NTC units by definition.

The discovery of the relationship between the March Azores High strength and Atlantic basin tropical cyclone activity led to the issuing of forecasts in early April by the CSU research team along with their regularly-scheduled forecasts issued in early December, early June and early August. An additional predictor that has been utilized by CSU in all their recent forecasts is the relationship between Atlantic basin sea surface temperatures and the upcoming hurricane season. In general, when waters in the tropical and North Atlantic are warmer, Atlantic basin hurricane seasons are more active (Dunn 1940; Gray 1968; Shapiro and Goldenberg 1998; Goldenberg et al. 2001). Figure 1.1 shows the locations of the statistical predictors utilized in the early August prediction during the early 1990s.

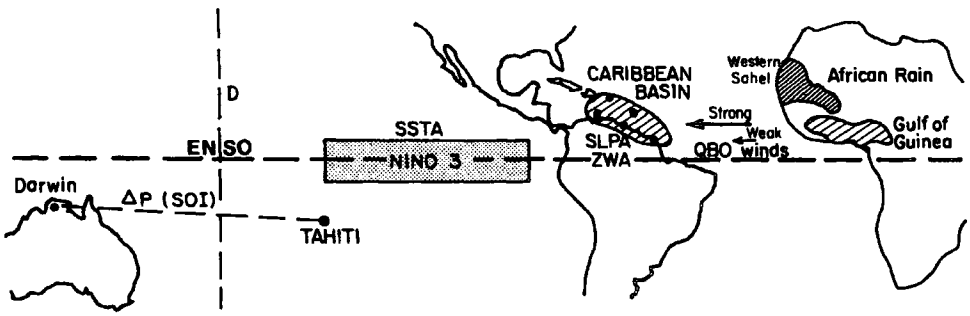

Figure 1.1: Predictors utilized in the early August statistical forecast during the early 1990s. Figure taken from Gray et al. 1993.

Early success showing operational skill in the issuing of seasonal hurricane forecasts for the Atlantic basin (Hastenrath 1990) has led other groups to begin forecasting tropical cyclone activity as well. These additional groups include the United States federal

government through the National Oceanic and Atmospheric Administration (NOAA) (began in 1998), Tropical Storm Risk (TSR) (began in 1999) and the Cuban Institute of Meteorology (began in 1999). These groups use somewhat different methodologies for arriving at their final forecast values. The next few portions of this chapter investigate these forecast methodologies in some detail.

1.3 NOAA seasonal forecast methodology

NOAA reviews a variety of predictors to make their seasonal predictions. Their forecast is based primarily on the observed state of the Atlantic Multi-decadal Oscillation (AMO) and a forecast of ENSO from the Climate Prediction Center (CPC). In general, when the AMO is positive, vertical wind shear is reduced across the tropical Atlantic, sea surface temperatures are warmer across the tropical Atlantic and sea level pressures are lower across the tropical Atlantic indicating greater instability and enhanced low-level convergence (Goldenberg et al. 2001). All of these features associated with a positive phase of the AMO are more favorable for development of tropical cyclones in the tropical Atlantic and the Caribbean Sea. Figure 1.2 displays the strong positive correlation between the phase of the AMO and an Accumulated Cyclone Energy (ACE) index. ACE is defined to be the sum of the squares of the estimated 6-hourly maximum sustained wind speeds for all systems when they have at least winds of tropical-storm strength (Bell et al. 2000).

A prediction of ENSO from the CPC is the other primary predictor that NOAA uses to issue its forecasts. The CPC utilizes a combination of currently-observed conditions along with a variety of statistical and dynamical forecast models to issue its forecast for ENSO. The relationship between ENSO and Atlantic basin tropical cyclone activity has

been well-documented in the literature (Gray 1984a; Goldenberg and Shapiro 1996; Pielke and Landsea 1999). In general, warm ENSO conditions are associated with anomalously strong vertical wind shear across the tropical Atlantic and subsidence in the Caribbean, while more favorable wind shear and vertical motion patterns are associated with cool ENSO anomalies.

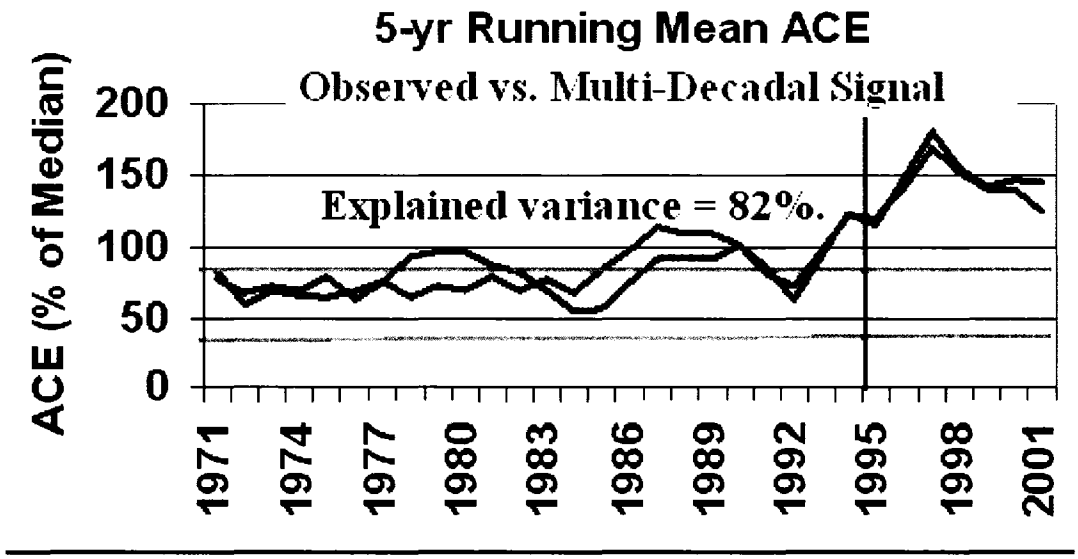

Figure 1.2: Five-year running mean ACE (dark line) plotted against a measure of the Atlantic Multi-decadal Oscillation (AMO) (light line). Note the strong measure of agreement between the two lines. Adapted from Bell and Chelliah (2006).

NOAA also uses estimated August-October Atlantic basin sea surface temperatures based on persistence and a forecast by the Climate Forecast System (CFS) model (Saha et al. 2006). As discussed previously, warmer sea surface temperatures in the tropical Atlantic generally indicate an increased likelihood for an active Atlantic basin hurricane season. A final predictor that NOAA utilizes is a forecast from the CFS model for August-October vertical wind shear across the tropical Atlantic (Chelliah and Saha 2004). Large amounts of vertical wind shear are detrimental for hurricane development and intensification (Gray 1984a; Frank and Ritchie 2001; Knaff et al. 2004). NOAA's final

forecast is derived from this predictor information and qualitatively adjusted by a consensus of forecasters located at several centers including the Climate Prediction Center, the National Hurricane Center and Hurricane Research Division (see http://www.noaa.gov for more information on NOAA's forecasts). NOAA issues predictions for the total number of named storms, hurricanes and major hurricanes expected to form in the Atlantic basin in a particular year. They also issue a prediction for the Accumulated Cyclone Energy (ACE) index.

1.4 TSR seasonal forecast methodology

Tropical Storm Risk (TSR), a private forecasting consortium based out of the United Kingdom, utilizes a methodology that predicts August-September trade wind speeds in the Caribbean and the tropical North Atlantic (7.5°N - 17.5°N, 100°W - 30°W) and August-September sea surface temperatures in the tropical North Atlantic (10°N - 20°N, 60°W - 20°W) (M. A. Saunders 2006, personal communication). From this prediction of trade wind speeds and sea surface temperatures, they arrive at a forecast for Atlantic basin tropical cyclone activity.

TSR's forecast of trade wind speeds is calculated from two predictors (M. A. Saunders 2006, personal communication). The first predictor is an August-September ENSO prediction based on a modified version of the ENSO-CLIPER model (Knaff and Landsea 1997). Sea surface temperatures are predicted for the tropical Pacific from 5°S - 5°N, 160°E - 90°W. The second predictor is a prediction of Atlantic/Caribbean sea surface temperatures from 7.5°N – 17.5°N, 85°W - 40°W. Atlantic/Caribbean sea surface temperatures are calculated from a 1-month lagged principal component analysis of

North Atlantic SST variability for the region from 0° - 50°N, 100°W - 0° (excluding the Pacific Ocean).

TSR's prediction of August-September tropical North Atlantic sea surface temperatures (10°N - 20°N, 60°W - 20°W) is derived from the same 1-month lagged principal component analysis technique mentioned in the previous paragraph. From these two predictors, TSR issues forecasts for the total number of named storms, hurricanes, and major hurricanes as well as the ACE index for the entire Atlantic basin. Utilizing these same two predictors, they also issue a forecast for the total number of named storms, hurricanes, major hurricanes and ACE expected in the Main Development Region (defined as 10°N - 20°N, 60°W - 20°W), the Caribbean Sea and the Gulf of Mexico (see http://tsr.mssl.ucl.ac.uk for more information on Tropical Storm Risk's forecasts).

TSR's hindcasts and forecasts have shown considerable skill when compared with climatology. Figure 1.3 displays improvement in mean-squared error (MSE) of TSR's forecasts of the ACE index for the entire Atlantic basin using hindcast data from 1984-2001 and real-time forecast data from 2002-2005 compared to a previous ten-year mean forecast. The scheme shows skill from early December with improving skill as the hurricane season approaches. It improves on the previous ten-year mean by approximately 30% in early June and by over 60% in early August using MSE as the skill metric.

1.5 Cuban Institute of Meteorology seasonal forecast methodology

The Cuban Institute of Meteorology utilizes a linear regression methodology involving several predictors to issue its forecast for the Atlantic basin hurricane season. The predictors that they utilize are quite similar to the predictors utilized by the other

forecast groups already discussed including sea level pressure and sea surface temperature values in the tropical Atlantic as well as the observed state of the QBO and the observed and predicted state of ENSO. In addition, the Cuban Institute of Meteorology also predicts the activity likely to develop in the Caribbean Sea, since this is the area that is obviously of greatest interest to individuals living in Cuba (see http://www.met.inf.cu for more information on the Cuban Institute of Meteorology forecasts).

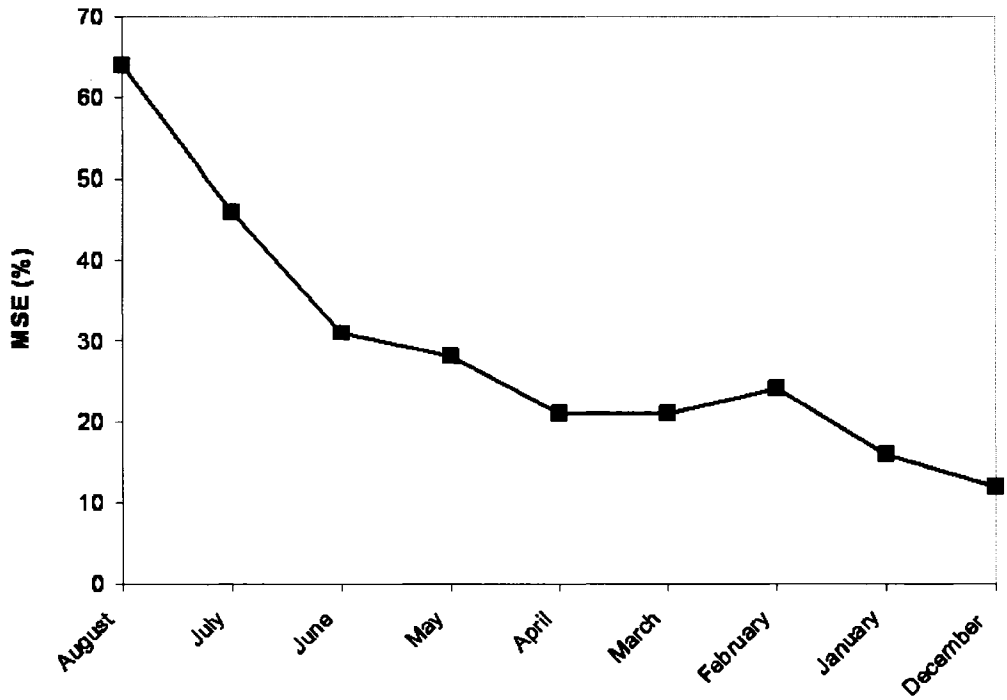

Figure 1.3: Tropical Storm Risk skill for the Atlantic basin ACE index (1984-2005) based on hindcasts (1984-2001) and forecasts (2002-2005). Skill is relative to mean-squared error (MSE) and is the percent improvement of the hindcast/forecast over the previous 10-year mean. Figure taken from Klotzbach (2007a).

The remainder of this manuscript begins by examining improvements in seasonal prediction of Atlantic basin tropical cyclones at the TMP since 2002. Chapter 2 discusses two of the primary sources of data utilized in developing new seasonal forecast methodologies, namely the National Centers for Environmental Prediction/National Center for Atmospheric Research (NCEP/NCAR) reanalysis, and the best track database developed and maintained by the National Hurricane Center (NHC). Chapter 3 examines the development of a new seasonal forecast methodology from early December (seven months prior to the start of the hurricane season). Chapter 4 discusses changes to the seasonal forecasts issued in early April and early June, while Chapter 5 reports on a new early August forecast scheme that shows considerable skill over a 106-year period. Chapter 6 discusses some developments in sub-seasonal forecasting (individual monthly forecasts for August, September and October), while Chapter 7 explains some of the recent developments in United States landfall probability forecasts. Chapter 8 examines multi-decadal variability in the Atlantic basin, while Chapter 9 examines potential changes in global TC activity over the past several decades. Chapter 10 summarizes and concludes with some ideas for future work.

Chapter 2
Data

2.1 NCEP-NCAR reanalysis

The National Centers for Environmental Prediction/National Center for Atmospheric Research (NCEP/NCAR) reanalysis was originally developed during the late 1990s and now includes data from 1948-present (Kalnay et al. 1996; Kistler et al. 2001). The reanalysis provides global data on a 2.5° by 2.5° grid for a large number of atmospheric and oceanic parameters including sea surface temperature, sea level pressure, zonal wind, meridional wind, etc. The model used to generate the reanalysis product was frozen at the beginning of the reanalysis, and therefore, there should not be any spurious jumps or discontinuities in the data due to model changes. It should also be noted that all data used as predictors for the various forecast schemes discussed in detail in the following chapters were selected from the reanalysis "A" variables (Kalnay et al. 1996). These variables have more consistency checks (e.g., wind-pressure relationships, thermal wind balance, etc.) and are more constrained by observations than some other variables (e.g., velocity potential, outgoing longwave radiation, etc.) and are therefore likely to be more accurate than other reanalysis variables. The reanalysis is currently run with an approximately three-day lag, so that accurate estimates of monthly predictor values can be made near the end of the month prior to the forecast issue date.

2.2 NHC best track database

Atlantic basin hurricane activity from 1900-2005 was calculated from the National Hurricane Center's "best track" data files (Jarvinen et al. 1984). This dataset provides the best estimate of a storm's intensity in five-knot increments for every six-hour period of the storm's existence. The "best track" dataset is updated following the end of each hurricane season. Recent changes made by the Atlantic Hurricane Database Re-analysis Project for tropical cyclones that occurred during the early part of the 20th century (1900-1914) (Landsea et al. 2004) have been included in this analysis.

Chapter 3

December prediction developments

During the next few chapters, I discuss revisions to seasonal forecasts issued at various lead times prior to the start of the active part of the hurricane season (approximately 1 August). This chapter focuses on revisions to the first prediction issued by the TMP in the early part of December (seven months prior to the start of the hurricane season on 1 June). Much of this discussion is taken from Klotzbach and Gray (2004). Additional information on the December statistical prediction is available in that paper.

3.1 Early December prediction background

Extended-range seasonal forecasts were issued beginning in 1992 with the development of a long-range statistical forecast of Atlantic seasonal hurricane activity. Gray et al. (1992a) found that cross-validated hindcast skill explaining approximately 50% of the variance in Atlantic basin tropical cyclone activity could be obtained based on the 1950-1990 time period. This first-ever 1 December forecast utilized predictors involving West African rainfall and the Quasi-Biennial Oscillation (QBO). They extrapolated the QBO 10 months into the future to estimate the wind strength at 30 mb, 50 mb, and the shear between these levels for the following September. Rainfall in the western Sahel during August-September of the previous year and rainfall in the Gulf of

Guinea during August-November of the previous year were utilized as African rainfall predictors.

Years that were in the west phase of the QBO were found to have many more intense hurricanes. Gray et al. (1992a) hypothesized that lower-stratospheric wind ventilation was reduced during west-phase years. In addition, the west phase of the QBO has been shown to enhance off-equatorial convection, while equatorial convection is favored in east QBO years (Gray et al. 1992b; Knaff 1993). Since hurricanes in the Atlantic basin do not form within 5° of the equator, off-equatorial convection is more favorable for African easterly waves developing into tropical cyclones. The West African rainfall-tropical cyclone relationship was largely based on persistence. Wet years in the Sahel are usually followed by wet years and vice versa. Landsea and Gray (1992) hypothesized that enhanced rainfall in West Africa during the prior year contributed to a strong monsoon the following year through feedbacks from both soil moisture and evapotranspiration. Increased West African rainfall during a particular year indicates that the easterly waves moving off the coast of Africa are likely stronger than normal.

Additional predictors were added to the early December statistical forecast since the original methodology was established in the early 1990s. The strength of the Azores ridge and several measures of ENSO were included by the late 1990s (Gray et al. 2000b). The strength of the Azores ridge during autumn has a similar relationship with Atlantic basin TC activity as that discussed with the springtime Azores high in Chapter 1. Strong high pressure near the Azores enhances trade winds and consequently increases upwelling over the tropical Atlantic which tends to feed back into a stronger springtime Azores ridge. This stronger springtime Azores ridge induces stronger trades, increased

vertical wind shear and cooler sea surface temperatures during the Atlantic basin hurricane season (Knaff 1998).

Warm ENSO conditions have been shown in many previous studies to inhibit Atlantic basin TC activity through a strengthening of upper-level westerlies and consequently an increase in vertical wind shear (e.g. Gray 1984a). However, the predictability of ENSO from the previous autumn to the following year's hurricane season is a very difficult task. The addition of both the Azores ridge and ENSO predictors added to the hindcast variance explained, but the addition of these predictors did not add skill to real-time forecasts issued during the 1990s. The recent-decade failure of this earlier statistical forecast is largely attributed to the failure of the African rainfall and Atlantic hurricane relationship. Although tropical cyclone activity has increased dramatically since 1994, West Africa has continued to report drought conditions typical of inactive hurricane seasons, although these drought-like conditions have diminished somewhat in recent years. At this point, considerable question remains whether the degraded African rainfall-Atlantic basin TC activity relationship is due to actual meteorological changes or an artifact of station measurement quality. It is also quite possible that other unrealized factors are playing a role.

Table 3.1 displays the degradation in seasonal forecast skill for the earlier December prediction methodology. Predictions of hurricane days and hurricane destruction potential (HDP) are displayed. HDP is calculated by squaring the wind speed (in knots) for each six-hour period for which a tropical cyclone is judged to have winds of hurricane strength (>=64 knots) and summing these together. Although jackknife (drop-one cross-validated) hindcast skill for 1950-1990 suggested that about 50% of the variance could be

explained in real-time forecasts, only 3-7% of the variance has been explained for hurricane days and HDP for forecasts issued between December 1991 – December 2001. The failure of the statistical scheme in recent years has been the primary motivation for the revision of the December statistical prediction technique.

Table 3.1: Early December forecast and observed values of hurricane days and HDP for 1992-2002. The average difference between forecast and observed values was taken without respect to sign.

Year	Forecast Hurricane Days	Observed Hurricane Days	Difference	Forecast HDP	Observed HDP	Difference
1992	15	16	-1	35	51	-16
1993	25	10	15	75	23	52
1994	25	7	18	85	15	70
1995	35	62	-27	100	173	-73
1996	20	45	-25	50	135	-85
1997	25	10	15	75	26	49
1998	20	49	-29	50	145	-95
1999	40	43	-3	130	145	-15
2000	25	32	-7	85	85	0
2001	20	27	-7	65	71	-6
2002	35	11	24	90	31	59
Average Difference			|15.5|			|47.3|
R^2			0.07			0.03
Jackknife Hindcast R^2			0.51			0.53

3.2 December seasonal prediction development methodology

This revised early December statistical forecast scheme attempts to maximize the hindcast skill in forecasting tropical cyclone activity based on the time period 1950-2001. Hindcasting involves selecting predictors that were useful in forecasting tropical cyclone activity during the period being hindcast. The forecast model operates on the premise that predictors that hindcast tropical cyclone activity accurately in the past will also be useful for forecasting tropical cyclone activity in the future. The process of obtaining

predictors began by seeing with the September-November period looked like in the year prior to an active or inactive hurricane season. NCEP/NCAR reanalysis data were utilized as the primary dataset for constructing composite analysis, and all composites were constructed using the Climate Diagnostic Center's (CDC) "Monthly/Seasonal Climate Composites" webpage available online at: http://www.cdc.noaa.gov/Composites. September, October and November were composited individually and grouped together to see what atmospheric and oceanic features prevailed in the years prior to the 10 most active and 10 most inactive years. Net tropical cyclone (NTC) activity was the tropical cyclone parameter utilized to classify years. By definition, the 1950-2000 climatological average value of NTC is 100 (Gray et al. 1994).

Several features that became evident from the composite maps were anomalously high heights in northern latitudes, indicating a negative Arctic Oscillation (AO) (Thompson and Wallace 1998) and negative North Atlantic Oscillation (NAO) (van Loon and Rogers 1978) and a midlatitude wave train pattern closely resembling a positive and slightly eastward-shifted Pacific-North American pattern (PNA) (Wallace and Gutzler 1981). A positive PNA is a typical wintertime midlatitude teleconnection associated with warm ENSO conditions (Horel and Wallace 1981), and the eastward shift of the PNA pattern is likely due to an eastward shift of sea surface temperature anomalies from the central to the eastern Pacific. A wave train propagates poleward and eastward from an area of thermal forcing (Hoskins and Karoly 1981), and therefore, if the warmest SST anomalies were located in the eastern Pacific, the Pacific North American pattern would also be shifted eastward. In general, warm SSTs in the tropical East Pacific are more unstable than in the tropical central Pacific and are therefore more likely to shift back to

neutral or cool conditions during the following year. Warm SSTs in the central tropical Pacific can sometimes persist for several years at a time, as was observed during the early 1990s as well as from 2002-2005.

The primary tool used in selecting predictors was the Climate Diagnostic Center's "Linear Correlations" webpage available online at: http://www.cdc.noaa.gov/Correation. This webpage allowed for the testing of correlations between global data fields and TC activity time series created by the user, such as NTC. Correlations between atmospheric data fields and Atlantic basin tropical cyclone activity indices were calculated. Figure 3.1 shows the correlation between the following year's NTC and November sea level pressure. Other predictors in the scheme were selected utilizing a residual approach. For this, one or two predictors already in the forecast model were used to predict the TC variable in question, for example, NTC. The difference between actual minus hindcast value for each year was considered the hindcast error, and a time series of these hindcast errors was created. Correlation maps between these residual time series and global atmospheric and oceanic features were then constructed to see if there were any large-scale areas that correlated strongly with both the residual and the predictand itself. September 500-mb geopotential height over the western United States and the QBO predictor were selected based on the residual approach. In addition, all predictors selected were required to span an area no less than 10° by 20° in extent to avoid "bull's-eye" features that are prevalent on some of the correlation maps.

3.3 Results

Nineteen predictors were evaluated for potential forecasting ability, and six predictors spanning various portions of the globe were selected to forecast Atlantic basin tropical

cyclones using the methodology outlined in the previous section. Predictors utilized zonal wind, sea level pressure, or geopotential height data that are defined, as discussed previously in Chapter 2, as reanalysis "A" variables. Table 3.2 lists the locations of the six predictors, while Figure 3.2 displays these predictors on a map. A listing of predictors chosen for forecasting each tropical cyclone activity parameter along with the variance explained and the cross-validated or jackknife variance explained are listed in Table 3.3. Jackknife or cross-validated variance explained is calculated using the technique outlined in Elsner and Schmertmann (1994). This methodology examines how well a year can be predicted utilizing an equation developed on the remaining 51 years of data. For example, a forecast for 1950 would be based on an equation developed on the years 1951-2001. Jackknifed hindcast skill gives a more accurate representation of actual forecast conditions and is often considered to be an upper bound on how much variance will likely be explained by the scheme when forecasts are issued in real time.

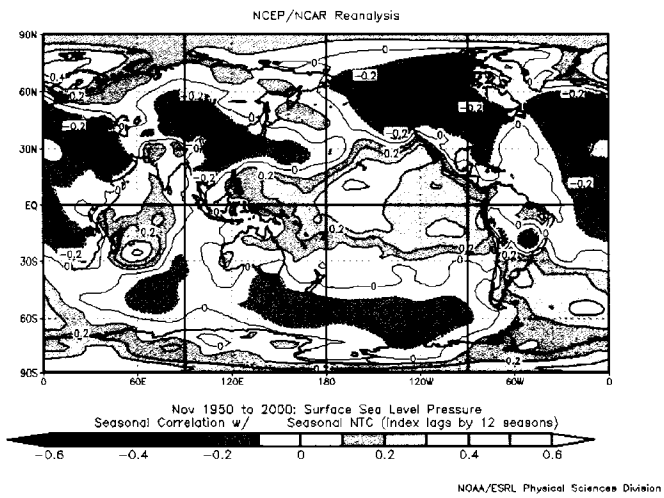

Figure 3.1: Correlation map between seasonal NTC and the previous year's November sea level pressure. Adapted from Klotzbach and Gray (2004).

Table 3.2: Predictors used in the early December forecast. The sign of the predictor associated with increased tropical cyclone activity the next year is in parentheses.

Predictor Name	Location
1) November 500-mb geopotential height in the far North Atlantic (+)	(67.5°-85°N, 10°E-50°W)
2) October-November SLP in the Gulf of Alaska (-)	(45°-65°N, 160°-120°W)
3) September 500 mb geopotential height in western North America (+)	(35°-55°N, 120°-100°W)
4) July 50 mb equatorial zonal wind (-)	(5°S-5°N, all longitudes)
5) September-November SLP in the Gulf of Mexico-southeastern United States (-)	(15°-35°N, 95°-75°W)
6) November SLP in the tropical northeast Pacific	(7.5°-22.5°N, 175°-125°W)

More intense tropical cyclone parameters tended to be better forecast than parameters dealing with weaker systems. For example, there was a nearly 30% better cross-validated hindcast variance explained for intense hurricanes compared to named storms. This result is to be expected, since weaker systems often form from higher-latitude baroclinically-generated systems that are impossible to predict months in advance, such as frontal boundaries or cold lows. In addition, weaker systems can form in marginal tropical cyclone environments that would not be conducive for hurricane or major hurricane development (i.e., fairly strong vertical wind shear, cool sea surface temperatures, etc.). Also, there are more observational problems in determining the intensity of weaker systems.

Predictors were selected using an all-subset technique similar to that used in Klotzbach and Gray (2003). This procedure differs from the stepwise regression technique in that it selects the best one predictor, the best two predictors, etc., up to the best five predictors for each tropical cyclone variable or until the jackknife hindcast skill no longer increases. No more than five predictors were selected for each TC parameter to

avoid statistical over-fitting of the data. An ordinary, least squares multiple regression technique was utilized for most predictands, but a Poisson regression model was utilized for intense hurricanes, since these typically have small integer values, as suggested by Elsner and Schmertmann (1993). A Poisson model does not allow negative numbers to be forecast for a predictand. This problem was sometimes observed when an ordinary least squares multiple regression equation was utilized for intense hurricanes.

Figure 3.3 displays a 52-year time series of observed versus cross-validated hindcast NTC for 1950-2001. Approximately 46% of the variance is explained by the five predictors utilized in the NTC prediction equation.

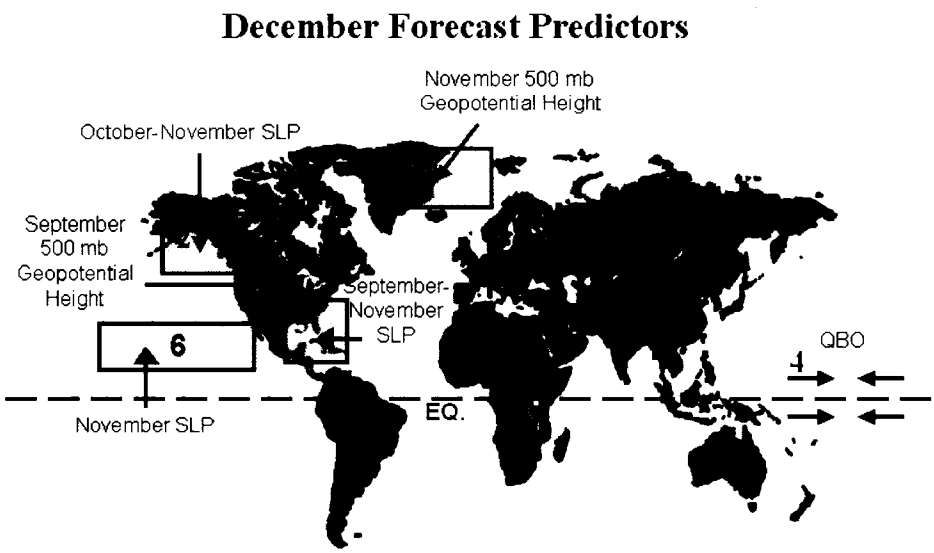

Figure 3.2: Map of predictors used in the early December statistical forecast. Adapted from Klotzbach and Gray (2004).

Table 3.3: Predictors chosen, hindcast variance explained, and jackknife variance explained for each TC activity parameter in the early December forecast of the following year's tropical cyclone activity. See Table 3.2 for predictor names and descriptions.

Forecast Parameter	No. of Predictors	Predictors Chosen from Table 3.2	Hindcast (r^2) (1950-2001)	Jackknife Hindcast (r^2) (1950-2001)
Named Storms	3	1, 2, 3	0.40	0.29
Named Storm Days	5	1, 3, 4, 5, 6	0.45	0.28
Hurricanes	5	1, 2, 3, 4, 5	0.53	0.38
Hurricane Days	5	1, 2, 3, 4, 5	0.53	0.35
Intense Hurricanes	5	1, 2, 3, 4, 5	0.69	0.57
Intense Hurricane Days	5	1, 3, 4, 5, 6	0.51	0.41
NTC Activity	5	1, 3, 4, 5, 6	0.62	0.46

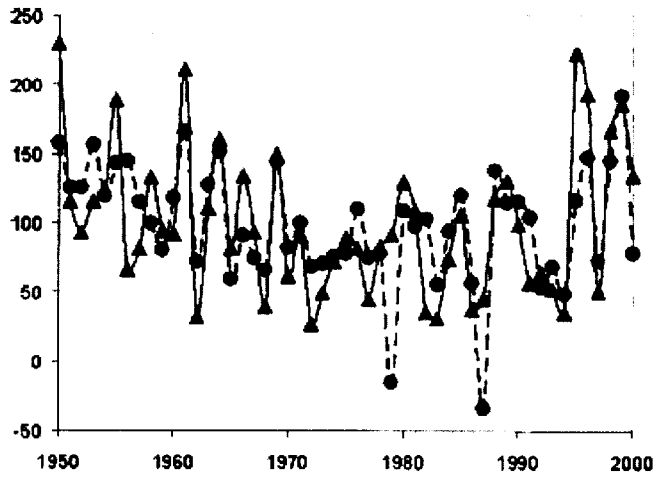

Figure 3.3: Actual NTC (solid line) versus early December cross-validated hindcast NTC (dashed line). Cross-validated variance (r^2) explained is 0.46. Adapted from Klotzbach and Gray (2004).

The new statistical forecast improves over the old statistical forecast considerably over the period from 1992-2002 (see Table 3.4). The old statistical forecast was developed on hindcast data from 1950-1990 and was first issued operationally in December 1991, but, although the scheme showed significant skill in hindcast mode, it

showed little skill in forecast mode. For this comparison, the forecasts for the new scheme were also developed on the hindcast years of 1950-1990. The new scheme explains approximately the same amount of variance during the 1992-2002 period as it did during the hindcast period compared with the complete failure of the earlier scheme during this same period. The average difference was reduced by about 30-35% for hurricane days and HDP when using the new statistical scheme over the 1992-2002 period.

Table 3.4: Improvement in skill with new December statistical forecast over the period from 1992-2002. The average difference between forecast and observed values was taken without respect to sign.

	Old Forecast Hurricane Days	New Forecast Hurricane Days	Old Forecast HDP	New Forecast HDP
Average Difference	|15.5|	|10.6|	|47.3|	|30.5|
r^2	0.05	0.52	0.03	0.58
Jackknife Hindcast r^2 (1950-1990)	0.51	0.46	0.53	0.50

Cross-correlations between individual predictors are quite small (see Table 3.5). All correlations are below r = |0.3| expect for the relationship between the Gulf of Alaska October-November sea level pressure and the November SLP in the tropical northeast Pacific which correlates at –0.57. According to a two-tailed Student's t test, 95% and 99% significance levels of inter-relationships between predictors are 0.28 and 0.36, respectively, based upon the 52 years of data evaluated for this scheme. Obtaining predictors that are mostly uncorrelated with each other is valuable in that each predictor provides mostly independent information from the other predictors in the scheme.

Table 3.5: Correlations between individual predictors for the December forecast. Most inter-correlations are below r = |0.3|. Average inter-correlations are computed without respect to sign. See Table 3.2 for predictor names and descriptions.

Predictor	1	2	3	4	5	6
1	---	-0.24	0.04	-0.14	-0.27	0.19
2	-0.24	---	-0.29	0.24	0.21	-0.57
3	0.04	-0.29	---	-0.07	-0.13	0.13
4	-0.14	-0.24	-0.07	---	0.09	0.01
5	-0.27	0.21	-0.13	0.09	---	-0.12
6	0.19	-0.57	0.13	0.01	-0.12	---
Average Inter-Correlation	**0.18**	**0.31**	**0.13**	**0.11**	**0.16**	**0.20**

3.4 Physical links between December predictors and seasonal Atlantic basin TC activity

Many of the predictors selected for forecasting the following year's tropical cyclone activity were not previously known to be related to current or future hurricane activity in the Atlantic basin; however, in combination with the other predictors in the forecast scheme, they were able to explain 46% of the cross-validated hindcast variance in Atlantic basin NTC activity 6-11 months in advance. One would not have expected the atmosphere-ocean to have such a long-term memory for the frequency of mesoscale events.

One way to better understand the predictors in the statistical forecast is to investigate the physical relationships between each predictor and tropical cyclone activity the following year. A method used to understand physical relationships between predictors and tropical cyclone activity was to correlate each predictor with other atmospheric fields during the month that the predictor was selected along with atmospheric fields during the following year's August-October period. By doing this, one can see global effects that occur concurrently with the predictor and also the teleconnected effects that happen 6-11

months later. These correlation maps were helpful in establishing the physical relationships discussed in the following paragraphs. Figure 3.4 displays three summer/fall features that were usually associated with an active hurricane season the following year. A discussion of hypothetical physical linkages between each of the predictors in the scheme and Atlantic basin tropical cyclone activity follows.

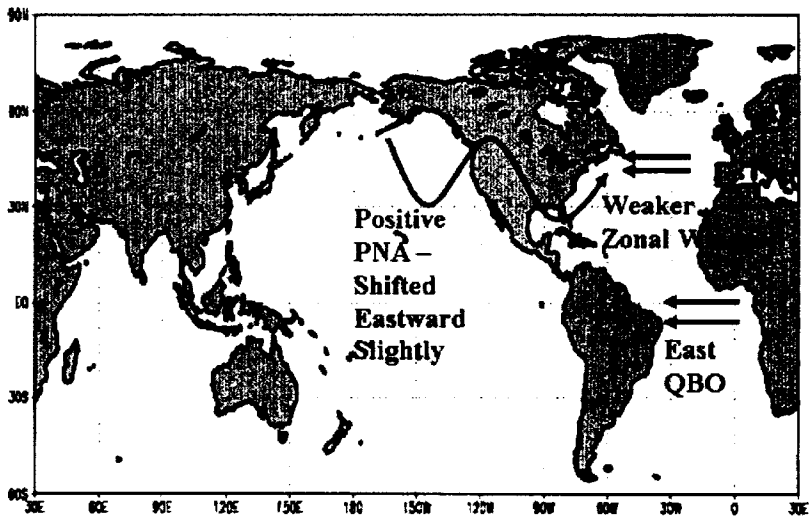

Figure 3.4: Summer/fall atmospheric features associated with an active hurricane season during the following year. Figure taken from Klotzbach and Gray (2004).

a. Predictor 1: November 500 mb geopotential height in the far North Atlantic (+)

Positive values of this predictor correlate very strongly (r = -0.7) with negative values of the AO and the NAO. Negative AO and NAO values imply more ridging in the central Atlantic and a generally warm North Atlantic Ocean (50°-60°N, 50°-10°W) due to stronger southerly winds during this period. Also, on decadal time scales, weaker zonal winds in the sub-polar areas (40°-60°N, 60°W-0°) across the Atlantic are indicative of a relatively strong thermohaline circulation. The change in strength of the zonal winds at

500 mb from the period inferred to have an active thermohaline circulation (1950-1969, 1995-1999) from the period inferred to have a weak thermohaline circulation (1970-1994) was found to be statistically significant at the 99% level (not shown). Also, positive values of this index in November (higher heights, weaker mid-latitude zonal winds) are correlated with weaker tropical Atlantic 200-mb westerly winds and weaker trade winds the following August-October. The associated reduced tropospheric vertical wind shear enhances TC development. Other following summer-early fall features that are directly correlated with this predictor are low sea level pressure in the Caribbean and a warm North and tropical Atlantic. Both of these features also enhance the likelihood of hurricane development.

b. Predictor 2: October-November SLP in the Gulf of Alaska (-)

Negative values of this predictor are strongly correlated with a positive "Alaska pattern" (Renwick and Wallace 1996) as well as a slightly eastward-shifted positive PNA, which implies reduced ridging over the central Pacific and increased heights over the western United States. The negative mode of this predictor is typically associated with warm current eastern Pacific equatorial SST conditions and a mature warm ENSO event. Low sea level pressure is observed to occur in the Gulf of Alaska with a decaying El Niño event, and anomalous high pressure is observed with a weakening La Niña event (Larkin and Harrison 2002). Negative values of this predictor indicate a likely change to cool ENSO conditions during the following year. Cool ENSO conditions enhance Atlantic hurricane activity.

c. Predictor 3: September 500-mb geopotential height in western North America (-)

Positive values of this predictor correlate very strongly (r = 0.8) with positive values of the PNA. PNA values are usually positive in the final year of an El Niño event (Horel and Wallace 1981). Therefore, cooler ENSO conditions are likely during the following year. Significant lag correlations exist between this predictor and enhanced 200-mb geopotential height anomalies in the subtropics during the following summer. Higher heights in the subtropics reduce the height gradient between the deep tropics and subtropics, resulting in easterly anomalies at 200 mb throughout the tropical Atlantic during the following summer. Easterly anomalies at 200 mb provide a strong enhancing factor for tropical cyclone activity.

d. Predictor 4: July 50-mb equatorial zonal wind (-)

Easterly anomalies of the QBO during the previous July indicate that the QBO will likely be in the west phase during the following year's hurricane season. According to Gray et al. (1992a), the average half-period of the QBO is approximately 14 months (average period 28-29 months). The QBO should therefore be of the opposite sign during the following year's August-October period. As mentioned briefly earlier, the west phase of the QBO has been shown in previous studies to provide favorable conditions in the deep tropics for the development of hurricanes, as discussed by Shapiro (1989) and Gray et al. (1992a, 1993, 1994). Hypothetical mechanisms for how the QBO affects hurricanes are as follows: a) Atlantic TC activity is inhibited during easterly phases of the QBO due to enhanced lower-stratospheric wind ventilation and increased upper-tropospheric-lower-stratospheric wind shear; b) the east phase of the QBO favors equatorial

convection (0°-10°N), and the west phase of the QBO favors higher-latitude convection (10°-20°N), which is more favorable for TC development; and c) the west phase of the QBO has a slower relative wind (advective wind relative to the moving system) than does the east phase (Gray and Sheaffer 1991). This allows for greater coupling between the lower stratosphere and the troposphere, which is an enhancing factor for Atlantic basin tropical cyclone activity.

e. Predictor 5: September-November SLP in the Gulf of Mexico-southeastern United States (-)

Low pressure in this area during September-November correlates quite strongly with a current positive phase of the PNA. As was stated earlier, the PNA is usually positive in the final year of a warm ENSO event, and therefore cooler ENSO conditions are likely the following year (Horel and Wallace 1981). This feature is strongly negatively correlated ($r \sim -0.5$) with the following year's August-September sea level pressure in the tropical and subtropical Atlantic. August-September SLP in the tropical Atlantic is one of the most important predictors for seasonal activity (e.g. Knaff 1997), indicating increased instability and a moister lower and middle troposphere. Easterly anomalies at 200 mb are also typical during the following year's August-October period indicating reduced vertical wind shear across the tropical Atlantic.

f. Predictor 6: November SLP in the tropical northeast Pacific (+)

According to Larkin and Harrison (2002), high pressure in the tropical northeast Pacific appears during most winters preceding the development of a La Niña event. High

pressure forces strong trade winds in the east Pacific, which increases upwelling and helps initiate La Niña conditions. These cool ENSO conditions eventually enhance Atlantic hurricane activity during the following summer due to a reduction in vertical wind shear. This predictor correlates with low geopotential heights at 500 mb throughout the tropics during the following summer, indicative of a weaker Hadley circulation which is typical of La Niña conditions. Also, high pressure in November in the tropical northeast Pacific correlates with low sea level pressure in the tropical Atlantic and easterly anomalies at 200 mb during the following August-October period.

The predictors discussed in detail above all relate to one or more of five global modes: the NAO, the AO, the PNA, ENSO, and the QBO. With a knowledge of the current value and a forecast of the future trends in these modes, one can explain up to approximately 50% of the variance of the following year's tropical cyclone activity based on 52 years of hindcast data.

3.5 Statistical analysis of predictors

The last section proposed physical linkages between predictors and Atlantic basin tropical cyclone activity. Another method used to add credibility to the forecast scheme is to use objective statistical bootstrap techniques to show that the predictors have statistically significant following-year correlations with tropical cyclone activity over the 52-year developmental dataset. One of the most common methods of evaluating statistical significance is to utilize a standard Student's *t* test. According to a two-tailed Student's *t* test, 95% and 99% significance levels of inter-relationships between predictors are 0.28 and 0.36, respectively, based upon the 52 years of data evaluated for this scheme. Table 3.6 displays correlations between all predictors and Atlantic TC

parameters. Predictors 1 and 2 show the highest correlation with Atlantic TC activity during the following year. Predictors 3 and 4 were selected from the residual analysis, and therefore it is expected that the individual correlations between the predictors and TC parameters are weakest for these features. It should also be noted that the power of this forecasting scheme does not lie simply in the strength of the individual predictors but in the strength of the predictors when used in combination.

An additional test to evaluate the strength of relationships between predictors and Atlantic TC parameters was to evaluate the top 10 and bottom 10 values of each predictor. For example, take the North Atlantic 500-mb geopotential height and compute a ratio for tropical cyclone activity that occurred during the top 10 versus the bottom 10 of those years. If there was a negative relationship between the predictor and TC activity, the ratio was inverted to allow for easy reference between each predictor-Atlantic TC parameter pair. Table 3.7 displays the top 10-bottom 10 ratios. Many of the ratios are of greater magnitude than 2:1, indicating significant relationships between the predictor and Atlantic hurricanes.

Table 3.6: Correlations between predictors and Atlantic tropical cyclone activity parameters. Correlations that exceed the 95% significance level as determined by the Student's *t* test are in italics and those that exceed the 99% significance level as determined by the Student's *t* test are in bold. See Table 3.2 for predictor names and descriptions.

Predictor	NS	NSD	H	HD	IH	IHD	NTC
1	**0.50**	**0.48**	**0.52**	**0.51**	**0.57**	**0.47**	**0.57**
2	**-0.45**	**-0.44**	**-0.53**	**-0.48**	**-0.49**	**-0.42**	**-0.52**
3	*0.30*	*0.31*	*0.31*	*0.35*	**0.41**	**0.40**	**0.40**
4	-0.25	-0.27	-0.19	-0.27	*-0.33*	*-0.29*	*-0.31*
5	*-0.29*	*-0.32*	**-0.43**	**-0.45**	*-0.32*	**-0.39**	**-0.41**
6	**0.36**	**0.40**	*0.34*	*0.35*	**0.36**	**0.37**	**0.40**

Table 3.7: Ratio of top 10-bottom 10 years for all predictors in the early December forecast scheme. See Table 3.2 for predictor names and descriptions.

Predictor	NS	NSD	H	HD	IH	IHD	NTC	Mean
1	1.61	1.86	1.68	2.27	3.58	3.56	2.30	2.41
2	1.52	1.70	1.72	2.05	2.82	3.75	2.09	2.24
3	1.52	1.63	1.59	1.78	2.50	2.27	1.81	1.87
4	1.19	1.28	1.17	1.32	1.65	1.53	1.35	1.36
5	1.22	1.46	1.54	2.09	1.76	3.13	1.75	1.85
6	1.35	1.63	1.46	1.71	1.88	2.53	1.72	1.75
Mean	**1.40**	**1.59**	**1.52**	**1.87**	**2.37**	**2.80**	**1.84**	**1.91**

3.6 December prediction – U.S. landfalling TC relationships

One of the most important aspects of any tropical cyclone forecast is the issuance of landfall probabilities. Previous work has been conducted on the predictability of landfall hurricanes (Lehmiller et al. 1997; Bove et al. 1998; Elsner et al. 2000), but the issuance of landfall probabilities has not been attempted until recently, by Gray et al. (1998). Although there are only small differences in landfalling TCs between individual active and inactive years, there are considerable differences in the number of intense hurricanes that make landfall along the U.S. coastline when one averages 4-5 active years versus 4-5 inactive years. With the upturn in Atlantic basin TC activity since 1995, the probability of an intense hurricane striking the U.S. coastline has increased accordingly, as evidenced by the seven major hurricane landfalls that occurred along the U.S. coastline during 2004 and 2005. For example, during the 15 years with the largest NTC hindcasts, 13 intense hurricanes made landfall along the U.S. coastline as opposed to only 8 intense hurricanes during the 15 least active years. These ratios are even more striking for the U.S. East Coast. The Gulf Coast-East Coast demarcation location is approximately 100 miles north of Tampa, Florida. Storms that made landfall near Tampa, Fort Myers and the Florida

Keys are considered to be East Coast landfalls. During the 15 highest NTC hindcasts, eight intense hurricanes made landfall along the East Coast as opposed to only three intense hurricanes during the 15 lowest NTC hindcasts. These types of strong relationships clearly indicate that there is a considerable amount of information regarding landfall probabilities for the following year's hurricane season seven months prior to the start of the hurricane season.

3.7 Current December prediction scheme and future work

The above-mentioned statistical scheme was implemented for the first time in December 2002 (Gray et al. 2002a). This was the sole statistical scheme utilized between 2002-2005. In December 2006, a new statistical scheme was investigated for the first time (Klotzbach and Gray 2006c). Following the success of a new August statistical forecast scheme (Klotzbach and Gray 2006b; Klotzbach 2007b), a similar scheme was developed for early December. This scheme is a simpler scheme that uses only three predictors. The predictor scheme selects predictors only utilizing sea level pressure and sea surface temperature data, and all predictors use two-month averaging periods, in an attempt to average out any variability due to Madden-Julian Oscillation (MJO) effects (Madden and Julian 1994).

The three predictors in the experimental statistical scheme were selected based upon data from 1950-1989. The predictors were then tested on independent data from 1990-2004, in an effort to ensure that the predictors showed comparable amounts of skill in both the dependent and independent data periods. The combination of these three predictors explained 51 percent of the variance in NTC on the dependent data (1950-1989), and using these same equations, 49 percent of the variance in NTC was explained

using independent data (1990-2004). It is hoped that testing these schemes on independent data will allow for continued skill for many years to come. Obviously, these statistical schemes are based on the fact that the future climate will behave in a way similar to the way that the past has behaved.

The scheme shows comparable hindcast skill to the six-predictor scheme that was used from 2002-2005. The relationships between individual predictors and seasonal tropical cyclone activity occurring the following year are somewhat better understood using this new prediction scheme, and the scheme also showed comparable skill on independent data. Similar to our newly-developed August seasonal forecast scheme (discussed in detail in Chapter 5), this scheme only predicts Net Tropical Cyclone (NTC) activity, and the other predictors are then derived from this NTC prediction. For example, if a typical season has 10 named storms and the predicted NTC value is 120%, the predicted number of named storms for the season would be 12 (10 * 120%). Table 3.8 discusses the locations of these new predictors, while Figure 3.5 displays the locations of these predictors on a map.

Table 3.8: Predictors used in the new December forecast. The sign of the predictor associated with increased tropical cyclone activity the next year is in parentheses.

Predictor Name	Location
1) October-November SLP in the North Atlantic (-)	(10°-60°N, 30°-10°W)
2) October-November SST in the North Atlantic (+)	(55°-65°N, 60°-10°W)
3) October-November SLP in the Subtropical NE Pacific (+)	(5°-25°N, 180°-150°W)

A brief discussion of how each of these three new experimental predictors may relate to Atlantic basin tropical cyclone activity follows:

a. Predictor 1: October-November SLP in the North Atlantic (-):

Low pressure in the North Atlantic in October-November SLP is generally related to weaker trade winds during the late fall/early winter which drives less evaporation and upwelling during the winter and spring in the tropical and subtropical Atlantic. Reduced upwelling and evaporation during the previous fall tends to relate to a warmer tropical North Atlantic the following summer and fall.

b. Predictor 2: October-November SST in the North Atlantic (+):

Warm North Atlantic sea surface temperatures in the fall are indicative of an active phase of the Atlantic Multi-decadal Oscillation (AMO) (Goldenberg et al. 2001) and a likely strong thermohaline circulation. An active AMO is associated with anomalously low vertical wind shear, warm tropical Atlantic sea surface temperatures and anomalously low sea level pressures during the hurricane season, all of which are favorable for an active Atlantic basin hurricane season.

c. Predictor 3: October-November SLP in the subtropical NE Pacific (+):

According to Larkin and Harrison (2002), high pressure in the tropical NE Pacific appears during most winters preceding the development of a La Niña event. High pressure forces stronger trade winds in the East Pacific which increases upwelling and helps initiate La Niña conditions which eventually enhance Atlantic hurricane activity during the following summer. This predictor correlates with low geopotential heights at 500 mb throughout the tropics the following summer, indicative of a weaker Hadley circulation typical of La Niña conditions. Also, high pressure in October-November in

the tropical NE Pacific correlates with low sea level pressure in the tropical Atlantic and easterly anomalies at 200 mb during the following August through October period.

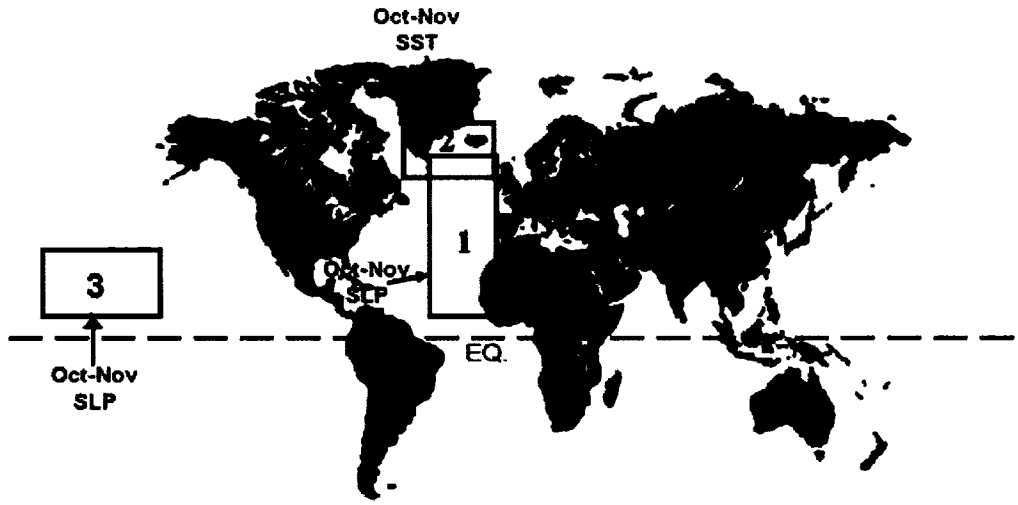

Figure 3.5: Map of predictors used in the experimental early December statistical forecast issued in December 2006.

Over the next couple of years, the skill of both December statistical forecasts will be evaluated. An additional predictor has also been suggested in recent months that may add skill to the December statistical forecast. A prediction of the following year's July-November Atlantic Meridional Mode (AMM) (Chiang and Vimont 2004), basically the meridional gradient in sea surface temperature between the northern tropical Atlantic and the southern tropical Atlantic, has been proposed as a possible additional predictor for the December statistical forecast. A positive AMM during the hurricane season indicates a northward-shifted Intertropical Convergence Zone (ITCZ), implying increased convergence, low-level vorticity, and reduced vertical wind shear, all of which favor an

active Atlantic basin hurricane season (Klotzbach and Gray 2006a). Approximately 50% of the variance of the following year's July-November AMM index can be hindcast by early December of the previous year. Additional efforts aimed at improving the December statistical forecast will continue for the foreseeable future.

Chapter 4

April and June prediction developments

The TMP issues several updates to their seasonal predictions that are first issued in early December. This chapter focuses on statistical techniques developed for the updated forecasts issued in early April and early June, respectively. Significant revamping of both the early April and early June statistical forecasts have occurred over the past few years. These forecasts are still being fine-tuned, and therefore these forecasts have not yet been subjected to the rigorous testing that both the early December (discussed in Chapter 3) and early August (discussed in Chapter 5) prediction schemes have been.

4.1 April prediction background

Early April predictions were first issued by the TMP in 1995. The original scheme utilized several predictors including the strength of the QBO at 30 and 50 mb, rainfall in the Sahel during the previous summer (June-September) and rainfall in the Gulf of Guinea during the previous August-November period. In addition, the strength of the Azores high during the current March and the previous October-November was evaluated. Lastly, several measures of North Atlantic sea surface temperatures and trends in ENSO temperatures were considered. This prediction scheme was utilized from 1995-

2002. Approximately 50% of the variance could be hindcast for individual predictands (i.e., named storms, named storm days, etc.) using combinations of these predictors based on the period from 1950-1997. However, the real-time skill of this scheme failed in the late 1990s, likely due to a weakening of the West African rainfall-Atlantic basin hurricane relationship as well as the QBO-Atlantic basin hurricane relationship. See Chapter 3 for more in-depth discussion of the recent failure of these relationships.

Since the statistical technique originally developed for issuing April forecasts was not skillful in real-time forecasting, it was decided to redo the statistical prediction scheme. The first revised April prediction was issued in April 2003, and the scheme has continued to undergo revisions over the past few years.

4.2 April seasonal prediction development methodology

As mentioned briefly earlier, the original early April statistical forecast scheme was initially revised in 2003 (Gray et al. 2003a). This scheme was adjusted slightly in 2004 (Gray and Klotzbach 2004). I will discuss the scheme utilized in the 2004-2006 seasons in further detail here. The new scheme used a total of six predictors that spanned the globe. As with the early December forecast, these predictors were selected from the NCEP/NCAR reanalysis data. No more than five predictors out of the pool of six predictors were selected for each individual predictand. Predictors were selected that maximized the hindcast variance over the period from 1950-2001. Composite and correlation analysis were constructed in a manner similar to what was done with the early December forecast (Klotzbach and Gray 2004). Table 4.1 presents a listing of the six predictors selected with the revised early April forecast scheme, while Figure 4.1 displays

the locations of these predictors. Table 4.2 displays the hindcast skill and cross-validated jackknife hindcast skill for this prediction scheme.

Table 4.1: Predictors used in the early April forecast scheme that was first issued in 2004. The sign of the predictor associated with increased tropical cyclone activity the next year is in parentheses.

Predictor Name	Location
1) February 200 mb U in the tropical Atlantic (-)	(5°S-10°N, 55°-35°W)
2) February-March 200 mb V in the South Indian Ocean (-)	(62.5°-35°S, 95°-70°E)
3) February SLP in the southeast Pacific (+)	(45°S-0°, 180°-90°W)
4) February SST in the northeast Atlantic (+)	(35°-50°N, 30°-10°W)
5) November 500-mb geopotential height in the far North Atlantic (+)	(67.5°-85°N, 50°W-10°E)
6) September-November SLP in the Gulf of Mexico-southeastern United States (-)	(15°-35°N, 95°-75°W)

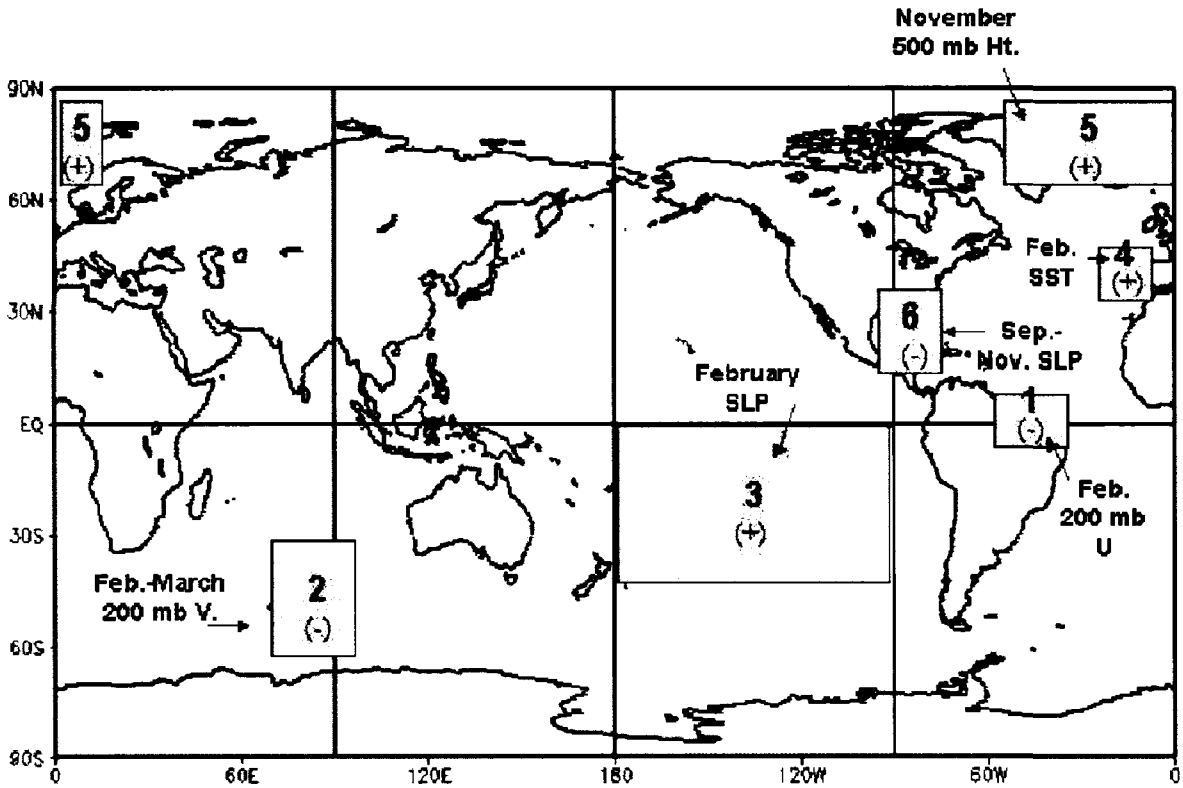

Figure 4.1: Location of predictors for the revised early April forecast scheme. The sign of the predictor associated with increased tropical cyclone activity the next year is in parentheses. This scheme was first used with the April 2004 forecast.

Table 4.2: Predictors chosen, hindcast variance explained, and jackknife variance explained for each TC activity parameter in the early April forecast of the following year's tropical cyclone activity. See Table 4.1 for predictor names and descriptions.

Forecast Parameter	No. of Predictors	Predictors Chosen from Table 3.2	Hindcast (r^2) (1950-2001)	Jackknife Hindcast (r^2) (1950-2001)
Named Storms	4	1, 2, 4, 5	0.45	0.34
Named Storm Days	4	1, 2, 4, 5	0.59	0.50
Hurricanes	4	2, 3, 5, 6	0.53	0.41
Hurricane Days	4	1, 2, 5, 6	0.65	0.57
Intense Hurricanes	4	2, 3, 4, 5	0.61	0.53
Intense Hurricane Days	5	1, 2, 4, 5, 6	0.55	0.46
NTC Activity	5	1, 2, 4, 5, 6	0.71	0.64

4.3 Physical links between April predictors and seasonal Atlantic basin TC activity

Brief descriptions of how predictors 1-4 are hypothesized to affect tropical cyclone activity in the Atlantic are provided below. Predictors 5 and 6 were already discussed in detail with the December prediction scheme. Refer to Chapter 3 for more information on how these predictors are thought to impact tropical cyclone activity in the Atlantic.

a. Predictor 1: February 200 mb U in the tropical Atlantic (-)

Easterly upper-level zonal wind anomalies off the northeast coast of South America imply that the upward branch of the Walker Circulation associated with ENSO remains in the western Pacific and that cool ENSO or La Niña conditions are likely to be present in the eastern equatorial Pacific for the next 4-6 months. El Niño conditions shift the upward portion of the Walker Circulation to the eastern Pacific and cause 200 mb westerly wind anomalies over the tropical Atlantic. These anomalies inhibit Atlantic hurricane activity.

b. Predictor 2: February-March 200 mb V in the South Indian Ocean (-)

Anomalous winds from the north at 200 mb in the southern Indian Ocean are associated with a northeastward shift of the South Indian Convergence Zone (Cook 2000), a more longitudinally concentrated upward branch of the Hadley Cell near Indonesia and warm sea surface temperatures throughout most of the Indian Ocean. This also implies that warm ENSO conditions have likely been prevalent throughout the past several months due to the lag teleconnected effect of a warm Indian Ocean with a warm eastern Pacific Ocean. Strong lag correlations ($r > 0.4$) with this predictor indicate that a change in phase of ENSO from warm to cool is likely during the latter part of the spring/early summer.

c. Predictor 3: February SLP in the southeast Pacific (+)

High sea level pressure in the eastern Pacific south of the equator indicates a positive Southern Oscillation Index (SOI) and stronger-than-normal trade winds across the equatorial Pacific. Increased trades drive enhanced upwelling off the west coast of South America that is typical of La Niña conditions. Cool sea surface temperatures in the eastern Pacific are associated with these higher surface pressures and tend to persist throughout the spring and summer thereby reducing vertical wind shear over the tropical Atlantic and providing more favorable conditions for tropical cyclone development.

d. Predictor 4: February SST in the northeast Atlantic (+)

Warm sea surface temperatures off the northwest coast of Europe correlate quite strongly with warm sea surface temperatures across the entire North Atlantic Ocean. A

warm North Atlantic Ocean indicates that the thermohaline circulation is likely stronger than normal, the subtropical high near the Azores is weaker than normal and consequently trade wind strength across the Atlantic is also reduced. Weaker trade winds induce less upwelling which keeps the tropical Atlantic warmer than normal. This pattern tends to persist throughout the spring and summer implying a warmer tropical Atlantic during the hurricane season which is an enhancing factor for developing tropical waves.

4.4 Current April prediction scheme and future work

The above-mentioned statistical scheme was implemented for the first time in April 2004 and was utilized through April 2006. A new statistical scheme was implemented for the April 2007 prediction (Klotzbach and Gray 2007a). This scheme utilizes a similar technique to what was done in early December. It utilizes only three predictors that are taken from sea level pressure and sea surface temperature data derived from the NCEP/NCAR reanalysis. Two-month averages are used, as was done with the early December forecast scheme in an attempt to average out any variability due to Madden-Julian Oscillation (MJO) effects (Madden and Julian 1994).

As was done with the December 2006 statistical prediction scheme, these three predictors were selected based on data from 1950-1989 and then tested on independent data from 1990-2004. The combination of these three predictors explained 53 percent of the variance in NTC on dependent data (1950-1989), and using these same equations, 66 percent of the variance in NTC was explained using independent data (1990-2004). When evaluated over the complete 1950-2004 time period, 55 percent of the variance was explained using these three predictors.

Similar to our newly-developed December and August seasonal forecasts, this scheme only predicts Net Tropical Cyclone (NTC) activity, and the other predictors are then derived from this NTC prediction. For example, if a typical season has 10 named storms and the predicted NTC value is 120%, the predicted number of named storms for the season would be 12 (10 * 120%). Table 4.3 discusses the locations of these new predictors, while Figure 4.2 displays the locations of these predictors on a map.

Table 4.3: Predictors used in the new April forecast. The sign of the predictor associated with increased tropical cyclone activity during the hurricane season is in parentheses.

Predictor Name	Location
1) February-March SST in the subtropical eastern Atlantic (+)	(30°-45°N, 30°-10°W)
2) February-March SLP in the subtropical southeastern Pacific (+)	(45°-20°S, 160°-100°W)
3) February-March SST in the South Atlantic (-)	(45°-30°S, 45°-20°W)

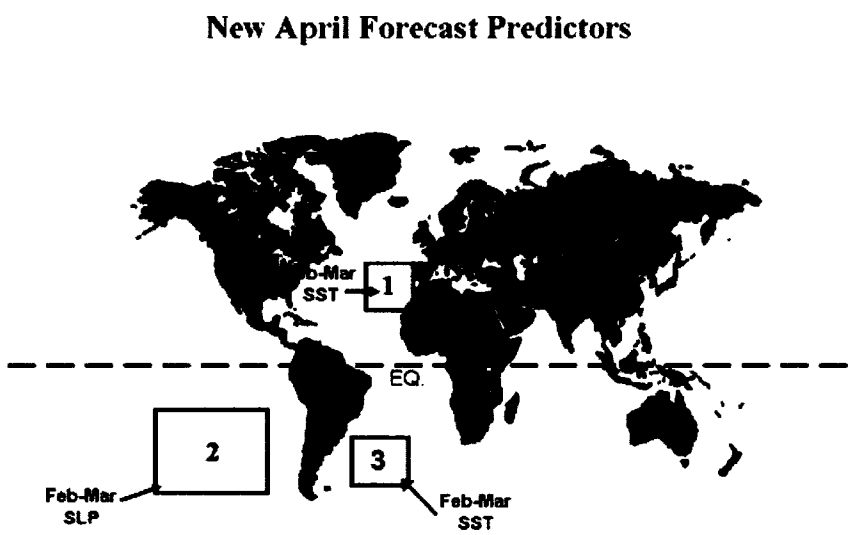

Figure 4.2: Location of predictors for the current early April forecast scheme. This scheme was first used with the April 2007 forecast.

A brief discussion of how each of these three predictors may relate to Atlantic basin tropical cyclone activity follows:

a. Predictor 1: February-March SST in the subtropical eastern Atlantic (+):

Above-normal sea surface temperatures (SSTs) in the eastern subtropical Atlantic are associated with a weaker-than-normal Azores high and reduced trade wind strength during the boreal spring (Knaff 1997). These above-average SSTs in February-March are strongly correlated with weaker trade winds, lower-than-normal sea level pressures and above-average SSTs in the tropical Atlantic during the following August-October period. All three of these August-October features are commonly associated with active Atlantic basin hurricane seasons, through reductions in vertical wind shear, increased vertical instability and increased surface latent and sensible heat fluxes, respectively.

b. Predictor 2: February-March SLP in the subtropical southeastern Pacific (+):

Anomalously high sea level pressure in this portion of the subtropical southeastern Pacific during February-March is associated with a positive Southern Oscillation Index and stronger trade winds across the tropical Pacific. Anomalously strong trade winds drive increased upwelling in the eastern tropical Pacific and are typically associated with cool ENSO conditions. Lag correlations for the August-October period indicate that La Niña conditions are much more likely with positive values of this predictor. Cool ENSO conditions are typically associated with more active Atlantic basin hurricane seasons through a reduction of vertical wind shear across the Caribbean and tropical Atlantic (e.g. Gray 1984a, Goldenberg and Shapiro 1996).

c. Predictor 3: February-March SST in the South Atlantic (-):

Above-average SSTs in February-March in the South Atlantic are associated with higher sea level pressures throughout the tropical Atlantic during the same time period. These higher pressures in the tropical Atlantic feed back and drive stronger trade winds across the tropical Atlantic during the August-October period. Warm ENSO conditions and above-average vertical wind shear across the tropical Atlantic are typically experienced during August-October with above-average SSTs in the South Atlantic in the February-March timeframe. More research is being conducted to tie down the physical linkage between this predictor and Atlantic basin TC activity.

As with the early December statistical forecast, the prediction of the following year's July-November AMM is also considered as a qualitative adjustment factor in the new early April prediction. This is not taken into account directly in the statistical scheme, but it is considered as a potential enhancing or detrimental factor in the upcoming season's prediction as a qualitative adjustment. Additional efforts aimed at improving the April statistical forecast will continue for the foreseeable future.

4.5 June prediction background

Seasonal predictions have been issued around June 1 since the TMP began issuing seasonal forecasts in 1984. Original predictors for the early June prediction scheme utilized the state of ENSO, the QBO and Caribbean basin sea level pressure values (Gray 1984a, 1984b). The prediction scheme was expanded to include measures of African rainfall and the strength of 200 mb zonal wind anomalies in the Caribbean in the early 1990s (Gray et al. 1994). Between 40-75% of the variance could be hindcast over the

period from 1950-1991 using a cross-validated Least Absolute Deviations (LAD) regression approach.

As happened with the early December forecast, the June forecast began to show diminishing skill during the early to mid 1990s, primarily due to the failure of the African rainfall and QBO relationships with Atlantic basin hurricane activity. It was therefore decided to redo the statistical prediction scheme using NCEP/NCAR reanalysis data. The first revised June prediction was utilized in 2003 and 2004, while the second was used in 2005 and 2006. A new statistical prediction has recently been developed and utilized for the first time with the early June prediction for 2007 Atlantic basin hurricane activity (Klotzbach and Gray 2007b). Brief discussions of all three schemes follow.

4.6 June seasonal forecast used in 2003 and 2004

The first revision to the early June prediction scheme was implemented in June 2003 (Gray et al. 2003b). This scheme was also utilized for the 2004 season. The new prediction used a total of seven predictors that spanned the globe. The first six predictors were the same six predictors used in the early April forecast scheme. The seventh predictor that helped increase the skill from the early April forecast scheme was the May sea surface temperature from 20-40°N and 30-15°W. May sea surface temperatures in the subtropical Atlantic are thought to influence Atlantic basin hurricanes during the upcoming summer and fall by the following mechanism: warm sea surface temperatures in this area indicate that the Atlantic subtropical ridge is weaker than normal, and therefore trade winds across the Atlantic are also weaker than normal. These anomalies in May correlate strongly with a generally warm Atlantic Ocean as well as with low sea

level pressure throughout the tropical Atlantic during the heart of the hurricane season from August-October. Weaker trade winds and easterly anomalies at upper levels during the summer throughout the tropical Atlantic are also associated with this feature.

Since only one additional predictor was added to the early April forecast scheme, the discussion of this scheme will remain brief. Please refer to Sections 4.2 and 4.3 for more information on the first six predictors utilized in the June prediction scheme. The May sea surface temperature predictor in the subtropical Atlantic was added as an additional predictor for intense hurricanes, intense hurricane days and NTC activity, and its addition caused an approximate 2-4% increase in variance explained for these three predictands.

4.7 June seasonal forecast used in 2005 and 2006

A new early June seasonal forecast was proposed in 2005 (Gray and Klotzbach 2005). This forecast utilized a total of four predictors and utilized data closer to the time of the forecast date. This is to be contrasted with the early June scheme issued in 2003 and 2004, which primarily used data prior to 1 April. By looking at climate signals closer to the forecast issuance date, it is thought that better real-time forecast skill will be achieved, even though hindcast skill may be reduced slightly. The new scheme was developed on data from 1949-1989 and then tested on independent data from 1990-2004. Predictors were selected that maximized the hindcast variance over the period from 1949-1989. Composite and correlation analysis were constructed in a manner similar to what was done with the early December forecast (Klotzbach and Gray 2004). Table 4.4 presents a listing of the four predictors selected with the revised early June forecast scheme, while Figure 4.3 displays the locations of these predictors. Table 4.5 displays

the variance explained over the developmental dataset (1949-1989), the independent dataset (1990-2004) and the entire dataset (1949-2004).

Table 4.4: Predictors used in the early June forecast scheme that was first issued in 2005. The sign of the predictor associated with increased tropical cyclone activity is in parentheses.

Predictor Name	Location
1) May SST in the eastern tropical Pacific – Nino 3 index (-)	(5°S-5°N, 150°-90°W)
2) April-May SST off the northwestern European coast (+)	(30°-45°N, 30°-10°W)
3) March-April SLP in the tropical Atlantic (-)	(0°-20°N, 40°-10°W)
4) Previous November 500-mb geopotential height in the far North Atlantic (+)	(67.5°-85°N, 50°W-10°E)

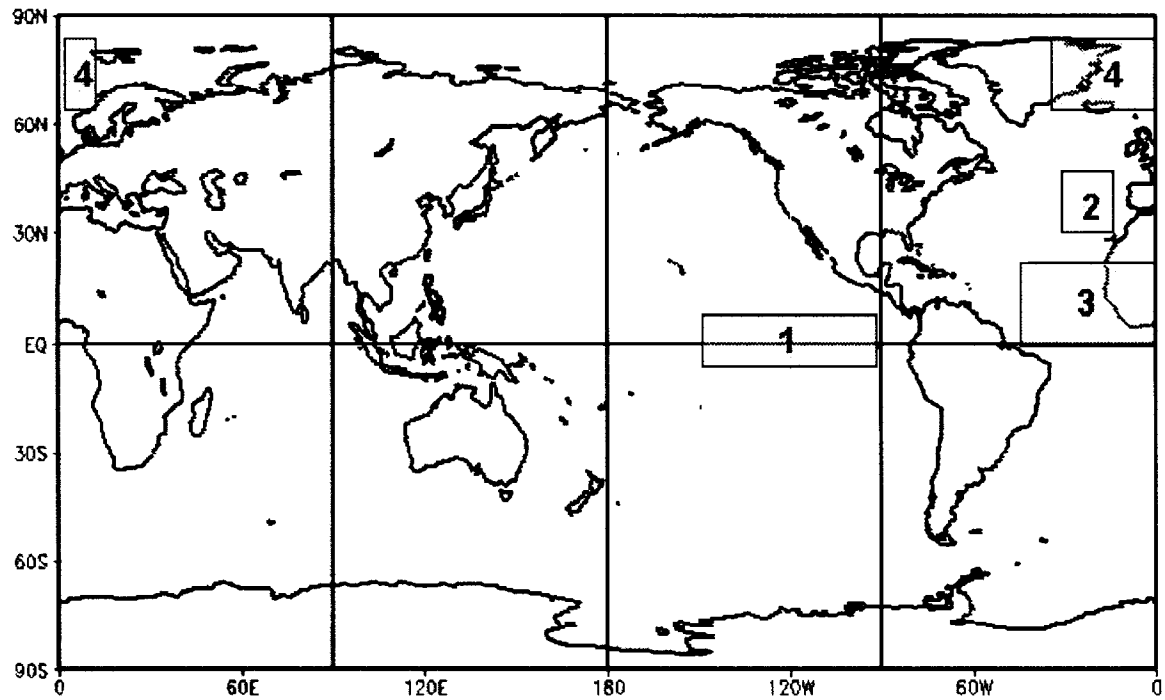

Figure 4.3: Location of predictors for the early June forecast scheme utilized in 2005 and 2006.

Table 4.5: Variance (r^2) explained for the early June forecast scheme utilized in 2005 and 2006 for the developmental dataset (1949-1989), the independent dataset (1990-2004) and the entire dataset (1990-2004).

Forecast Parameter	Developmental Dataset (1949-1989) r^2	Independent Dataset (1990-2004) r^2	Entire Dataset (1949-2004) r^2
Named Storms	0.27	0.49	0.29
Named Storm Days	0.40	0.65	0.37
Hurricanes	0.31	0.67	0.36
Hurricane Days	0.51	0.63	0.49
Intense Hurricanes	0.45	0.67	0.49
Intense Hurricane Days	0.54	0.38	0.48
NTC Activity	0.54	0.70	0.52

4.8 Physical links between June predictors and seasonal Atlantic basin TC activity

Brief descriptions of how the four predictors utilized in the early June forecast scheme are thought to impact tropical cyclone activity in the Atlantic follows:

a. Predictor 1: May SST in the eastern equatorial Pacific (-)

Sea surface temperatures in this area are taken to be a measure of ENSO conditions. When sea surface temperatures are much cooler than normal, La Niña conditions are present, and when sea surface temperatures are much warmer than normal, El Niño conditions are occurring. Although there is some changeover during the summer and fall, in general, anomalies in this area tend to persist from the late spring through the summer and fall. El Niño conditions during the summer and fall tend to decrease Atlantic hurricane activity by increasing westerlies at upper levels across the Atlantic (Gray 1984a, Goldenberg and Shapiro 1996). These increased westerlies increase vertical wind shear across the area where Atlantic tropical cyclones develop.

b. Predictor 2: April-May SST off the northwestern European coast (-)

Warm sea surface temperatures in this area indicate that the Atlantic subtropical ridge is weaker than normal, and therefore trade winds across the Atlantic are also weaker than normal. These anomalies in April-May correlate strongly with a generally warm Atlantic Ocean as well as with low sea level pressure throughout the tropical Atlantic during the heart of the hurricane season from August-October. Weaker trade winds and easterly anomalies at upper levels during the summer throughout the tropical Atlantic are also associated with this feature.

c. Predictor 3: March-April SLP in the tropical Atlantic (-)

Low sea level pressure in the tropical Atlantic during March-April implies increased instability, reduced trade wind strength and warm sea surface temperatures during the spring. In general, these favorable conditions for tropical cyclone activity tend to persist through the summer and fall, as evidenced by strong lag correlations ($r > |0.4|$) between this feature and warm sea surface temperatures in the tropical Atlantic during the late summer/early fall. Also, reduced vertical wind shear and continued low sea level pressure during the late summer/early fall are associated with low values of this feature in March-April.

d. Predictor 4: Previous November 500 mb geopotential height in the far North Atlantic (+)

Positive values of this predictor correlate very strongly ($r \sim -0.7$) with negative values of the Arctic Oscillation (AO) and the North Atlantic Oscillation (NAO). Negative AO

and NAO values imply more blocking in the central Atlantic and a likely warm north Atlantic Ocean (50-60°N, 50-10°W). Also, on decadal timescales, weaker zonal winds in the subpolar areas are indicative of a relatively strong thermohaline circulation which is favorable for hurricane activity. Positive values of this November index are negatively correlated with both 200 mb zonal winds and trade wind strength the following September in the tropical Atlantic. The associated reduced tropospheric vertical wind shear enhances conditions for TC development. Other features that are directly correlated with this predictor are low sea-level pressure in the Caribbean and a warm North and tropical Atlantic. Both of the latter are also hurricane-enhancing factors.

4.9 Current June prediction scheme and future work

The statistical scheme discussed in detail in the previous section was utilized for the early June prediction in 2005 and 2006. A new statistical scheme was implemented for the June 2007 prediction (Klotzbach and Gray 2007b). This scheme utilizes a similar technique to what was done in early December and in early April. It utilizes a total of three predictors. Two of these predictors are derived from sea surface temperature data derived from the NCEP/NCAR reanalysis. The third predictor is the previous year's early December prediction of the Atlantic Meridional Mode (AMM) discussed in previous sections regarding the new early December and early April forecasts. Unlike those schemes where the predicted AMM is evaluated in a qualitative manner, it is ingested in a quantitative manner in the new early June statistical forecast.

As was done with the new early December and early April statistical prediction schemes, these three predictors were selected based on dependent data from 1950-1989 and then tested on independent data from 1990-2004. The combination of these three

predictors explained 42 percent of the variance in NTC on dependent data (1950-1989), and using these same equations, 54 percent of the variance in NTC was explained using independent data (1990-2004). When evaluated over the complete 1950-2004 time period, 49 percent of the variance was explained using these three predictors.

The reader will note that the variance explained in the early June statistical scheme is actually slightly less than that achieved in either early December or early April. However, the author feels that utilizing a statistical scheme that includes data from the two months immediately prior to the forecast date is critical for evaluating the current state of the atmosphere/ocean system.

As with all of the other new forecast schemes that have been outlined, this new scheme only predicts Net Tropical Cyclone (NTC) activity, and the other predictors are then derived from this NTC prediction. Table 4.6 provides the locations of these new predictors, while Figure 4.4 displays the locations of these predictors on a map.

Table 4.6: Predictors used in the new early June forecast. The sign of the predictor associated with increased tropical cyclone activity during the hurricane season is in parentheses.

Predictor Name	Location
1) April-May SST in the eastern Atlantic (+)	(25°-60°N, 30°-15°W)
2) April-May SST in the eastern and central tropical Pacific – Nino 3.4 index (-)	(5°S-5°N, 170°-120°W)
3) July-November Predicted AMM Index (+)	(21°S-32°N, South American Coastline – West African Coastline)

A brief discussion of how each of these three predictors in the current early June forecast scheme may relate to Atlantic basin tropical cyclone activity follows:

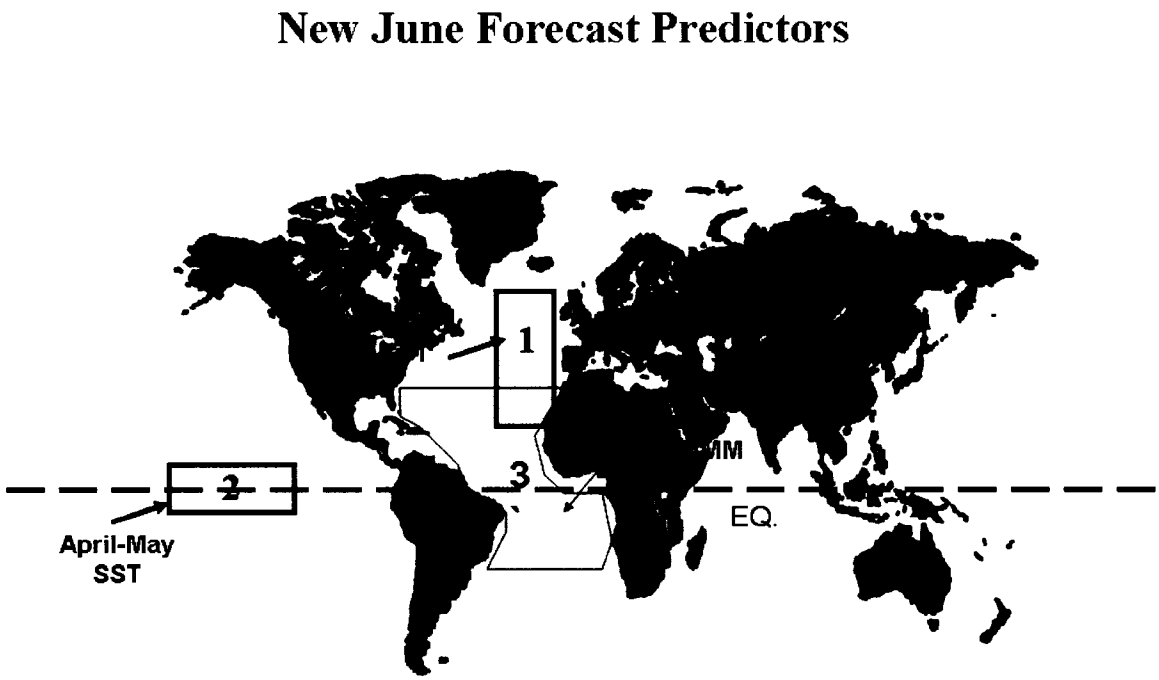

Figure 4.4: Location of predictors for the current early June forecast scheme. This scheme was first used with the June 2007 forecast.

a. Predictor 1: April-May SST in the eastern Atlantic (+):

Above-normal sea surface temperatures (SSTs) in the eastern Atlantic during April-May are associated with a weaker-than-normal Azores high and reduced trade wind strength during the boreal spring (Knaff 1997). As was observed with warm SSTs in the subtropical eastern Atlantic during February and March, above-average SSTs in April-May are strongly correlated with weaker trade winds, lower-than-normal sea level pressures and above-average SSTs in the tropical Atlantic during the following August-October period. All three of these August-October features are commonly associated with active Atlantic basin hurricane seasons, through reductions in vertical wind shear,

increased vertical instability and increased surface latent and sensible heat fluxes, respectively. In addition, warmer-than-normal sea surface temperatures in the eastern Atlantic are typically associated with a positive phase of the Atlantic Multi-decadal Oscillation (AMO) and a strong thermohaline circulation (Klotzbach and Gray 2007, manuscript submitted to *Geophys. Res. Lett.*).

b. Predictor 2: April-May SST in the eastern and central tropical Pacific – Nino 3.4 index (-):

When sea surface temperatures in the Nino 3.4 region during April-May are below average, it indicates that a La Niña event is likely taking place. Typically, by the end of May, the springtime ENSO predictability barrier (e.g., Samelson and Tziperman 2001) has passed, and therefore the persistence of either warm or cold anomalies is likely to continue through the upcoming Atlantic basin hurricane season. As has been discussed extensively in previous sections, El Niño conditions during the summer and fall tend to decrease Atlantic hurricane activity by increasing vertical wind shear across the area where Atlantic tropical cyclones develop (e.g., Gray 1984a).

c. Predictor 3: July-November AMM Prediction (+):

The Atlantic meridional mode evaluates the strength of the SST gradient between the northern tropical and southern tropical Atlantic, spanning from 21°S-32°N and the South American coastline to the West African coastline. A positive AMM is in place when the meridional gradient of SST between the northern tropical Atlantic and southern tropical Atlantic is greater than the long-period average. When the AMM is positive, the

Intertropical Convergence Zone (ITCZ) shifts northward. Consequently, convergence is enhanced in the northern tropical Atlantic, while trade wind strength and vertical wind shear in the tropical Atlantic are reduced. Also associated with a northward-shifted ITCZ are enhanced low-level vorticity and below-normal sea level pressures (Knaff 1997). When all these conditions occur, more active Atlantic basin tropical cyclone seasons are typically observed (Chiang and Vimont 2004, Klotzbach and Gray 2006a). This AMM prediction, issued in early December of the previous year, explains approximately 40% of the variance of the observed AMM during the following year's July-November period.

As with the other new statistical forecasts, additional research will continue to further improve the early June statistical forecast scheme.

Chapter 5
August prediction developments

This chapter focuses on revisions to the early August prediction issued by the TMP, prior to the climatologically most active portion of the Atlantic basin hurricane season. Approximately 90-95% of all tropical cyclone activity occurs after 1 August in an average season. Much of this discussion is taken from Klotzbach (2007b). Additional information on the August statistical prediction is available in that paper.

5.1 Background

Earlier prediction schemes for Atlantic basin tropical cyclone activity from early August utilized statistical relationships between El Niño, the QBO and spring and early summer values of Caribbean basin sea level pressure (Gray 1984b). When eastern and central Pacific Ocean equatorial sea surface temperatures were above normal (i.e., El Niño conditions), Atlantic basin hurricane activity tended to be reduced due to an increase in upper-level westerlies and a concomitant increase in vertical wind shear (Gray 1984a). The east phase of the QBO was hypothesized to increase upper tropospheric-lower stratospheric vertical wind shear and increase ventilation at upper levels in tropical cyclones thereby inhibiting their intensification. Lastly, although not completely explained in the original paper, high values of Caribbean sea level pressure imply

increased subsidence, drier air and likely stronger trade winds (Knaff 1997). All three of these factors inhibit tropical cyclone development.

Additional predictors were added to the early August forecast scheme during the first part of the 1990s. These predictors included measures of West African rainfall and upper-tropospheric zonal wind anomalies in the Caribbean (Gray et al. 1993). Drought in the Sahel during the early part of the hurricane season (June-July) was hypothesized to indicate weaker African easterly waves and increased dry air and vertical wind shear in the tropical Atlantic (Landsea and Gray 1992). Positive upper-tropospheric zonal wind anomalies (e.g., stronger westerlies) imply increased vertical wind shear and a southward-shifted Intertropical Convergence Zone (ITCZ), causing anomalous low-level divergence and upper-level convergence in the tropical Atlantic. Both of these conditions are unfavorable for an active hurricane season (Goldenberg and Shapiro 1996, Knaff et al. 2004). Figure 5.1 shows the location of the predictors utilized in the early 1990s version of the 1 August forecast scheme.

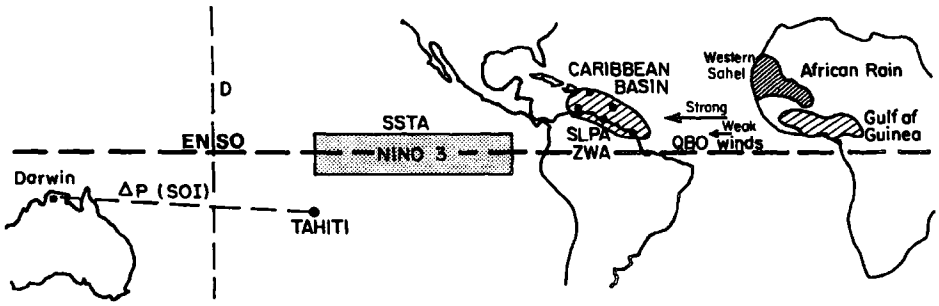

Figure 5.1. Location of areas from which meteorological parameters used in the earlier 1 August Atlantic basin seasonal forecast were derived. Figure taken from Gray et al. (1993).

The Atlantic basin seasonal hurricane forecast from 1 August showed considerable hindcast skill over the period from 1950-1990, explaining over 60 percent of

the variance in major hurricane activity (Gray et al. 1993). However, this scheme has not worked as well in real-time forecasting since the mid-1990s when the Atlantic returned to very active hurricane conditions associated with the onset of a positive phase of the AMO (Goldenberg et al. 2001).

The primary reason for the failure of the statistical scheme in recent years is due to the failure of the African rainfall predictors, as well as a noticeable weakening of the relationship between Atlantic hurricanes and the QBO. As discussed in detail in Chapter 3, it is difficult to say why the African rainfall predictors have failed in recent years. It could be due to a breakdown in the linkage between African rainfall and Atlantic hurricane activity, or it could be an artifact of changing station measurement quality in West Africa. In addition, Bell and Chelliah (2006) have noted that upper-level divergence over West Africa varies on multi-decadal timescales. Therefore, it could be possible that this is more of a multi-decadal than a year-to-year relationship. Research is ongoing as to why the QBO-Atlantic hurricane relationship has weakened in recent years. Recently, an unpublished manuscript has noted the strong degradation of the QBO-Atlantic hurricane relationship over the past 10-15 years (Chris Landsea 2007, personal communication).

Another reason for re-doing the early August statistical forecast was to develop a simple, more concise scheme. The original statistical scheme expanded over time, to include consideration of 16 predictors by August 2001. Mostly different predictors were utilized to predict each tropical cyclone metric (i.e., named storms, hurricanes, etc.). Since the pool of predictors was so large, it often led to somewhat divergent statistical forecasts for individual tropical cyclone parameters. Therefore, these statistical forecasts

lacked internal consistency. For example, in August 2001, 6.7 named storms were predicted (about 75% of the post 1-August climatological average); whereas, 5.5 major hurricane days were predicted (about 110% of the post 1-August climatological average) (Gray et al. 2001). For reference, a total of 15 named storms and 4.25 major hurricane days occurred during 2001, so clearly, for this particular forecast, the statistical prediction of major hurricane days was much closer to the mark than the named storm prediction.

Several new datasets have recently been developed which provide data on a global grid for a variety of meteorological and oceanic parameters including zonal wind, sea level pressure, SST, etc. Some of these datasets, especially those that evaluate surface parameters, extend back to 1900 or even as far back as the mid-nineteenth century. It was decided to develop a new 1 August seasonal forecast scheme that utilizes these new datasets as well as some recent new physical insights into other potential modulators of Atlantic hurricane activity. The remainder of this chapter discusses the development and results of this new 1 August seasonal statistical forecast in detail.

5.2 Data used in August seasonal forecast development

Atlantic basin hurricane activity from 1900-2005 was calculated from the National Hurricane Center's "best track" data files (Jarvinen et al. 1984). This dataset provides the best estimate of a storm's intensity in five-knot increments for every six-hour period of the storm's existence. Recent changes made by the Atlantic Hurricane Database Re-analysis Project for tropical cyclones that occurred during the early part of the 20th century (1900-1914) (Landsea et al. 2004) have been included in this analysis.

As was done with the other statistical schemes that have been discussed in prior chapters, the primary data source used for selecting predictors in the early August forecast scheme is the NCEP/NCAR reanalysis from 1949-2005 (Kalnay et al. 1996; Kistler et al. 2001).

One of the predictors selected for forecasting Atlantic basin hurricane activity was the Nino3 index located in the tropical eastern Pacific. This index is a measure of sea surface temperatures from 5°S - 5°N, 150°W - 90°W. The Climate Prediction Center's analysis of the Nino3 index is utilized in this paper for the 1950-2005 period. Values were obtained from the Climate Prediction Center's webpage (http://www.cpc.ncep.noaa.gov/data/indices/sstoi.indices). The Nino3 index from 1900-1949 was derived from the HadISST1 dataset (Rayner et al. 2003) using calculations available from the Climate Diagnostics Center's time series webpage (http://www.cdc.noaa.gov/Pressure/Timeseries/).

Two additional datasets were utilized for the earlier independent dataset from 1900-1948. Sea level pressure values were calculated from the Hadley Center SLP dataset (Basnett and Parker 1997). Earlier-period sea surface temperatures were calculated from the Kaplan SST dataset (Kaplan et al. 1998).

5.3 August seasonal prediction development methodology

One of the likely reasons why earlier statistical forecasts of Atlantic basin hurricane activity have had a significant reduction in forecast skill when applied to independent data was due to the general lack of data for independent tests. This was largely due to the unavailability of earlier-period datasets (e.g., 1900-1950) when the older August statistical forecasts were being developed in the 1980s and 1990s. With the

recent development of new surface datasets for the first half of the 20th century, it is believed that more robust forecast schemes can be formulated, since they can be developed on 40+ years of dependent data and then tested on an additional 40+ years of independent data. If a scheme shows skill in both long-term periods, it is much less likely to fail when applied on new independent data sets.

As was done with the new early December, early April and early June schemes, I attempt to find predictors that explain variance in both dependent and independent datasets for the Net Tropical Cyclone (NTC) activity metric (Klotzbach and Gray 2004). Following the prediction of NTC, all other Atlantic seasonal predictands (e.g., named storms, named storm days, hurricanes, hurricane days, etc.) are then adjusted from their climatological average values by the NTC prediction. This methodology helps keep the statistical scheme much simpler by using many fewer predictors than if each predictand were hindcast individually.

Predictors were selected from the NCEP/NCAR reanalysis using the Climate Diagnostic Center's "Linear Correlations" webpage which allows for correlating various atmospheric and oceanic fields with a particular index (http://www.cdc.noaa.gov/Correlation). In this case, sea level pressure and SST fields were correlated with NTC activity for 1949-1989. The 1990-2005 period was set aside as an independent dataset, and the predictors selected were also tested over an earlier 49-year period (1900-1948). The earlier period (1900-1948) correlation tests are done utilizing the Hadley SLP and Kaplan SST datasets discussed earlier. Figure 5.2 shows an example of the linear correlation map between June-July sea level pressure and post 1-August Net Tropical Cyclone (NTC) activity from 1949-1989.

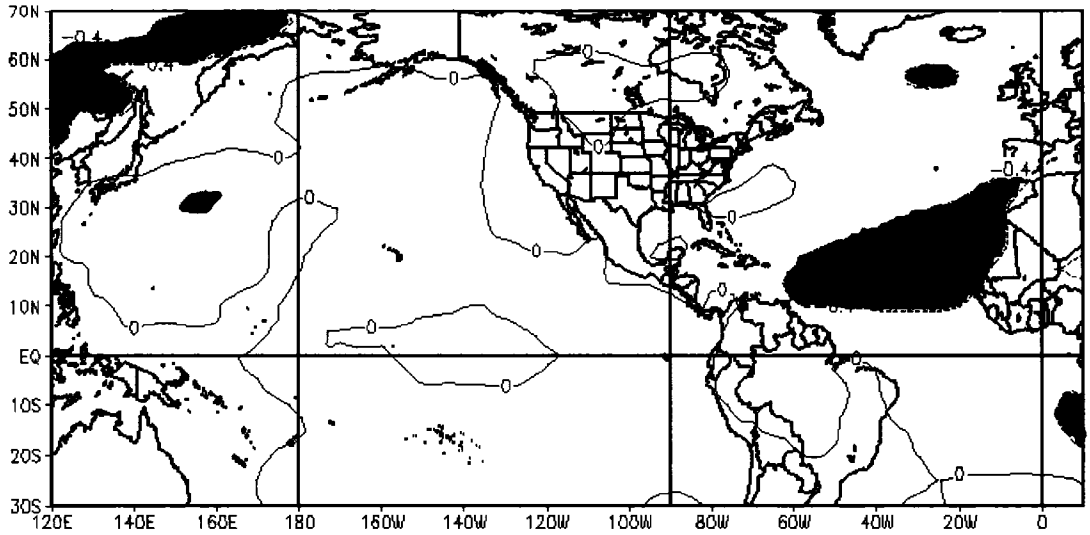

Figure 5.2: Linear correlation map between June-July sea level pressure and post-1 August NTC from 1949-1989. Areas shaded in gray correlated at (r > |0.4|), which is approximately the 99% confidence level of statistical significance for a two-tailed Student's t-test. Figure taken from Klotzbach (2007b).

Predictors were added using a stepwise regression technique (Wilks 1995), and they were only kept in the forecast scheme if they explained an additional two percent of the variance in the dependent data (1949-1989), the recent independent data (1990-2005), and the older independent data (1900-1948). It is believed that if a predictor added additional variance in all three datasets, it is likely robust and is explaining additional variance not explained by the other predictors.

5.4 August statistical forecast results

Table 5.1 and Figure 5.3 describe and display the predictors selected for the 1 August forecast for the remainder of the hurricane season. Table 5.2 shows the increase in variance explained for NTC using the stepwise regression technique for each time period (1949-1989, 1990-2005, 1900-1948, 1949-2005 and 1900-2005). The increase in

variance explained for the time periods of 1990-2005, 1900-1948, 1949-2005 and 1900-2005 were calculated using the equations developed on 1949-1989. The variance explained is even higher in the 1990-2005 independent dataset than over the 1949-1989 developmental dataset. This is a testament to the remarkable stability of the scheme. It should also be noted that this independent dataset is only sixteen years in length. Often large correlations can be obtained when evaluating a scheme over a short time period. If the scheme were to fail in one or two years, the variance explained would fall to values more similar to what were observed during the 1949-1989 period.

Table 5.1: Location of predictors utilized in the new 1 August forecast for Atlantic basin hurricane activity. The sign of the predictor associated with increased Atlantic basin tropical cyclone activity is in parentheses.

Predictor Number	Predictor Name	Location
1	June-July SST in the subtropical Atlantic (+)	(20°-40°N, 35°-15°W)
2	June-July SLP in the tropical and subtropical Atlantic (-)	(10°-20°N, 60°-10°W)
3	June-July Nino3 SST index (-)	(5°S-5°N, 150°-90°W)
4	Before-1 August tropical Atlantic Named Storm Days (+)	(South of 23.5°N, East of 75°W)

Note that the addition of each predictor to the forecast scheme adds at least two percent in additional variance explained for each time period. The equations for 1949-1989 were derived from the predictor's standardized anomaly values. This was done since data from 1900-1948 use different time series, and therefore, the means and standard deviations are likely to be slightly different.

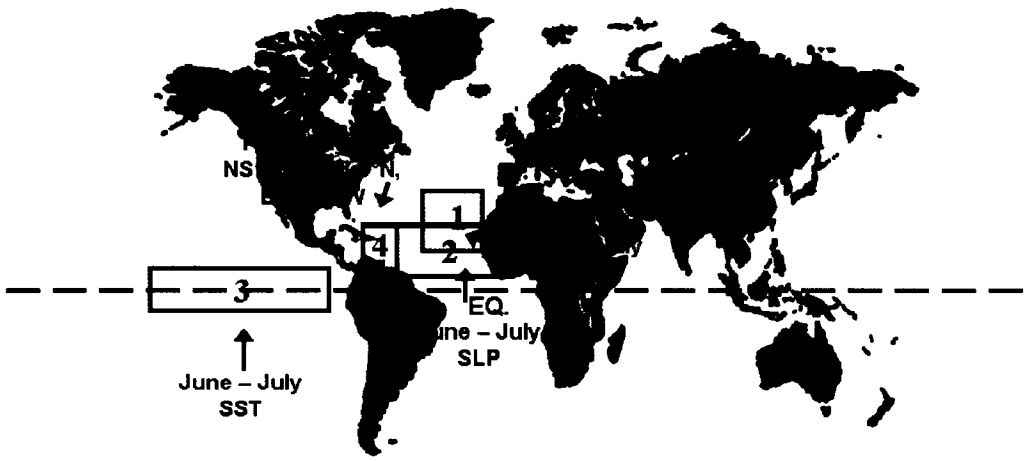

Figure 5.3: Map of the predictors utilized in the new 1 August forecast scheme for Atlantic basin hurricane activity. See Table 5.1 for exact locations. Figure taken from Klotzbach (2007b).

Table 5.2: Stepwise regression technique showing the improvement in variance explained for NTC with the addition of predictors to the August forecast scheme for seasonal Atlantic basin hurricane activity from 1949-1989, 1990-2005, 1900-1948, 1949-2005 and 1900-2005, respectively. The variance explained values are calculated based on equations developed over 1949-1989. Predictor numbers are the same as in Table 5.1.

Predictor	1949-1989 (r^2) (41 Years)	1990-2005 (r^2) (16 Years)	1900-1948 (r^2) (49 Years)	1949-2005 (r^2) (57 Years)	1900-2005 (r^2) (106 Years)
1	0.16	0.41	0.23	0.25	0.32
1, 2	0.39	0.56	0.32	0.37	0.45
1, 2, 3	0.43	0.67	0.38	0.41	0.51
1, 2, 3, 4	0.45	0.71	0.45	0.49	0.60

The forecast scheme showed considerable stability between time periods, and therefore, it was decided that for real-time forecasts of post-1 August NTC in 2006 and in

future years, equations from 1949-2005 would be used. Table 5.3 displays the stepwise regression technique for 1949-2005 using equations developed over the full period (e.g., 1949-2005). Also, the skill of the independent dataset from 1900-1948 and over the full period (1900-2005) is evaluated using equations developed from 1949-2005. Note that the skill over the 1900-1948 time period improves slightly using the equations developed over the longer period (e.g., 1949-2005 compared with 1949-1989).

Table 5.3: Stepwise regression technique showing the improvement in variance explained for NTC with the addition of predictors to the August forecast scheme for seasonal Atlantic basin hurricane activity from 1949-2005, 1900-1948 and 1900-2005, respectively. The variance explained values are calculated based on equations developed over 1949-2005. Predictor numbers are the same as in Table 5.1.

Predictor	1949-2005 (r^2) (57 Years)	1900-1948 (r^2) (49 Years)	1900-2005 (r^2) (106 Years)
1	0.25	0.23	0.32
1, 2	0.38	0.34	0.47
1, 2, 3	0.43	0.39	0.53
1, 2, 3, 4	0.52	0.47	0.63

When evaluating the hindcast skill of the equations developed over the 1949-2005 period, it is encouraging to note that the variance explained over the independent dataset from 1900-1948 shows similar levels of variance explained (47% (1900-1948)) compared with 52% (1949-2005) in the dependent dataset. This level of forecast degradation is slightly less than would be expected from jackknife or cross-validation regression techniques (Elsner and Schmertmann 1994). In a cross-validation exercise, the year that is being hindcast is omitted from the development dataset. This exercise is generally considered to provide an upper-bound on likely real-time forecast skill for the statistical scheme. When cross-validation is applied to the 1949-2005 dependent dataset, the

variance explained over the period is 42%, which is smaller than the variance explained in the earlier independent dataset. This adds increased confidence that this forecast scheme is quite stable between time periods and should be reasonably skillful in the future. The prediction scheme shows remarkable skill over the entire time period (1900-2005), explaining 63% of the variance in NTC activity over the past 106 years.

Figure 5.4 displays a time series of post-1 August NTC hindcasts compared with observed post-1 August NTC from 1949-2005. Note that the hindcasts generally follow the observations quite closely, as evidenced by the 52% variance explained over the 1949-2005 time period.

Table 5.4 displays the individual correlations between each predictor and post-1 August NTC for the dependent dataset of 1949-2005 and the independent dataset of 1900-1948. The statistical significance of each predictor is tested using a two-tailed Student's t-test. Although several of these predictors had already been known to be related to upcoming hurricane activity, it was decided to use a two-tailed Student's t-test in order to be conservative with statistical significance estimates.

For the 1949-2005 time period, a correlation of 0.26 is required for 95% significance and a correlation of 0.34 is required for 99% significance. For the 1900-1948 time period, a correlation of 0.28 is required for 95% significance and a correlation of 0.37 is required for 99% significance. All correlations are significant at the 95% level except for the Nino3 index from 1900-1948. However, this correlation is just slightly below the 95% level, and it has been well-documented that ENSO effects Atlantic hurricane activity (Gray 1984a; Goldenberg and Shapiro 1996; Klotzbach and Gray 2004). In addition, the quality of sea surface temperature data prior to 1949 is somewhat

suspect, especially in data void regions such as Nino3. In earlier-period SST datasets such as the Hadley SST dataset during the period 1900-1948, EOF analysis was used to spatially smooth data, and therefore, some of the predictive signal may have been lost in the smoothing. The stability of the correlations in both dependent and independent datasets gives us increased confidence in the use of these predictors in the forecast scheme.

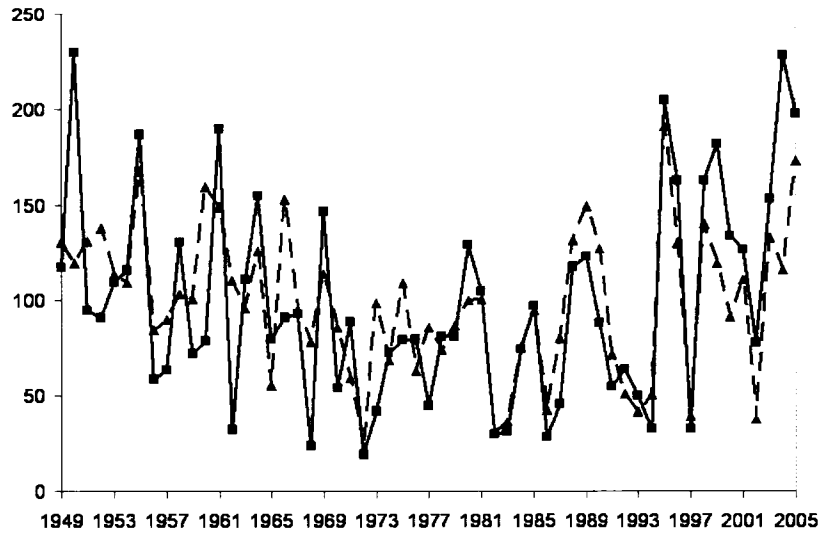

Figure 5.4: Observed post-1 August NTC (solid line) versus hindcast post-1 August NTC (dashed line) for 1949-2005. Non-jackknifed variance explained (r^2) is 0.52. Figure taken from Klotzbach (2007b).

Table 5.5 displays the inter-correlations between the four predictors over the dependent dataset from 1949-2005, while Table 5.6 displays these inter-correlations over the independent dataset from 1900-1948. All correlations are below r = |0.4| ($r^2 < 0.16$). There is a marginally significant (90% level) negative correlation between the subtropical Atlantic SST and tropical Atlantic SLP predictor over both time periods (1949-2005 and

1900-1948). This is to be expected, as higher sea level pressure values indicate stronger trade winds, driving more upwelling and cooling sea surface temperatures. However, the location of these two predictors is such that they are only weakly positive correlated, and there is considerable additional information added by considering both predictors. The inter-correlations between individual predictors tend to be fairly stable between the two time periods. Having predictors that are mostly independent of each other is important, because this implies that new independent information is being added to the scheme with the addition of another predictor. The independence of these predictors is not surprising, as it has already been noted that each predictor added at least an additional two percent to the variance explained in the forecast scheme.

Table 5.4: Correlations between individual predictors and post-1 August NTC for 1900-1948 and 1949-2005. Correlations significant at the 95% level for a two-tailed Student's t test are italicized while correlations significant at the 99% level are bold-faced. Predictor numbers are the same as in Table 5.1.

Predictor	1900-1948 (r)	1949-2005 (r)
1	**0.48**	**0.50**
2	**-0.46**	**-0.49**
3	-0.25	*-0.33*
4	**0.56**	**0.39**

Table 5.5: Inter-correlations between predictors over the dependent dataset from 1949-2005. Predictor numbers are the same as in Table 5.1.

Predictor	1	2	3	4
1	___	-0.28	0.02	0.14
2	-0.28	___	0.36	-0.17
3	0.02	0.36	___	0.01
4	0.14	-0.17	0.01	___

Table 5.6: Inter-correlations between predictors over the independent dataset from 1900-1948. Predictor numbers are the same as in Table 5.1.

Predictor	1	2	3	4
1	___	-0.32	-0.02	0.32
2	-0.32	___	0.04	-0.36
3	-0.02	0.04	___	-0.21
4	0.32	-0.36	-0.21	___

As was briefly mentioned earlier, the forecast scheme works quite well on independent data as well. Using the exact same equations as were used from 1949-2005, 47 percent of the variance is explained over the 1900-1948 time period. It is interesting to note that NTC values are over-forecast considerably during the first part of the 20th century. The mean for observed NTC from 1900-1948 is 68, while the mean for predicted NTC from 1900-1948 is 97 based on equations developed on 1949-2005. This is likely due to the fact that the observational network during the first part of the 20th century missed several tropical cyclones each year, especially systems that formed and dissipated over the open Atlantic, as noted in Landsea (2007). Therefore, observed NTC values during the first part of the 20th century are most likely under-estimated somewhat.

Equations for the 1900-1948 time period using data for that same time period are then developed. In a sense, this is making the earlier period also a hindcast dataset. The variance explained only increases slightly when this is done (improves r^2 from 47 percent to 51 percent), but it removes any NTC over- or under-estimate, since the equations are now trained to the earlier-period dataset. Figure 5.5 displays a time series of post-1 August NTC hindcasts compared with observed post-1 August NTC from 1900-1948 using these new equations.

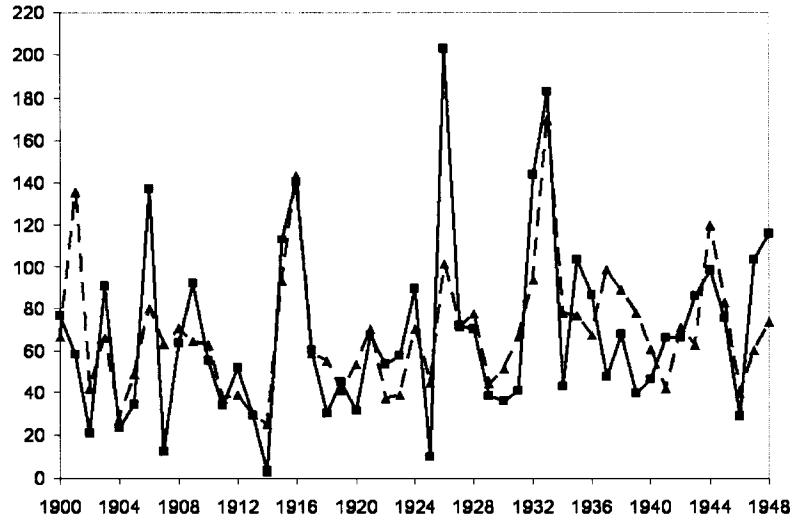

Figure 5.5: Observed post-1 August NTC (solid line) versus hindcast post-1 August NTC (dashed line) for 1900-1948. Non-jackknifed variance explained (r^2) is 0.51.

The stability of the forecast scheme and the stability of the individual correlations between predictors and post-1 August NTC gives increased confidence that this forecast scheme will likely have long-term stability. The next section discusses the likely physical relationships between individual predictors and Atlantic basin hurricane activity.

5.5 Physical links between August predictors and seasonal Atlantic basin TC activity

One method to better understand physical relationships between predictors and Atlantic basin hurricane activity is to use the NCEP/NCAR reanalysis correlations webpage (http://www.cdc.noaa.gov/Correlation). For example, using this webpage, a user can correlate a predictor field, for example tropical Atlantic sea surface temperatures in June and July, and see how that field correlates with Atlantic basin NTC. Since these predictors occur just before the start of the busy part of the hurricane season, it is somewhat easier to tie them physically to the Atlantic basin hurricane season than some

earlier season predictors. I now discuss the hypothesized physical relationships between each individual predictor and post 1-August Atlantic basin hurricane activity.

a. Predictor 1. June-July SST in the Northeastern Subtropical Atlantic (+)

Warm sea surface temperatures in this area in June-July correlate very strongly with anomalously warm sea surface temperatures in the tropical Atlantic throughout the upcoming hurricane season. Anomalously warm sea surface temperatures are important for development and intensification of tropical cyclones by infusing more latent heat into the system (Shapiro and Goldenberg 1998). Warmer SSTs reduce static stability which weakens subsidence associated with the subtropical high and consequently reduces trade winds during the remainder of the season (e.g., Namias 1973). Weaker trade winds cause less evaporation and upwelling of the sea surface which therefore feeds back into keeping the tropical Atlantic warm. In addition, weaker trade winds imply that there is less vertical wind shear across the tropical Atlantic. Weak wind shear is favorable for tropical cyclone development and intensification (Gray 1968; Goldenberg and Shapiro 1996; Knaff et al. 2004). Lastly, there is a strong positive correlation ($r \sim 0.5$) between anomalously warm June-July SSTs in the subtropical northeastern Atlantic and low sea level pressures in the tropical Atlantic and Caribbean basin during the heart of the hurricane season (August-October). Low sea level pressures imply decreased subsidence and enhanced mid-level moisture. Both of these conditions are favorable for tropical cyclogenesis and intensification (Knaff 1997).

b. Predictor 2. June-July SLP in the Tropical Atlantic (-)

Low sea level pressure in the tropical Atlantic in June-July implies that early summer conditions in the tropical Atlantic are favorable for an active tropical cyclone season with increased vertical motion, decreased stability and enhanced mid-level moisture. There is a strong auto-correlation ($r > 0.5$) between June-July sea level pressure anomalies and August-October sea level pressure anomalies in the tropical Atlantic. Low sea level pressure in the tropical Atlantic also correlates quite strongly ($r > 0.5$) with reduced trade winds (weaker easterlies) and anomalously easterly upper-level winds (weaker westerlies). The combination of these two features implies weaker vertical wind shear and therefore more favorable conditions for tropical cyclone development in the Atlantic (Gray 1968; Goldenberg and Shapiro 1996). In addition, lower-than-normal sea level pressure usually indicates more mid-level moisture which is an important ingredient for tropical cyclone genesis and intensification (Gray 1968).

c. Predictor 3. June-July Nino3 Index (-)

Cool sea surface temperatures in the Nino3 region during June-July imply that a La Niña event is currently present. In general, positive or negative anomalies in the Nino3 region during the early summer persist throughout the remainder of the summer and fall. El Niño conditions shift the center of the Walker Circulation eastward which causes increased convection over the central and eastern tropical Pacific. This increased convection in the central and eastern Pacific manifests itself in anomalous upper-level westerlies across the Caribbean and tropical Atlantic, thereby increasing vertical wind shear and reducing Atlantic basin hurricane activity. The relationship between ENSO

and Atlantic hurricane activity has been well-documented in the literature (e.g., Gray 1984a; Goldenberg and Shapiro 1996; Elsner 2003; Bell and Chelliah 2006).

d. Predictor 4. Named Storm Days South of 23.5°N, East of 75°W (+)

Most years do not have named storm formations in June and July in the tropical Atlantic; however, if tropical Atlantic formations do occur, it indicates that an active hurricane season is likely to occur. For example, the six years with the most named storm days in the deep tropics in June and July (since 1949) are 1966, 1969, 1995, 1996, 1998 and 2005. All six of these seasons were very active. When storms form in the deep tropics in the early part of the hurricane season, it indicates that conditions are already very favorable for TC development. In general, the start of the hurricane season is restricted by thermodynamics (warm SSTs, unstable lapse rates, mid-level moisture) (DeMaria et al. 2001), and therefore deep tropical activity early in the hurricane season implies that the thermodynamics in the tropical Atlantic are already quite favorable for TC development. Also, this predictor's correlation with seasonal NTC is 0.39 over the 1949-2005 period, and when tested on independent data (1900-1948), the correlation actually improves to 0.56, which gives increased confidence in its use as a seasonal predictor.

5.6 August prediction – U.S. landfalling TC relationships

It has been shown in previous forecast papers and in previous chapters of this manuscript that there is a strong relationship between hindcast values of NTC and United States landfalling tropical cyclones (Klotzbach and Gray 2003; Blake and Gray 2004; Klotzbach and Gray 2004). These relationships are usually strongest for major

hurricanes, which are the storms that are of greatest importance. Major hurricanes, although accounting for only 20-25% of all named storms, do approximately 80-85% of the total economic damage when normalized by population, inflation and wealth per capita (Pielke and Landsea 1998). The relationship between landfalling tropical cyclones after 1 August and hindcast values of post 1-August NTC is quite significant. For example, using the hindcast equations developed over the 1949-2005 period, in the 10 years from 1949-2005 where the largest values of NTC were hindcast, 23 hurricanes made United States landfall after 1 August compared with only 9 hurricanes in the 10 years with the lowest hindcast NTC values; a ratio of greater than 2.5 to 1. Eight major hurricanes made landfall in the top 5 hindcasts compared with only one major hurricane in the 5 lowest hindcasts. Table 5.7 displays landfalling named storms, hurricanes and major hurricanes for the East Coast (EC), the Gulf Coast (GC) and United States coastline for the top 5 – bottom 5, top 10 – bottom 10 and top 15 – bottom 15 NTC hindcast values from 1949-2005. For reference, the East Coast/Gulf Coast breakdown for landfalling storms is approximately 100 miles north of Tampa, Florida. Storms making landfall in SW Florida including the Florida Keys are counted as East Coast storms in this analysis. The breakdown of the coastline was done this way, because, in general, storms making landfall along the Florida Panhandle and westward tend to have their genesis in the Gulf of Mexico, while storms in SW Florida and eastward tend to have their genesis in the North Atlantic.

To provide a visualization of some of the significant differences between storms making landfall in high and low NTC hindcast years, Figure 5.6 displays East Coast landfalling hurricanes for the top 10 and bottom 10 NTC hindcast years. Thirteen storms

made landfall in the top 10 NTC hindcast years compared with only four storms in the bottom 10 NTC hindcast years.

These ratios become even stronger in the independent dataset from 1900-1948. The equations developed on 1949-2005 were used to predict NTC activity from 1900-1948, and then seasons from 1900-1948 were ranked using these predictions. Twenty-six hurricanes made landfall in the top 10 predicted NTC years compared with only 10 hurricanes in the 10 lowest years. Also, 15 major hurricanes made landfall in the top 10 predicted NTC years compared with only 2 major hurricanes in the 10 lowest years.

It is clear from these significant ratios that the use of NTC predictions certainly has the potential to add skill to landfall probabilities beyond that specified by climatology. These NTC predictions will be integrated into the landfall probability forecasts issued by the TMP.

5.7 Summary

A significant amount of skill has been demonstrated using a simple hurricane prediction scheme that uses only four predictors to forecast hurricane activity after 1 August. This scheme not only showed skill on a dependent dataset of 1949-1989 but also shows nearly equivalent levels of skill during an earlier period from 1900-1948 and during a more recent period from 1990-2005. In addition, an independent forecast for the 2006 hurricane season called for a post-1 August forecast NTC of 88, which is quite close to the observed value of 80 that occurred after 1 August. Since this scheme showed considerable stability over an 106-year period, it likely will show similar amounts of skill in the future.

Table 5.7: Number and ratio of landfalling named storms, hurricanes and major hurricanes for the US, the East Coast (EC), and the Gulf Coast (GC) for the top 5 and bottom 5, the top 10 and bottom 10 and the top 15 and bottom 15 post 1-August NTC hindcast years from 1949-2005.

Hindcast Landfall Occurrences	US NS	US H	US IH	EC NS	EC H	EC IH	GC NS	GC H	GC IH
Top 5	18	14	8	11	9	5	7	5	3
Bottom 5	13	3	1	5	0	0	8	3	1
Ratio (as percentage)	138	467	800	220	n/a	n/a	88	167	300
Top 10	35	23	10	18	13	6	17	10	4
Bottom 10	23	9	6	12	4	3	11	5	3
Ratio (as percentage)	152	256	167	150	325	200	155	200	133
Top 15	46	28	12	25	16	8	21	12	4
Bottom 15	33	15	7	18	7	3	15	8	4
Ratio (as percentage)	139	187	171	139	229	267	140	150	100

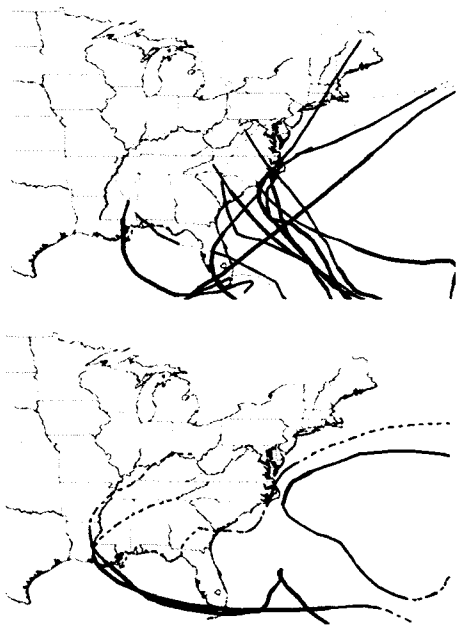

Figure 5.6: Hurricanes making landfall along the East Coast of the United States in the top 10 and bottom 10 NTC hindcast years from 1949-2005. Dotted lines represent tropical storm strength, thin solid lines represent hurricane strength and thick solid lines represent major hurricane strength. Figure taken from Klotzbach (2007b).

Chapter 6
Sub-seasonal prediction developments

This chapter focuses on developments in sub-seasonal prediction by the TMP. The TMP currently issues predictions for the individual months of August, September and October. Full documentation of the August-only scheme is provided in a project report by Eric Blake (Blake 2002) and in Blake and Gray (2004), while full documentation of the September-only scheme is provided in a project report by Klotzbach (Klotzbach 2002) and in Klotzbach and Gray (2003). The October-only forecast scheme has been discussed in various forecast publications. Since the August-only and September-only forecasts have already been discussed extensively in project reports and in the peer-reviewed literature, they will be described briefly, while the remainder of the chapter will focus on the October-only forecast.

6.1 Sub-seasonal prediction background and motivation

While seasonal predictions have been issued by the TMP since 1984, sub-seasonal forecasts were not issued until the early August forecast release in 2000 (Gray et al. 2000a). Included in this seasonal forecast update was the first-ever monthly forecast for August. The primary motivation for issuing sub-seasonal forecasts was that hindcast skill for an August-only forecast was comparable to that obtained for seasonal forecasts (Blake

2002; Blake and Gray 2004). Following the considerable hindcast skill shown with the August-only forecast, additional monthly forecasts were developed for September (Klotzbach 2002; Klotzbach and Gray 2004) and October (Gray and Klotzbach 2003).

Sub-seasonal forecasts are important because active seasons can have inactive months and inactive seasons can have active months. The 2005 season was quite rare in that it witnessed well above-average activity in all three months of August, September and October. More common are seasons like 2004 and 2006. In 2004, one of the most active seasons on record, August and September had activity at well above-average and near-record levels, respectively, while October recorded below-average activity, likely due to a late developing El Niño event (Klotzbach and Gray 2006a). Slightly below-average activity occurred during the 2006 season. August and October both witnessed activity at well below-average levels, while activity in September was somewhat above-average. Based on this evidence over the past few years, it is clear that sub-seasonal forecasts are quite important, and in the next few sections, I examine the August-only, September-only and October-only forecasts in more detail.

6.2 August monthly forecast

The August-only monthly forecast was developed by Eric Blake who was an M.S. student at CSU from 1998-2002. His pioneering research in sub-seasonal forecasting indicated that comparable hindcast skill to that shown for seasonal forecasts could be achieved for the prediction of August monthly activity by the start of the month. A total of twelve predictors were selected from the NCEP/NCAR reanalysis that showed hindcast skill over the 1949-1999 period. Blake found that a combination of four to five predictors for each predictand (i.e., named storms, named storm days, hurricanes, etc.)

led to cross-validated hindcast skill over the 1949-1999 period of approximately 40-70 percent. Table 6.1 describes the locations of these predictors, while Figure 6.1 displays the locations of the predictors utilized in the August-only forecast scheme. Full description of the methodology used to develop the scheme and additional information on the predictors is available in Blake (2002) and Blake and Gray (2004).

Table 6.1: Location of predictors utilized in the August-only forecast scheme for Atlantic basin hurricane activity. The sign of the predictor associated with increased Atlantic basin tropical cyclone activity is in parentheses.

Predictor Number	Predictor Name	Location
1	July Galapagos 200 mb V (-)	(4°S-8°N, 105°-79°W)
2	July Bering Sea SLP (-)	(47°-62°N, 156°E-164°W)
3	July Atlantic Ocean SLP (-)	(25°-37.5°N, 47.5°-25°W)
4	July SE Pacific 200 mb U (-)	(40°-35°S, 110°-85°W)
5	July S. Indian Ocean 500 mb Ht. (-)	(42.5°-27.5°S, 72.5°-95°E)
6	July Coral Sea 200 mb U (+)	(17.5°-7.5°S, 145°E-180°)
7	July Galapagos 200 mb U (-)	(5°S-5°N, 110°-85°W)
8	June North Greenland 200 mb U (+)	(80°-85°N, 45°W-10°E)
9	June Northwest Pacific SLP (+)	(18°-30°N, 134°-154°E)
10	April South Atlantic Ocean SLP (-)	(10°S-5°N, 35°W-15°E)
11	February Scandinavia SLP (-)	(52.5°-75°N, 5°W-35°E)
12	January Southwest United States SLP (-)	(30°-40°N, 110°-95°W)

August-only forecasts have been issued in real-time over the past seven years (2000-2006). These forecasts have shown moderate skill when compared with climatology. Table 6.2 displays the final August-only forecast for NTC activity

compared with a climatology NTC activity forecast and observed August-only NTC values. August-only forecasts have improved upon a climatological forecast in five of the seven years that forecasts have been issued, and August-only forecasts have also had a slightly smaller average error than a climatological forecast when evaluated over the full seven-year period. If the 2006 forecast bust is excluded from the dataset, the average August forecast error was approximately 20% less than the forecast error using climatology.

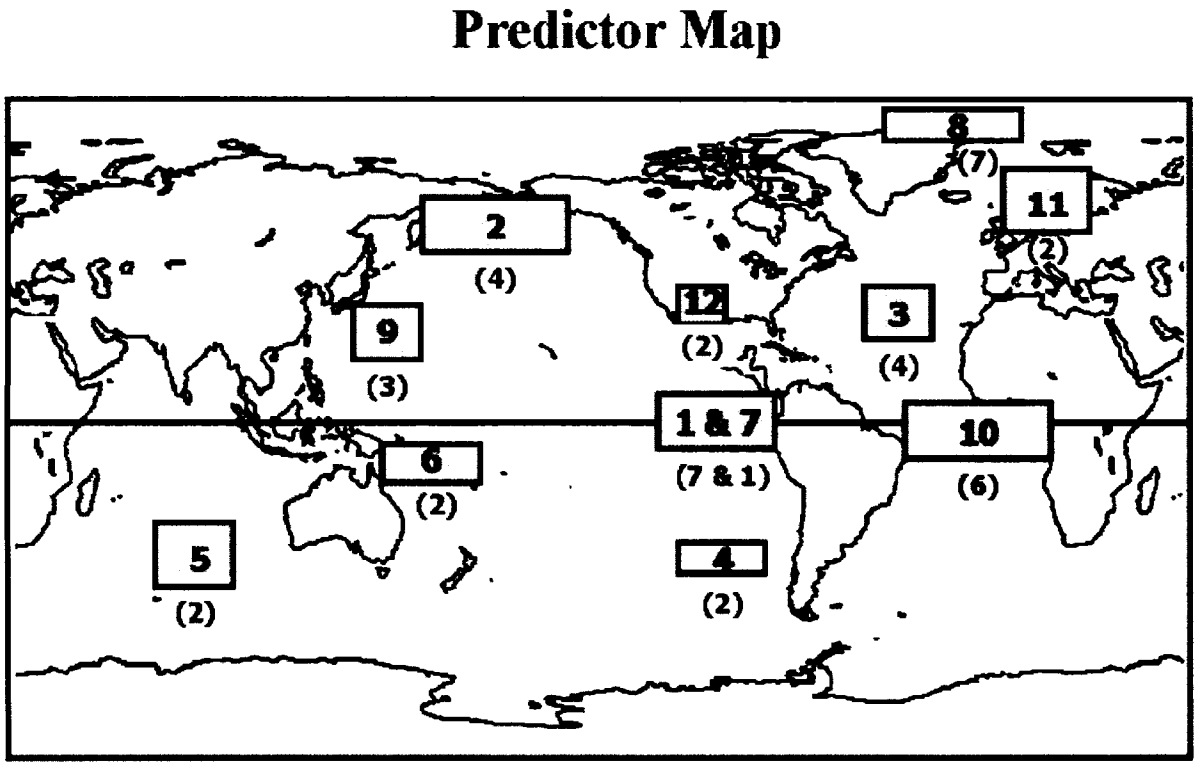

Figure 6.1: Global map showing locations of August-only tropical cyclone predictors. Table 6.1 provides a listing and description of these predictors. The numbers in the boxes are keyed to the description in Table 6.1. The numbers in parentheses beneath each box indicate how many predictive equations are used for each predictor. Figure taken from Blake and Gray (2004).

Table 6.2: Real-time August-only NTC prediction, observed August-only NTC values, difference between a real-time prediction and the August-only NTC observation, and difference between a forecast of climatology and the August-only NTC observation. For reference, a climatological value of August-only NTC is 26, based on data from 1949-1999.

Year	Real-Time August-only NTC Prediction	Observed August-only NTC	Difference (Forecast – Observation)	Difference (Climatology – Observation)
2000	33	42	-9	16
2001	22	9	13	-17
2002	18	7	11	-19
2003	22	26	-4	0
2004	35	89	-54	63
2005	50	41	9	15
2006	50	12	38	-14
Average Difference			**|19.7|**	**|20.6|**

The August-only statistical forecast currently utilizes a total of twelve predictors and attempts to hindcast individual seasonal activity metrics such as named storms, named storm days, hurricanes, etc. In the next couple of years, I intend to update the August-only statistical forecast to utilize predictors only from the two months immediately prior to the forecast issue date (i.e., June-July data), and as is currently done for the seasonal forecasts, only NTC activity will be predicted. I also intend to develop the forecast scheme over a dependent dataset (1950-1989) and then test the scheme on recent independent data (1990-2004) as well as on earlier independent data (1900-1949), in a manner similar to what was done with the early August seasonal forecast.

6.3 September monthly forecast

The September-only monthly forecast was developed by the author while an M.S. student at CSU from 2000-2002. The September-only monthly forecast showed comparable hindcast skill to that obtained for the August-only forecast scheme (i.e., 30-

70 percent of the cross-validated variance explained over the developmental dataset from 1950-2000). An initial September-only monthly forecast was issued in early August with an update provided in early September in 2002 (Gray et al. 2002b). A total of seven predictors were utilized for the September-only forecast issued in early August, with a total of nine predictors utilized in the early September update. The same seven predictors utilized in the early August prediction for September monthly activity are utilized in the early September prediction, along with two additional August sea level pressure predictors. Table 6.3 describes the locations of the nine predictors utilized in the early September update of the September-only forecast scheme, while Figure 6.2 displays the locations of the predictors utilized in the early September update of the September-only forecast scheme. A full description of the predictors utilized in this scheme is available in Klotzbach (2002) and Klotzbach and Gray (2003).

September-only forecasts have been issued in real-time over the past five years (2002-2006). As was evident with the August-only forecast, these forecasts have also shown moderate skill when compared with climatology. Table 6.4 displays the early September prediction of September-only NTC activity compared with a climatological NTC activity forecast and observed September-only NTC values. September-only forecasts have improved upon a climatological forecast in four of the five years that forecasts have been issued, and the average September forecast error was approximately 28% less than the forecast error using climatology.

As was the case with the August-only forecast, the September-only statistical forecast attempts to hindcast individual seasonal activity metrics such as named storms, named storm days, hurricanes, etc. In the next couple of years, I intend to update the

September-only statistical forecast to utilize predictors only from the two months immediately prior to the forecast issue date (i.e., June-July data), and as is currently done for the seasonal forecasts, only NTC activity will be predicted. I also intend to develop the forecast scheme over a dependent dataset (1950-1989) and then test the scheme on recent independent data (1990-2004) as well as on earlier independent data (1900-1949), in a manner similar to what was done with the early August seasonal forecast.

Table 6.3: Location of predictors utilized in the early September prediction of September-only Atlantic basin hurricane activity. The sign of the predictor associated with increased Atlantic basin tropical cyclone activity is in parentheses.

Predictor Number	Predictor Name	Location
1	April South Atlantic 1000 mb U (-)	(30°-12.5°S, 40°-10°E)
2	July Asian 200 mb Ht. (+)	(32°-42°N, 100°-160°E)
3	July-August 1000 mb U (+) (-)	(5°-15°N, 30°-50°W) – (22.5°-35°N, 35°-65°W)
4	February West Africa 1000 mb U (-)	(20°-30°N, 15°W-15°E)
5	April NE Siberia 200 mb U (-)	(67.5°-85°N, 110°-180°E)
6	August Indonesia SLP (-)	(30°-0°S, 120°-160°E)
7	August South Indian Ocean SLP (-)	(45°-20°S, 60°-90°E)
8	May Central Africa 200 mb V (+)	(20°S-0°, 15°-30°E)
9	January-February West Pacific 200 mb U (-)	(15°-25°N, 120°E-160°W)

6.4 October monthly forecast overview

The October-only monthly forecast made its debut with the 2003 hurricane season forecasts (Gray and Klotzbach 2003b). Since that time, October-only forecasts have been issued with each August seasonal forecast. These forecasts are then updated in early

September and early October, to take into account trends in various atmospheric/oceanic parameters. Unlike the August-only forecast and September-only forecasts, only the NTC index was hindcast with the October-only forecast scheme, resulting in a statistical prediction scheme with fewer predictors.

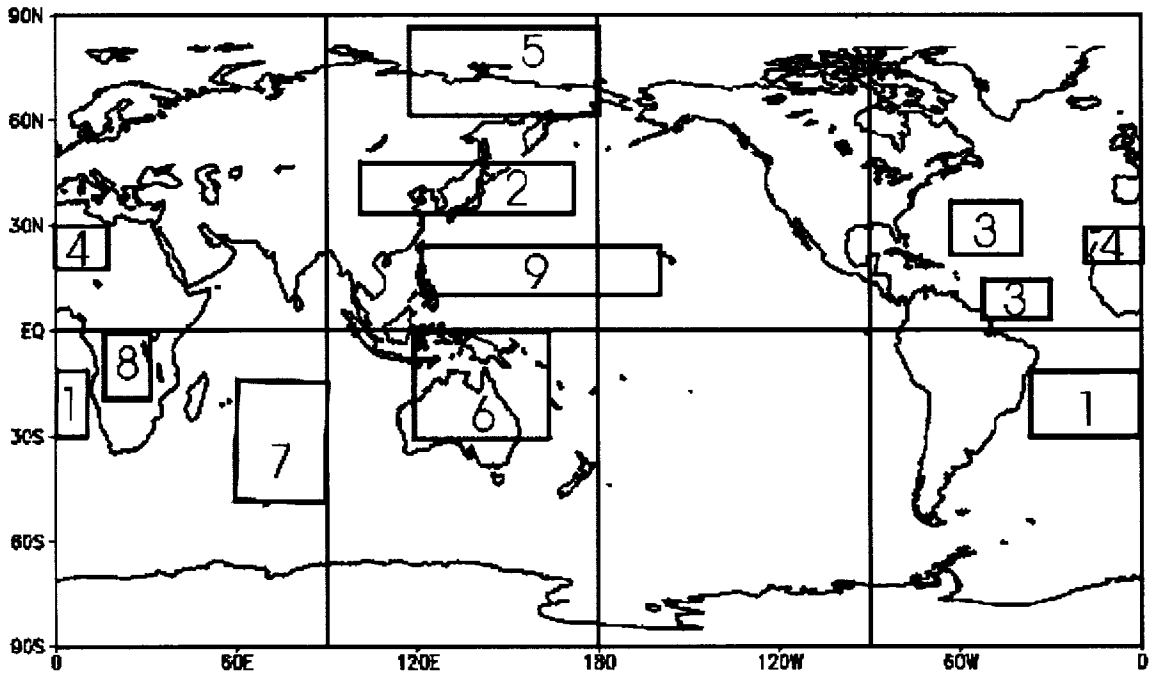

Figure 6.2: Global map showing locations of early September predictors for September-only tropical cyclone activity. Table 6.3 provides a listing and description of these predictors. The numbers in the boxes are keyed to the description in Table 6.3. Figure taken from Klotzbach and Gray (2003).

Table 6.4: Real-time September-only NTC prediction, observed September-only NTC values, difference between a real-time prediction and the September-only NTC observation, and difference between a forecast of climatology and the September-only NTC observation. For reference, a climatological value of September-only NTC is 48, based on data from 1949-1999.

Year	Real-Time September-only NTC Prediction	Observed September-only NTC	Difference (Forecast – Observation)	Difference (Climatology – Observation)
2002	26	56	-30	-8
2003	55	95	-40	-47
2004	85	131	-46	-83
2005	80	72	8	-24
2006	59	63	-4	-15
Average Difference			**|25.6|**	**|35.4|**

6.5 Early August prediction of October Atlantic basin hurricane activity

Based on data for the 1950-2001 period, approximately 50 percent of the cross-validated variance in October-only NTC activity could be explained over the 1950-2001 development period by the early August prediction. A total of four predictors were utilized to make this prediction. As was done with the August-only and September-only prediction schemes, the October-only predictors were selected from the NCEP/NCAR reanalysis. These predictors are listed in Table 6.5 and displayed in Figure 6.3.

A brief discussion of how each of the four predictors likely effects October Atlantic basin tropical cyclone activity follows:

a. Predictor 1: June-July SLP in the tropical Atlantic (-):

Low sea level pressure in June-July in this part of the subtropical Atlantic is the most important predictor for October tropical cyclone activity. Low pressure indicates that a weak subtropical ridge is present, trade winds are weaker, and consequently, due to

evaporation decreases, the tropical Atlantic is warmer than normal. On a climatological average, tropospheric vertical wind shear and sea level pressure are directly related. Lower than normal sea level pressure indicates that late-season tropical cyclones are more likely to occur due to a combination of reduced wind shear and a warm tropical Atlantic.

Table 6.5. Location of predictors utilized in the early August prediction of October-only Atlantic basin hurricane activity. The sign of the predictor associated with increased Atlantic basin tropical cyclone activity is in parentheses.

Predictor Number	Predictor Name	Location
1	Tropical Atlantic June-July SLP (-)	(10°-25°N, 40°-10°W)
2	Subtropical Atlantic July 200 mb Ht. (+)	(20°-35°N, 45°-5°W)
3	South Pacific July 200 mb U (+)	(47.5°-35°S, 160°E-160°W)
4	NW North America Previous November SLP (-)	(45°-65°N, 145°-115°W)

b. Predictor 2: July 200 mb geopotential height in the subtropical Atlantic (+):

High heights in the northern subtropical Atlantic indicate that there is an increased height gradient between the tropical and subtropical Atlantic which decreases the area and strength of upper-level westerly winds. Anomalous easterlies at upper levels tend to persist throughout the remainder of the hurricane season thereby reducing vertical wind shear and providing more favorable conditions for October tropical cyclone development.

c. Predictor 3: July South Pacific 200 mb U (+):

Increased upper-level westerlies near New Zealand indicate increased Southern Hemisphere winter baroclinicity which is typically associated with favorable conditions

for tropical cyclones in the Atlantic. These conditions tend to persist through October, increasing the likelihood of late-season tropical cyclones.

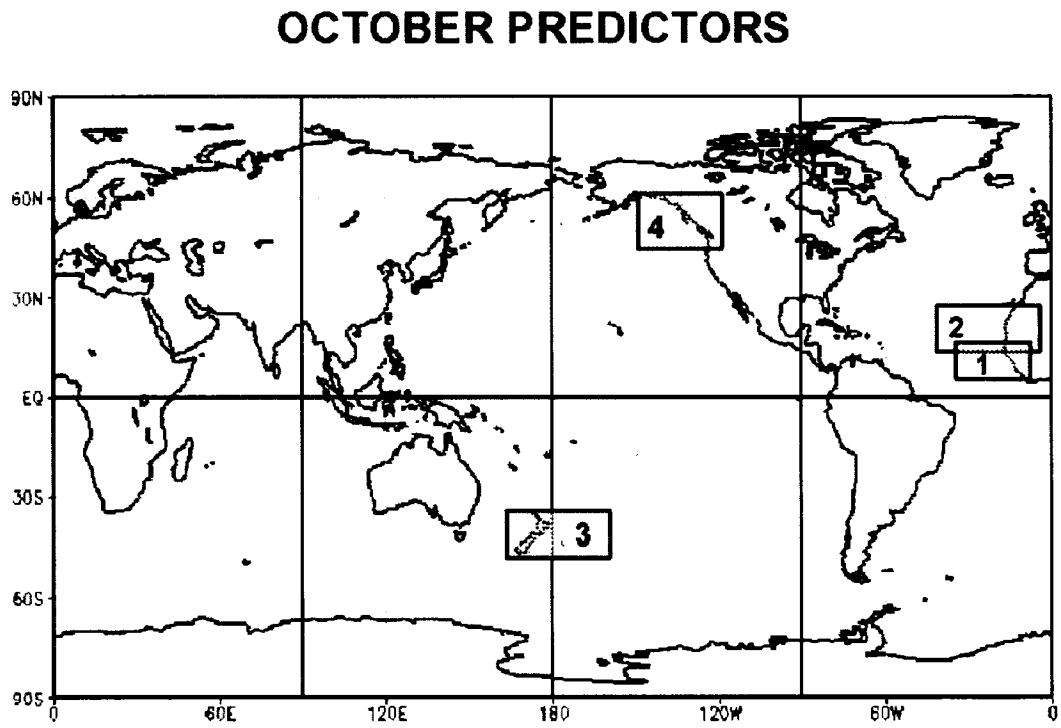

Figure 6.3: Global map showing locations of early August predictors for October-only tropical cyclone activity.

d. Predictor 4: Previous November Northwest North America SLP (-):

Low sea level pressure in this area during November of the previous year implies a deeper and eastward-shifted Aleutian Low which is typical of a positive Pacific North American Pattern (PNA). A positive PNA is frequently associated with the final year of warm ENSO conditions (Horel and Wallace 1981) and therefore, a return to cooler conditions in the eastern tropical Pacific during the following year. Cool ENSO conditions provide a favorable environment for the development of October tropical cyclones.

6.6 Early September prediction of October Atlantic basin hurricane activity

An update to the October-only monthly forecast has been issued in early September for each season since 2003. By including August NCEP/NCAR reanalysis data in the prediction scheme, cross-validated variance explained over the 1950-2001 period improves from 50% in early August to 60% in early September. This is to be expected, since as the month being predicted is approached, one is likely to have a better idea of how the atmosphere and ocean are interacting. The early September prediction of October-only activity uses one of the same predictors that was utilized in the early August prediction of October-only activity (the previous November SLP values in northwest North America), while two other predictor simply use a two-month average and a slightly different location than was used in early August (the South Pacific 200 mb U and tropical/subtropical Atlantic sea level pressure). The fourth predictor measures sea surface temperatures in the North Pacific. The four predictors utilized in the early September prediction of October-only activity are listed in Table 6.6 and displayed in Figure 6.4.

A brief discussion of how the sea surface temperatures in the North Pacific are thought to affect October-only tropical cyclone activity follows:

d. Predictor 4: August North Pacific SST (+):

Warm waters in the Pacific Ocean south of Japan are well-linked to a cold Pacific Decadal Oscillation (PDO). In general, a cold PDO is associated with blocking over the central Pacific and low pressure and reduced wind shear over the tropical Atlantic.

Table 6.6: Location of predictors utilized in the early September prediction of October-only Atlantic basin hurricane activity. The sign of the predictor associated with increased Atlantic basin tropical cyclone activity is in parentheses.

Predictor Number	Predictor Name	Location
1	July-August Subtropical Atlantic SLP (-)	(12.5°-27.5°N, 45°-15°W)
2	July-August South Pacific 200 mb U (+)	(47.5°-35°S, 160°E-155°W)
3	Previous November NW North America SLP (-)	(45°-65°N, 145°-115°W)
4	August North Pacific SST (+)	(22.5°-35°N, 120°-150°E)

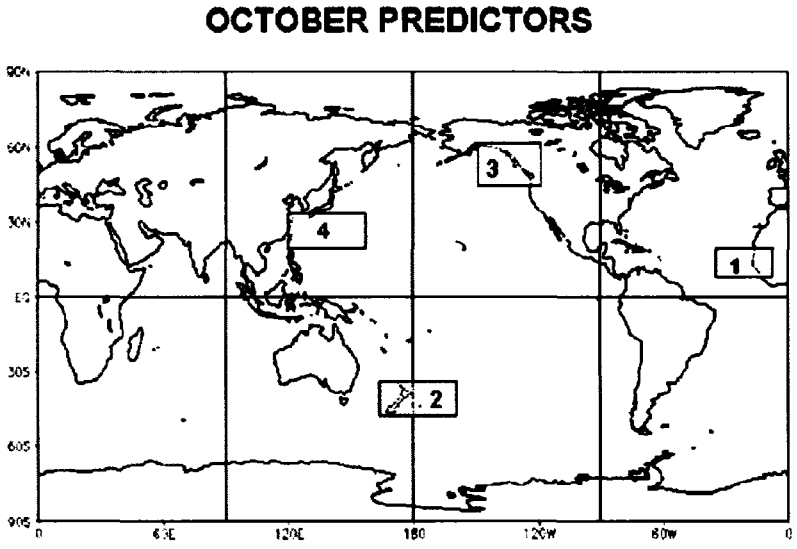

Figure 6.4: Global map showing locations of early September predictors for October-only tropical cyclone activity.

6.7 Early October prediction of October Atlantic basin hurricane activity

A final update to the October-only monthly forecast has been issued in early October for each season since 2003. One predictor is added to the four-predictor pool consulted in the early September prediction scheme for October-only activity. The

inclusion of this additional predictor (200 mb zonal winds in the South Atlantic) increases cross-validated variance explained over the 1950-2001 period from 60% in early September to 64% in early October. All four other predictors are the same as are used in the early September prediction of October-only activity. The five predictors utilized in the early October prediction of October-only activity are listed in Table 6.7 and displayed Figure 6.5.

A brief discussion of how 200 mb zonal winds in the South Atlantic are thought to affect October-only tropical cyclone activity follows:

e. Predictor 5: September South Atlantic 200 mb U (+):

Increased westerlies throughout the Southern Hemisphere are commonly associated with active years in the tropical Atlantic. Heightened winter baroclinicity off the coast of Brazil is typically seen during years with reduced wind shear over the tropical Atlantic.

6.8 October Atlantic basin hurricane activity forecast verification

October-only forecasts have been issued in real-time for the past four years (2003-2006). As was seen with the August-only and September-only schemes, these forecasts have shown moderate skill when compared with climatology. Table 6.8 displays the final October-only forecast for NTC activity issued in early October compared with a climatological NTC activity forecast and observed October-only NTC values. October-only forecasts have improved upon a climatological forecast in three of the four years that

forecasts have been issued, and the average October forecast error is approximately 20% less than the forecast error using climatology.

Table 6.7: Location of predictors utilized in the early October prediction of October-only Atlantic basin hurricane activity. The sign of the predictor associated with increased Atlantic basin tropical cyclone activity is in parentheses.

Predictor Number	Predictor Name	Location
1	July-August Subtropical Atlantic SLP (-)	(12.5°-27.5°N, 45°-15°W)
2	July-August South Pacific 200 mb U (+)	(47.5°-35°S, 160°E-155°W)
3	Previous November NW North America SLP (-)	(45°-65°N, 145°-115°W)
4	August North Pacific SST (+)	(22.5°-35°N, 120°-150°E)
5	September South Atlantic 200 mb U (+)	(47.5°-37.5°S, 30°W-0°)

6.9 Ideas for future work for the October forecast

In the future, the October-only forecast will be revised to include data from the two months prior to the forecast issue date, as is done with the seasonal forecasts and will be done in the next couple of years for the August-only and September-only forecasts. In addition, recent studies by the author and colleagues (e.g., Klotzbach and Gray 2006d) have shown that there is a marked relationship between October tropical cyclone activity and ENSO. Since October is a marginal month for formation due largely to vertical wind shear approaching untenable values (Demaria et al. 2001), any enhancement of vertical wind shear during the month due to ENSO effects can cause an early end to the season, as evidenced by the early end of the season in 2006, when the last storm dissipated on October 2. I intend to include an explicit ENSO predictor in the October-only statistical scheme in the future.

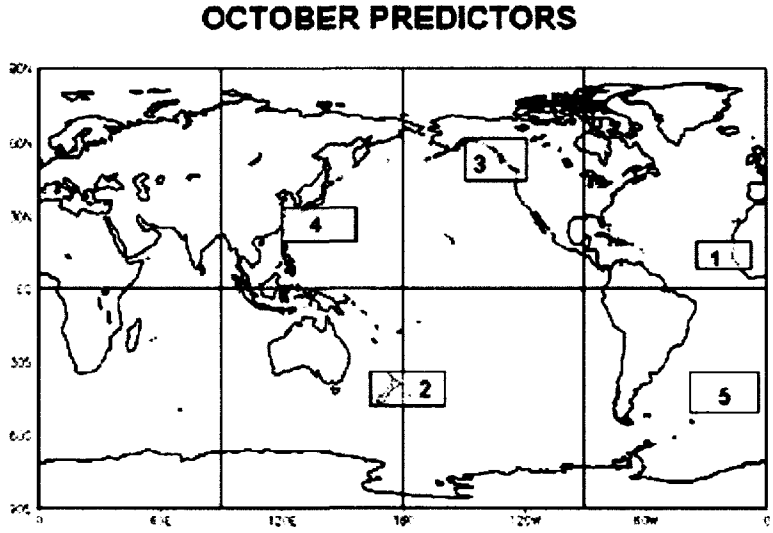

Figure 6.5: Global map showing locations of early October predictors for October-only tropical cyclone activity.

Table 6.8: Real-time October-only NTC prediction, observed October-only NTC values, difference between a real-time prediction and the October-only NTC observation, and difference between a forecast of climatology and the October-only NTC observation. For reference, a climatological value of October-only NTC is 18, based on data from 1949-1999.

Year	Real-Time October-only NTC Prediction	Observed October-only NTC	Difference (Forecast – Observation)	Difference (Climatology – Observation)
2003	21	28	-7	-10
2004	20	6	14	12
2005	30	67	-37	-49
2006	12	2	10	-16
Average Difference			**|17.0|**	**|21.8|**

Chapter 7

United States landfall probabilities

7.1 Background

Probabilities of landfall of tropical storms, hurricanes and intense hurricanes were first issued by the TMP in 1998 (Gray 1998). These probabilities were calculated based upon intensities of 20th century landfalling tropical cyclones taken from the NHC's HURDAT file (Jarvinen et al. 1984). Probabilities of landfall are currently issued by the TMP for the entire United States coastline from Brownsville, Texas to Eastport, Maine, and for the Gulf Coast and Florida Peninsula and East Coast, respectively. The United States has been further sub-divided into eleven regions which were created based upon 20th century major hurricane landfall frequency. Regions 1-4 are considered the Gulf Coast, while Regions 5-11 are defined to be the Florida Peninsula and East Coast. Figure 7.1 displays the regions for which landfall probabilities are currently issued by the TMP. The total number of major hurricanes that made landfall in each region are displayed in a schematic form.

The total number of named storms, hurricanes and major hurricanes making landfall for each region were tabulated. Then, the probabilities of landfall were calculated using a Poisson distribution, since more than one storm can make landfall in any given hurricane season. The formula for a Poisson distribution is given below:

$$EP = p^x/e^p x!$$

where the terms are defined as follows:

- *EP – expected probability,*
- *p – the annual number of storms that have occurred over the past 100 years,*
- *x – the number of storms expected to occur in the upcoming year based on the Poisson formula,*

Equation 7.1: Poisson distribution formulas.

This formula allows for the calculation of the probability of zero named storms, one or more named storms, two or named storms, etc. occurring in any particular year.

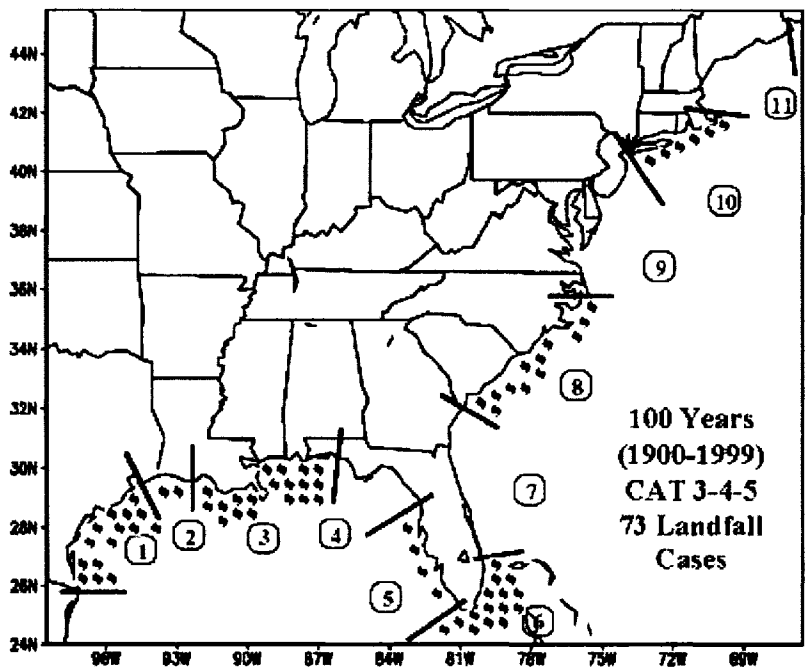

Figure 7.1: The eleven regions for which landfall probability forecasts are provided. Regions were created based upon 20th century major hurricane landfall frequency. Major hurricane landfalls are as indicated by the hurricane symbol.

Landfall probabilities are then adjusted by the prediction of the likely amount of tropical cyclone activity that is expected in the upcoming season. As has been shown earlier in this manuscript, there are clear relationships between predicted amounts of tropical cyclone activity and the observed number of United States landfalls that occur in any particular year. Climatological probabilities are adjusted to current-year probabilities by multiplying the predicted NTC activity divided by 100 times the number of storms that made landfall during the 20th century. This new adjusted number of storms is then placed in Equation 7.1 to derive the current-year probabilities.

It should be noted that until recently, Regions 5-11 were also adjusted by an additional parameter termed SSTA*. This parameter was a weighted average of North Atlantic sea surface temperatures, with warmer SSTs indicating a strong thermohaline circulation (more on this in chapter 8) and an increased likelihood of East Coast landfall. However, upon further analysis, SSTA* does not appear to add any additional skill beyond the NTC prediction, and therefore, landfall probabilities are currently only being adjusted by the upcoming season's prediction.

7.2 United States landfall probability webpage motivation

There is a considerable lack of knowledge amongst the general population along the East Coast, the Florida Peninsula and Gulf Coast of the United States regarding the likelihood of tropical cyclone landfall along a particular portion of coastline in any particular area. Some individuals believe that if they have not been hit by a hurricane in the past few years, they are more likely or "due" to be hit by a hurricane in the upcoming season. Other individuals think that if they were hit by a hurricane last year, their odds of landfall in the upcoming season are much less. In an effort to correct these

misconceptions, and due to the fact that individuals have an inherent curiosity for this type of information, the TMP decided to develop the United States Landfalling Hurricane Probability Webpage. This webpage was put together as a joint partnership with the Geo-Graphics Laboratory at Bridgewater State College in Bridgewater, Massachusetts.

As part of this project, probabilities for the eleven regions discussed in the previous section have been further subdivided into probabilities for 55 sub-regions and 205 coastal and near-coastal counties. Sub-regions were created based upon coastal population density. All coastal counties from Brownsville, Texas to Eastport, Maine are included, while some counties that are slightly inland from the coastline are also included. The webpage utilizes a Geographic Information System (GIS) program known as Maptitude for the Web. This program allows the user to be able to select any county along the coastline and obtain probabilities of landfall for that county along with the larger sub-region and region that it is located. In addition, an MS Excel spreadsheet has been created that allows for a quick comparison of landfall likelihood between different regions, sub-regions and counties. This webpage went online on June 1, 2004, and since that time, the webpage has received over 500,000 hits. The next few pages provide details on how the various data available on the webpage were calculated.

7.3 Sustained wind probability calculations

Probabilities of a tropical storm, hurricane and intense hurricane making landfall are calculated at the region level only. For the sub-region and county level, it was decided that these probabilities should not be provided, since with only ~100-150 years of data available for probability calculations, whether a storm made landfall in any particular county or in an adjacent county can alter probabilities dramatically, and a

distance of a few miles in terms of landfall location is deemed to be within the noise of the data that is currently available. More complicated statistical techniques including many hundreds of years of Monte Carlo simulations would likely be necessary to simulate accurately the probability of landfall between one county and an immediately adjacent county.

Probabilities that are provided for the region level, the sub-region level and the county level are the probabilities of receiving sustained winds of tropical storm force, hurricane force, and intense hurricane force. Maximum wind speeds at landfall were taken from the HURDAT database. For hurricanes that made landfall between 1851-1914 and 1980-2004, maximum landfalling wind speeds were taken from the HURDAT datasheet available online at http://aoml.noaa.gov/hrd/hurdat/ushurrlist.htm. For 1915-1979, maximum landfalling wind speeds were taken to be the midpoint of the Saffir-Simpson category intensity that the hurricane was assigned at landfall.

For tropical storm landfalls from 1851-1914, maximum landfall wind speeds were taken from the HURDAT database. For 1915-1994, tropical storm landfall intensity was taken from the 6-hour intensity immediately prior to landfall, and from 1995-2004, tropical storm landfalling intensities were taken directly from the National Hurricane Center Tropical Cyclone Reports.

To calculate sustained wind probabilities, it was necessary to consider a crude relationship between tropical cyclone intensity and extent of damaging winds, since wind radii information for individual storms has only been made routinely available with the HURDAT database since 2004. The extended best track database, constructed by Mark DeMaria and colleagues at NOAA, which contains wind radii information, only extends

back to 1988, and therefore, to calculate damaging wind radii for all storms since the start of the 20th century, it was necessary to make some assumptions in order to obtain the wind radii necessary for making sustained wind calculations. The relationship between tropical cyclone intensity and wind radii is not valid on an individual storm basis, as it has been shown that a tropical cyclone's wind radii is only crudely correlated with its intensity (e.g., Weatherford and Gray 1988); however, when considering all tropical cyclones that made landfall during the 20th century, it was considered valid.

Wind radii were calculated using the following formula:

$$V_T r^x = \text{constant}$$

where the terms are defined as follows:

- V_T – *maximum sustained wind at landfall,*
- r – *radius from the center of the storm,*
- x – *a constant which is taken to be 0.5 for hurricane-force winds and 0.65 for major hurricane-force winds,*

Equation 7.2: Formula for calculating damaging wind radii.

Figure 7.2 displays the wind speed at various radii away from the center of the tropical cyclone using the above-discussed approximation. It should also be noted that for tropical cyclones that are of tropical storm-strength, the wind radii is assumed to increase linearly from 30-90 kilometers as the storm intensifies from a 35 knot marginal tropical storm to a 60 knot strong tropical storm. The radii of tropical-storm force winds are assumed to be three times the radii of hurricane-force winds.

Using the above-discussed approximations, a table with approximate radii of tropical storm-force, hurricane-force and intense hurricane-force winds for tropical cyclones that made landfall at various intensities has been created. Table 7.1 shows these calculations for cyclones at five-knot intensity increments from 35 knots to 165 knots.

Table 7.2 shows the wind radii assigned to all tropical cyclones that made landfall in Region 2 (the eastern part of Texas and the western part of Louisiana) from 1900-1999.

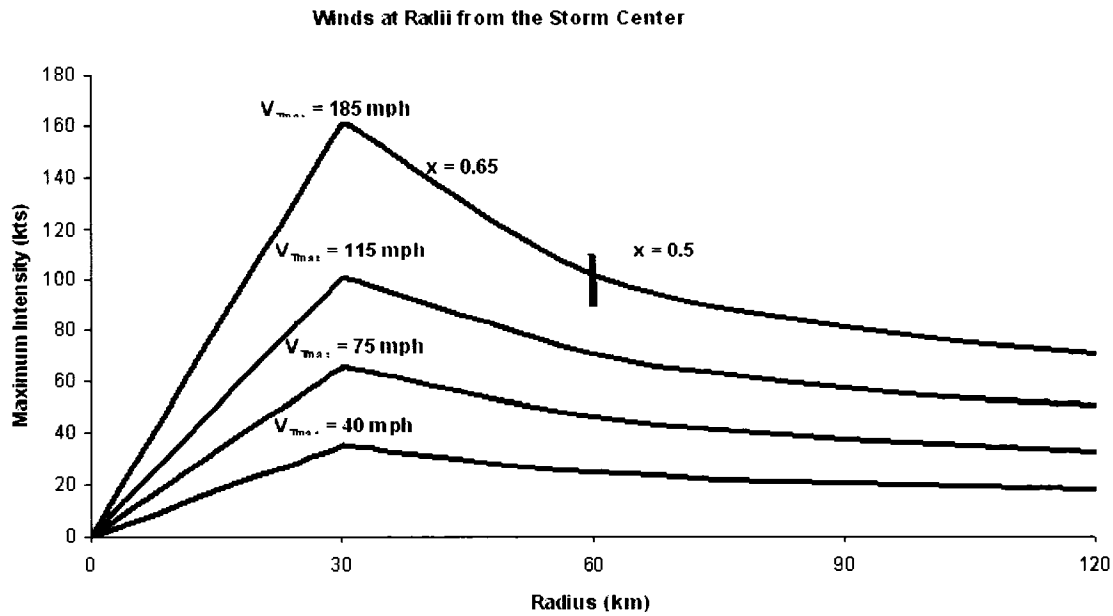

Figure 7.2: Intensity of winds at various radii away from the center of tropical cyclones with maximum intensities of 35, 65, 100 and 160 knots respectively.

From this information, calculations were made for the probability of obtaining tropical storm-force, hurricane-force, and intense hurricane-force winds as follows. The total radius covered by a particular strength wind, for example, tropical storm-force winds was calculated. The radii of all tropical storm-force winds over the entire 100-year period (1900-1999) were then added and multiplied by 2 to obtain the diameter of tropical storm-force winds. Then, divide by the coastal length of the region, resulting in the probability per year of obtaining winds of tropical storm-force strength. This calculation would be made for tropical storm-force winds in Region 2 as follows:

1. Begin by summing the radii of tropical storm-force winds in the region: 1757 km
2. Multiply by 2 to obtain the total diameter of tropical storm-force winds over the 100 year period: (1757 km * 2) = 3514 km
3. Lastly, divide by the coastal length of the region (257 km). This gives the probability per year (in percent) of obtaining tropical storm-force winds in Region 2: (3514 km / 257 km = 13.7%)

The climatological probability of winds of various forces for a subregion was calculated by taking the coastline distance of the subregion and dividing it by the total coastline distance. That ratio was then multiplied by the probability for the entire region (13.7%). For example, the coastline distance of subregion 2C is 145 km and the total coastline distance of Region 2 is 257 km, giving a ratio of 145 km/257 km = 0.56. Therefore the probability of tropical storm-force winds affecting subregion 2C is 0.56 * 13.7% = 7.7%.

The climatological probability of winds of various forces for a coastal county was calculated by taking the coastline distance of the county and dividing it by the distance of the subregion. That ratio was then multiplied by the probability for the entire subregion (7.7%). For example, the coastline distance of Cameron County is 102 km and the total coastline distance of subregion 2C is 145 km, giving a ratio of 102 km/145 km = 0.70. Therefore the probability of tropical storm-force winds affecting Cameron County is 0.70 * 7.7% = 5.4%.

Table 7.1: Assumed radial extent of tropical storm, hurricane and intense (Category 3-4-5) hurricane-force winds for cyclones of different intensities.

Wind Speed (kts)	TS Radius (km)	H Radius (km)	IH Radius (km)
35	30	0	0
40	40	0	0
45	50	0	0
50	60	0	0
55	70	0	0
60	80	0	0
65	90	30	0
70	104	35	0
75	120	40	0
80	136	45	0
85	154	51	0
90	173	58	0
95	192	64	0
100	213	71	30
105	227	76	32
110	241	80	35
115	255	85	37
120	270	90	40
125	285	95	42
130	300	100	45
135	316	105	48
140	332	111	51
145	349	116	53
150	365	122	56
155	382	127	59
160	399	133	62
165	417	139	65

For inland counties, the border distance of the county relative to the aspect of the coastline was measured. Then, the probability was calculated in the same way as that for a coastal county. The probability was then multiplied by 0.75 to take into account the fact that storms weaken as they move inland.

Table 7.2: Damaging wind swaths for all tropical cyclones making landfall in Region 2 from 1900-1999.

Year	Storm Name	Winds (kts)	TS Rad. (km)	H Rad. (km)	IH Rad. (km)
1905	Storm 3	45	50	0	0
1918	Storm 1	85	154	51	0
1938	Storm 2	75	120	40	0
1940	Storm 2	70	104	35	0
1940	Storm 6	40	40	0	0
1941	Storm 1	40	40	0	0
1943	Storm 6	40	40	0	0
1946	Storm 1	35	30	0	0
1954	Barbara	40	40	0	0
1957	Audrey	125	285	95	42
1957	Bertha	60	80	0	0
1959	Arlene	40	40	0	0
1971	Edith	85	154	51	0
1978	Debra	50	60	0	0
1979	Claudette	45	50	0	0
1982	Chris	55	70	0	0
1985	Danny	80	136	45	0
1985	Juan	70	104	35	0
1986	Bonnie	75	120	40	0
1987	Unnamed (1)	40	40	0	0
	Total		**1757**	**392**	**42**
	Prob. Per Year		**13.67%**	**3.05%**	**0.33%**

7.4 50-Year probabilities

Fifty-year probabilities of landfalling tropical cyclones have been included on the United States Landfalling Hurricane Probability Webpage because most structures are built to last at least 50 years, and construction decisions on the cost of hurricane-protecting building materials should be based on these longer period odds. The odds of any one county along the United States coastline experiencing hurricane-force winds in any one particular year is quite small; however, these probabilities grow considerably when considering longer-term probabilities. If a county has a rather large likelihood of a

hurricane making landfall over a 50-year period, one would want to construct the building to withstand at least minimal hurricane-force winds.

The 50-year probability is calculated by taking the individual year climatological probability into account and then using a binomial distribution. For Subregion 2C, the 50-year probability of tropical storm-force winds (individual year probability is 7.7%) is calculated as follows (using decimals for all calculations, i.e. 7.7% = 0.077):

$$\text{50-Year Prob.} = 1 - (1 - \text{One-Year Prob.})^{50}$$

$$= 1 - (1 - 0.077)^{50}$$

$$= 1 - (0.923)^{50}$$

$$= 1 - 0.018$$

50-Year Prob. = 0.982 or 98.2%

Therefore, one would expect a 98.2% chance of getting tropical storm-force winds in Subregion 2C during any 50 year period.

The probability of tropical storm-force winds affecting an area grows considerably as the number of years increases. The example below shows the growth of individual-year probabilities when 1, 5, 10, 25, 50 and 100-year periods are considered for climatological conditions. For ease of comparison, probabilities of getting tropical storm-force winds in Subregion 2C will be calculated:

1-Year Prob. = $1 - (1 - 0.077)^{1} = 0.077$ or 8%
5-Year Prob. = $1 - (1 - 0.077)^{5} = 0.330$ or 33%
10-Year Prob. = $1 - (1 - 0.077)^{10} = 0.551$ or 55%
25-Year Prob. = $1 - (1 - 0.077)^{25} = 0.865$ or 87%
50-Year Prob. = $1 - (1 - 0.077)^{50} = 0.982$ or 98%
100-Year Prob. = $1 - (1 - 0.077)^{100} = 0.999$ or ~100%

This serves as an example that even though there is only a small chance of tropical-storm force winds in Subregion 2C in any one year, these probabilities grow considerably when considering longer periods of time, and these time periods are important when determining building construction practices.

7.5 Storm vicinity probabilities

In addition to calculating probabilities of sustained winds affecting regions, sub-regions and counties, calculations have been made of the potential of winds of tropical storm-force, hurricane-force and intense hurricane-force influencing all coastal counties from Brownsville, TX to Eastport, ME. These values take into account the inherent uncertainty in tropical cyclone track and intensity forecasting. For example, when a tropical cyclone is located in the Gulf of Mexico, many residents along the entire Gulf begin to take preliminary action to protect life and property. Tropical storm and hurricane watches are often issued for a much larger area than actually experiences winds of these magnitudes. In addition, individuals immediately outside of the watch and warning areas may also make some hurricane preparations as a precautionary measure.

To take this uncertainty into account, the probability of each region and subregion being in the vicinity of winds of various magnitudes is calculated by multiplying the probability of sustained winds by 9. Then, the Poisson distribution formula is utilized (Equation 7.1). All counties in a subregion are assigned the same probability of being in the vicinity as the subregion itself. This is done because all counties in a subregion are going to be within the vicinity of the same tropical cyclone.

In this case, the probability of having zero storms making landfall in a particular year is calculated, and the resulting difference from 1 is the probability of having tropical

storm-force winds at least once during a particular hurricane season in the vicinity of that area. For Subregion 2C, the calculation would be made using the Poisson formula provided in Equation 7.1, resulting in an expected probability of 50% for Subregion 2C being in the vicinity of tropical storm-force winds in any particular year.

7.6 Future work

Currently, the strength of tropical cyclones that made United States landfall from 1915-2004 are being reanalyzed as part of the Atlantic Hurricane Database Re-Analysis Project (Landsea et al. 2004), and as this new data becomes available, probability specifications will be re-calculated to include this new source of more accurate landfall intensities. Several additional landfall probability calculations are planned in the next couple of years. Since monthly predictions of NTC activity are issued, I intend to include probabilities of landfall for the individual months of August, September and October on the webpage. Also, I intend to include a user interface where the user can select a particular county and a time period that they are going to be there, and the interface will return a likelihood of tropical cyclone landfall during that time period. This functionality will likely be of considerable use to the travel industry by indicating that the odds of landfall, although not zero, are quite small over a short-term period for any particular coastal location.

Currently, the United States Landfalling Hurricane Probability Webpage only provides probabilities based on one-minute sustained winds. Obviously, shorter period gusts are often what does the real damage, and therefore, over the next couple of years, I intend to include gust probabilities to take into account these shorter-period winds that often can be devastating to coastal properties. Lastly, I intend to include some estimates

of potential future damage using a methodology similar to that outlined in Pielke and Landsea (1998) whereby all tropical cyclones that made landfall during the 20th century were normalized to the damage that they would cause in the year 2000 based upon coastal population, inflation and wealth per capita.

Chapter 8

Atlantic Basin multi-decadal variability

This chapter focuses on observed multi-decadal variability in the Atlantic basin. With the marked increase in Atlantic basin hurricane activity that has occurred since 1995, there has been increased attention focused on this important phenomenon. Much of the information in this chapter is taken from Klotzbach and Gray (2007, manuscript submitted to *Geophys. Res. Lett.*).

8.1 Introduction

The recent increase in both Atlantic basin activity as a whole as well as US landfalling activity had been anticipated as early as the late 1980s (Gray 1989; Gray 1990). Considerable debate has ensued over the past few years as to the cause of this increase. Recent papers by Emanuel (2005) and Webster et al. (2005) have implied that there has been a large increase in global TC intensity since the 1970s, while others have questioned this interpretation of the data (Landsea et al. 2006) or have found little trend in global TC activity when evaluating subsets of the data (Klotzbach 2006; Kossin et al. 2007). Regardless of global trends, there is a general consensus that Atlantic basin TC activity has increased dramatically since 1995, similar to amounts of activity observed from the late 1940s through the mid-1960s (e.g., Goldenberg et al. 2001).

Using "best track" data from the NHC (Jarvinen et al. 1984), previous studies have documented multi-decadal variability in TC activity in the Atlantic basin back to the latter part of the 19th century (Gray 1990; Gray et al. 1997). Associated with this variability are fluctuations in basinwide North Atlantic SSTs (Goldenberg et al. 2001) and Atlantic sea level pressure (SLP). This variability is most pronounced in SSTs for the far North Atlantic (north of 50°N) and in Atlantic SLP equatorward of 50°N.

One of the primary questions that has been recently raised is the likely cause of this multi-decadal variability in SST and SLP. Several studies have postulated that these changes may be due to variability in the Atlantic thermohaline circulation (THC) [Gray 1990; Delworth et al. 1993; Gray et al. 1997; Delworth and Greatbatch 2000; Goldenberg et al. 2001), while another hypothesis that has recently been raised is that some of the variability may be due to human-caused sulfate aerosols (Mann and Emanuel 2006). The causes of this variability in North Atlantic SST are still under debate. This chapters augments previous research on Atlantic basin multi-decadal variability by documenting that through the combined use of far North Atlantic SSTs and a basinwide measure of North Atlantic SLP, multi-decadal variability in atmospheric/oceanic conditions can be clearly documented backward to the latter part of the 19th century. This variability in Atlantic basin atmospheric/oceanic conditions can be clearly linked to variability in both Atlantic basin TC activity as a whole as well as to US landfalling TCs. A combination of SST and SLP appears to work better than either of these two parameters by themselves in defining these multi-decadal periods.

8.2 Data utilized for multi-decadal variability analysis

As was done with all other tropical cyclone calculations utilized in this manuscript, information on basinwide TC activity for the North Atlantic as well as US landfalling TCs was calculated from the "best track" dataset produced by the NHC from 1878-2006 (Jarvinen et al. 1984). Storm data from 1878-1914 were tabulated using the updated best track data which are based upon revisions from the Atlantic Hurricane Database Re-Analysis Project (Landsea et al. 2004). If a storm made landfall in two distinct locations, and the center of the circulation traveled over open ocean in between the two landfalls (i.e., Hurricane Katrina in 2005 in Florida and Louisiana), it was counted as two landfalls.

SST data from 1878-2006 were calculated from the Kaplan SST dataset (Kaplan et al. 1998). SLP data from 1878-2006 were obtained from the Hadley SLP2 dataset (Allan and Ansell 2006). With all datasets used in this study, it is acknowledged that individual-year data in the latter part of the nineteenth and earlier part of the twentieth century may be less reliable. However, since multi-decadal variability is being evaluated in this study, any errors in year-to-year variability will likely be averaged out over the lengthy time periods being analyzed.

8.3 Atlantic basin multi-decadal variability observed in SST and SLP fields

Gray et al. (1997) and Goldenberg et al. (2001) have previously shown that multi-decadal variability is quite strong when evaluating SSTs in the far North Atlantic. Their study and others have referred to this variability as fluctuations in the strength of the Atlantic multi-decadal mode, the strength of the Atlantic multi-decadal oscillation (AMO), or the strength of the THC. For the remainder of this chapter, I will refer to this

multi-decadal variability in the Atlantic basin as the AMO, which will be shown later is likely synonymous with increases or decreases in strength of the THC. This study finds that an even stronger AMO signal is obtained when evaluating a combination of far North Atlantic SSTs in the region from 50-60°N, 50-10°W and North Atlantic SLP in the region from 0-50°N, 70-10°W.

The index of the AMO is calculated by taking annually-averaged standardized anomalies (subtract the mean and divide by the standard deviation) of SST and SLP fields in the aforementioned latitude-longitude regions. The standardized anomalies of SLP and SST are then added together, and this combination is taken as the index of the AMO. Figure 8.1 displays annually-smoothed values of North Atlantic SST, SLP and the combined AMO index from 1880-2004. A 1-2-3-2-1 filter has been applied to the data to smooth out some of the year-to-year variability, and therefore, the first two years and last two years of the data record are not displayed in the figure. In general, the AMO index is positive from 1880-1899, then negative from 1900-1925, then positive from 1926-1969, then negative from 1970-1994, and finally positive from 1995-2004. Table 8.1 displays standardized values for both SST anomalies (SSTA) and SLP anomalies (SLPA). Actual deviations in °C (for SSTA) and mb (for SLPA) are given in parentheses as well as the combined SSTA minus SLPA or AMO index for various multi-decadal periods. When the AMO is judged to be in its positive phase, SSTAs in the far North Atlantic are usually above normal while SLPA values in the North Atlantic equatorwards of 50°N are usually below normal. The opposite conditions occur when the AMO is in its negative phase.

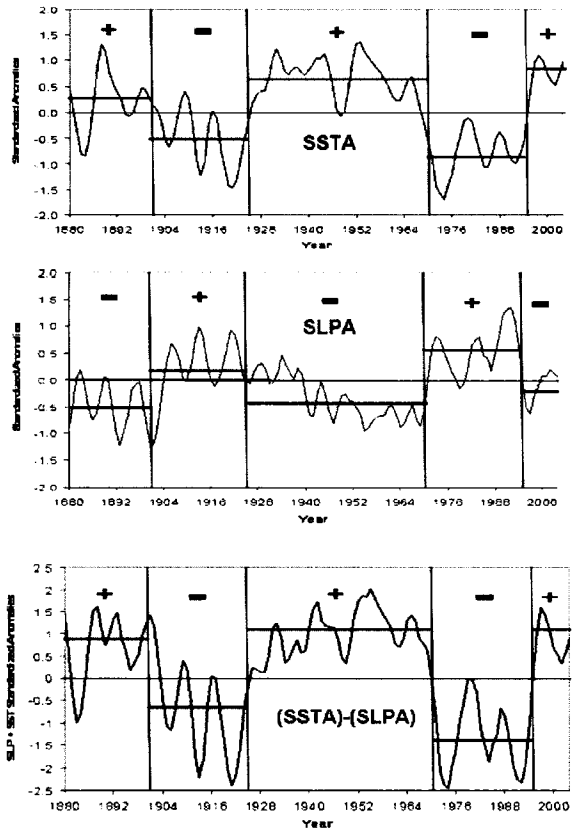

Figure 8.1: Standardized values of North Atlantic SSTA for the area from 50-60°N, 50-10°W (top panel), North Atlantic SLPA for the area from 0-50°N, 70-10°W (middle panel), and the combination of these two parameters (SSTA-SLPA) – taken to be the strength of the AMO - from 1880-2004 (bottom panel). Horizontal lines indicate average values for the multi-decadal period, while (+) and (-) symbols indicate that positive or negative values of the particular index predominated during that period. A 1-2-3-2-1 filter has been applied to the data.

8.4 Atlantic basin multi-decadal variability in tropical cyclone activity

There is a considerable amount of inter-annual and multi-decadal variability observed in Atlantic basin TC activity (Goldenberg et al. 2001; Klotzbach 2006). Previous studies (Gray 1990; Gray et al. 1997; Goldenberg et al. 2001) have shown that TC multi-decadal variability is most significant for major (Category 3-4-5) hurricanes, and results from this study confirm these previous research studies. We stratified our multi-decadal periods using the AMO index derived in the previous section.

Table 8.1. Values of annually-averaged standardized North Atlantic SSTA (50-60°N 50-10°W), annually-averaged standardized North Atlantic SLPA (0-50°N, 70-10°W) and the combined (SSTA minus SLPA) annually-averaged value (taken as the AMO index) over various multi-decadal periods. Note the multi-decadal periods when the AMO index was judged to be positive or to be negative. Actual annually-averaged deviations in °C for SST and mb for SLP are provided in parentheses. The bottom two rows provide annually-averaged data for the 77 years during which the AMO was judged to be positive and the 51 years when it was judged to be negative.

Period	SSTA (1)	SLPA (2)	AMO Index (1) – (2)
1878-1899	+0.3 (+0.08°C)	-0.5 (-0.15 mb)	+0.8
1900-1925	-0.5 (-0.18°C)	+0.2 (+0.08 mb)	-0.7
1926-1969	+0.7 (+0.16°C)	-0.4 (-0.07 mb)	+1.1
1970-1994	-0.8 (-0.27°C)	+0.6 (+0.19 mb)	-1.4
1995-2006	+0.9 (+0.21°C)	-0.2 (-0.03 mb)	+1.1
All Positive	+0.6 (+0.14°C)	-0.4 (-0.09 mb)	+1.0
All Negative	-0.7 (-0.22°C)	+0.4 (+0.13 mb)	-1.0

Table 8.2 displays the average annual number of hurricanes (H), hurricane days (HD), major hurricanes (MH) and major hurricane days (MHD) for the five consecutive positive/negative multi-decadal periods from 1878-1899, 1900-1925, 1926-1969, 1970-1994, and 1995-2006, respectively. Note the large amount of multi-decadal variability between positive and negative AMO periods, especially for MH and MHD. Activity in the earlier periods was likely somewhat underestimated due to a lack of aircraft reconnaissance prior to 1944 and a lack of satellite data prior to the mid-1960s.

This variability is even more striking when evaluating the 20 years when the AMO was judged to be the most positive (in descending order from highest positive - 1955, 1942, 1878, 1888, 1893, 1952, 1966, 1958, 1997, 1902, 1909, 2005, 1932, 2006, 1899, 1960, 1945, 1881, 1937, 1998) compared with the 20 years when the AMO was judged to be the most negative (in ascending order from lowest negative – 1913, 1914, 1986, 1972, 1922, 1974, 1921, 1883, 1920, 1973, 1991, 1993, 1976, 1994, 1982, 1990,

1992, 1984, 1923, 1983). Figure 8.2 displays the average number of H, HD, MH and MHD for the top 20 and bottom 20 AMO years, respectively. Note the large differences between the two periods, with a ratio approaching 5:1 for MHD. Very similar ratios would be obtained if the 10 most positive AMO years since 1950 were compared with the 10 most negative AMO years since 1950.

Table 8.2: Observed annually-averaged Atlantic basin H, HD, MH and MHD during the multi-decadal periods of 1878-1899, 1900-1925, 1926-1969, 1970-1994 and 1995-2006. The bottom row provides the annually-averaged ratio for the 77 positive AMO years and the 51 negative AMO years.

Period	AMO Phase	H	HD	MH	MHD
1878-1899	Positive	5.9	29.0	1.6	4.4
1900-1925	Negative	3.6	15.4	1.2	3.2
1926-1969	Positive	5.6	24.8	2.6	6.5
1970-1994	Negative	5.0	16.0	1.5	2.5
1995-2006	Positive	8.2	35.3	3.9	10.1
Ratio (1878-1899/1900-1925)	Positive/Negative	1.6	1.9	1.3	1.4
Ratio (1926-1969/1900-1925)	Positive/Negative	1.6	1.6	2.2	2.0
Ratio (1926-1969/1970-1994)	Positive/Negative	1.1	1.6	1.7	2.6
Ratio (1995-2006/1970-1994)	Positive/Negative	1.6	2.2	2.6	4.0
All Positive /All Negative	Positive/Negative	1.4	1.8	1.8	2.2

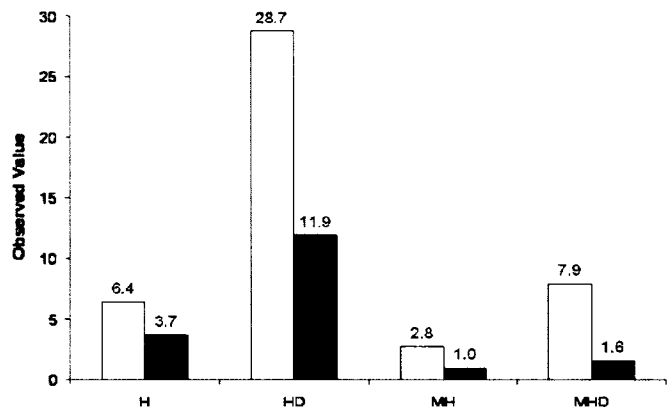

Figure 8.2: Annually-averaged Atlantic basin hurricanes (H), hurricane days (HD), major hurricanes (MH) and major hurricane days (MHD) for the top 20 AMO years (white bar) and the bottom 20 AMO years (black bar).

8.5 Atlantic basin multi-decadal variability in United States tropical cyclone landfalls

There is a strong multi-decadal signal in US TC landfalls, as there is with Atlantic basin activity as a whole. There were 50-100% more H and MH which made landfall in active multi-decadal periods compared with inactive multi-decadal periods. For the top 20-bottom 20 AMO years, the ratio is even more striking, with a total of 19 MH making US landfall in the top 20 years compared with only 7 MH making landfall in the bottom 20 years (nearly a 3 to 1 ratio). Similar ratios would be obtained if the 10 most positive AMO years since 1950 were compared with the 10 most negative AMO years since 1950.

Multi-decadal variability in landfalls is even stronger when considering storms making landfall along the Florida Peninsula and the East Coast of the US. The Florida Peninsula is defined from approximately 100 miles north of Tampa, Florida southward to the Florida Keys and then up the east coast of the state. MH landfalls occurred three times more frequently along the Florida Peninsula and East Coast of the US during 1926-1969 then during either the 1900-1925 period or the more recent 1970-1994 period (Table 8.3). For the top 20-bottom 20 AMO years, the ratio is also quite striking, with a total of 11 MH making landfall in the top 20 years compared with only 4 MH making landfall in the bottom 20 years (nearly a 3 to 1 ratio).

This dramatic multi-decadal landfall variability is even more pronounced when considering MH landfalls along the Florida Peninsula. During the 33-year period from 1933-1965, 11 MH made landfall, while during the following 38-year period (1966-2003), only one MH made landfall (Hurricane Andrew in 1992) – a yearly average difference of over 12 to 1.

Table 8.3: Observed annually-averaged Florida Peninsula and East Coast named storm (NS), H and MH landfalls during the multi-decadal periods of 1878-1899, 1900-1925, 1926-1969, 1970-1994 and 1995-2006. The bottom row provides the annually-averaged ratio for the 77 positive AMO years and the 51 negative AMO years.

Period	AMO Phase	NS	H	MH
1878-1899	Positive	2.2	1.1	0.3
1900-1925	Negative	1.3	0.7	0.2
1926-1969	Positive	2.0	1.3	0.6
1970-1994	Negative	1.3	0.6	0.2
1995-2006	Positive	2.4	1.2	0.3
Ratio (1878-1899/1900-1925)	Positive/Negative	1.7	1.6	1.5
Ratio (1926-1969/1900-1925)	Positive/Negative	1.5	1.9	3.0
Ratio (1926-1969/1970-1994)	Positive/Negative	1.5	2.2	3.0
Ratio (1995-2006/1970-1994)	Positive/Negative	1.8	2.0	1.5
All Positive /All Negative	Positive/Negative	1.7	1.8	2.1

8.6 Possible physical mechanism behind Atlantic basin multi-decadal variability

Multi-decadal variability in the Atlantic basin has been observed to occur from the mid-19th century to the present, and proxy data including Greenland ice core data indicates that this variability has likely occurred for the past four centuries (Delworth and Mann 2000) and possibly the last millennium (Fischer and Mieding 2005). This variability has been tied to fluctuations in the strength of the THC (Delworth et al. 1993; Gray et al. 1997; Delworth and Greatbatch 2000; Goldenberg et al. 2001). A stronger THC is typically associated with a warmer and saltier far North Atlantic and therefore with more sinking of deep water in the far North Atlantic. Salinity content is a much more important factor for the density of salt water than is temperature when the ocean water cools to values of a few degrees above freezing.

Figure 8.3 displays the top 10 AMO years minus the bottom 10 AMO years for both annually-averaged SST and annually-averaged SLP. Hadley SLP2 data is used for the SLP composites (Allan and Ansell 2006), while due to its availability for plotting on

the Climate Diagnostics Center's website, HadISST1 data is used for the SST composite (Rayner et al. 2003). When the AMO is in its positive phase, data clearly shows that the Atlantic subtropical high (or gyre) is weaker than normal. This anomalously weak subtropical gyre is associated with more Atlantic warm salty water moving poleward and sinking to deep levels. This stronger than average THC acts to slowly reduce the Atlantic's salinity content, and with time the THC becomes weaker than normal. This was observed during a rapid weakening of the THC associated with the Great Salinity Anomaly in the North Atlantic that began in the late 1960s (Dickson et al. 1988). When this happens, the THC reverses its polarity and goes into its negative phase. This is associated with the subtropical high (or gyre) becoming stronger. Less salty water is then advected poleward, and salt begins to slowly accumulate within the broad subtropical gyre area until its content is high enough to begin a new multi-decadal period of strong advection of salty subtropical water to high latitudes. We think that this is the primary mechanism by which the Atlantic basin undergoes its multi-decadal variability.

8.7 Future work

Much additional work is needed in tying down the physical relationships between the AMO and the THC. More discussion of the physics behind the THC and its relationship to the AMO has recently been submitted as a manuscript for publication (Gray and Klotzbach 2007, manuscript submitted to *J. Geophys. Res.)*. An additional piece of evidence lending support to the argument that the recent warming of Atlantic SSTs is likely driven by natural causes and not human-induced global warming has recently come to light. In a study recently published (Vecchi and Soden 2007), the authors reviewed a total of 18 climate models. A statistically robust result using climate

models from the Intergovernmental Panel on Climate Change (IPCC) report is an increase in vertical wind shear across the tropical Atlantic and in the Caribbean. This chapter has briefly discussed the fact that vertical wind shear has decreased across the tropical Atlantic over the past decade. Therefore, assuming the results from the Vecchi and Soden study are correct, it lends one to believe that the recent increase in tropical and North Atlantic SSTs is due primarily to natural causes. Much additional research is needed in this area.

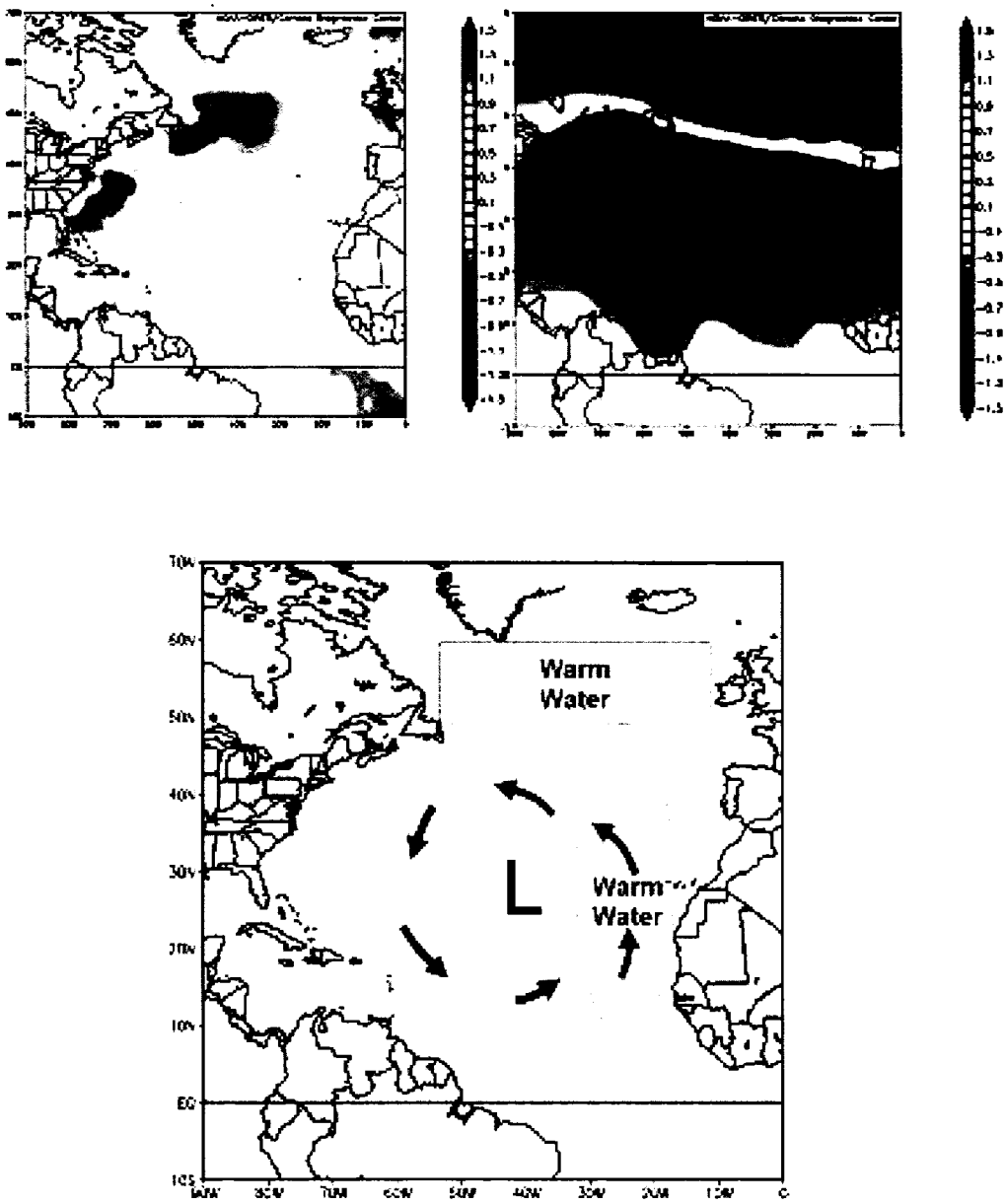

Figure 8.3: Observed SST differences between the top 10 and bottom 10 AMO years (top left panel), observed SLP differences between the top 10 and bottom 10 AMO years (top right panel) and a schematic of how these patterns likely impact the AMO (bottom panel).

Chapter 9

Global tropical cyclone trends

This chapter focuses on trends in global tropical cyclone activity over the past twenty years. Atlantic tropical cyclone activity has clearly increased since 1995, as discussed in the previous chapter; however, a question that remains unanswered is: have global tropical cyclones increased worldwide? I attempt to help shed some light on this question in this chapter. Much of the information in this chapter is taken from Klotzbach (2006).

9.1 Introduction

Recent papers by Emanuel (2005) and Webster et al. (2005) have caused a flurry of debate about the relationship between increasing tropical SSTs and intense TCs. Emanuel (2005) found that a Power Dissipation Index (PDI), effectively the six-hour TC one-minute maximum sustained wind speed cubed, had increased by approximately 50% for both the Atlantic basin and the Northwest Pacific basin since the mid 1970s. Webster et al. (2005) analyzed Category 4-5 hurricanes (maximum sustained winds >= 115 knots) for all TC basins over the past 30 years and found that their numbers had nearly doubled between an earlier (1975-1989) and a more recent (1990-2004) 15-year period.

Many questions have been raised regarding the data quality in the earlier part of their analysis periods (Landsea et al. 2006; Landsea 2007). Before the early 1980s, the Dvorak Technique (Dvorak 1975), a method which utilizes satellite imagery to assign an intensity to TCs, was only applicable to visible satellite imagery and therefore could not be used at night. Since 1984, improved technology has allowed the technique to be applied to both infrared and visible imagery (Dvorak 1984), and more accurate estimates of real-time intensity have become available. In addition, the quality and resolution of satellite imagery has continued to improve over time, and with this improved imagery, operational forecasters can be more confident of their satellite-derived intensity estimates. The elimination of aircraft reconnaissance in the Northwest Pacific in 1987 raised the importance of satellite-based intensity estimates even more. Also, the Joint Typhoon Warning Center urges caution in utilizing data prior to 1985 (Chu et al. 2002). Because of these earlier period limitations and the desire to obtain a near-homogeneous dataset, only the twenty years from 1986-2005 are examined in this paper. If the trends shown in Emanuel (2005) and Webster et al. (2005) are to be accepted, then one should also find a similar increasing trend in global TC datasets over the last 20 years.

9.2 Methodology

Global TC activity was tabulated using "best track" datasets from 1986-2004 for all TC basins (the North Atlantic, the Northeast Pacific, the Northwest Pacific, the North Indian, the South Indian, and the South Pacific). The "best track" datasets are the best estimates of intensities of TCs at six-hour intervals produced by the international warning centers. The "best track" datasets from the National Hurricane Center (NHC) were utilized for the North Atlantic (Jarvinen et al. 1984) and the Northeast Pacific basins, and

"best track" data from the Joint Typhoon Warning Center (JTWC) (Chu et al. 2002) were utilized for the North Indian and Northwest Pacific basins.

For the South Indian and South Pacific basins, a dataset created by Neumann (Neumann 1999) was used for 1986-2001 because it was utilized by Webster et al. (2005) in their study. The South Indian and South Pacific basins were divided at 135°E with storms forming east of this longitude being classified as South Pacific storms and storms forming west of this longitude being classified as South Indian storms. If a storm crossed 135°E longitude, it was classified into the basin in which it accrued more named storm days. The Neumann dataset ended in June 2002, and after this point, the JTWC's "best track" dataset was used. The JTWC dataset overlaps the Neumann dataset from 1970-2002, and the correlation between TC statistics calculated from these datasets is greater than 0.95. The consistency between datasets suggests that the JTWC "best track" dataset can be utilized from July 2002-June 2004 without causing any spurious jumps in the data. For 2005 for the Northern Hemisphere and for July 2004-2005 for the Southern Hemisphere, operational TC intensity estimates were utilized. These data were obtained from the NHC for the North Atlantic and the Northeast Pacific. JTWC data were utilized for all other basins. In the Southern Hemisphere, JTWC advisories were occasionally supplemented with data from the advisory centers in Perth, Darwin, Brisbane and Reunion to extend a storm's length or increase its intensity slightly per the suggestion of Gary Padgett (personal communication, 2006). This was done for storms where the JTWC advisory intensities were considerably below the intensity recorded at the other centers. The combination of these datasets provides a comprehensive evaluation of global TC activity over the past twenty years (1986-2005).

9.3 Trends in Accumulated Cyclone Energy

Figure 9.1 displays Accumulated Cyclone Energy (ACE) index values for all TC basins from 1986-2005. ACE is defined to be the sum of the maximum one-minute sustained surface wind speed squared at six-hourly intervals for all periods when the TC is at least of tropical storm strength (>= 34 knots) (Bell et al. 2000). Linear trends have been fitted to all six TC basins. This ACE index is quite similar to the Power Dissipation Index (PDI) created by Emanuel (2005), since PDI is defined to be the sum of the maximum one-minute sustained wind speed cubed at six-hourly intervals for all periods when the TC is at least of tropical storm strength. The largest trends noticeable on this figure are a large increase over the past twenty years in the North Atlantic and a considerable decrease over the Northeast Pacific. The large recent increase in North Atlantic activity has been noted extensively throughout the literature and has been attributed to an increase in strength of the Atlantic Thermohaline Circulation (THC) (alternatively referred to as a change in sign to a positive phase of the Atlantic multi-decadal mode) (Gray et al. 1997; Goldenberg et al. 2001; Pielke et al. 2005). The trends in all other basins are quite small.

Figure 9.2 takes the ACE index values for all TC basins and sums them into values for the Northern Hemisphere, the Southern Hemisphere, and the entire globe. A five-year running mean of tropical SST anomalies (23.5°S – 23.5°N, all longitudes) obtained from the NCEP Reanalysis (Kistler et al. 2001) are also plotted for reference. A linear trend has been fitted to all three curves, and it is noted that there is a slight increase in ACE for the Northern Hemisphere, the Southern Hemisphere and consequently for the globe for the 1986-2005 period. However, it is also to be noted that most of this increase

occurred during the earliest part of the dataset, where there are still some questions regarding data quality (Landsea et al. 2006). As seen in Figure 9.3, if the last 16 years of the dataset are examined (1990-2005), the trend in global ACE is actually slightly downward, although tropical SSTs increased by approximately 0.2°-0.3°C during this period.

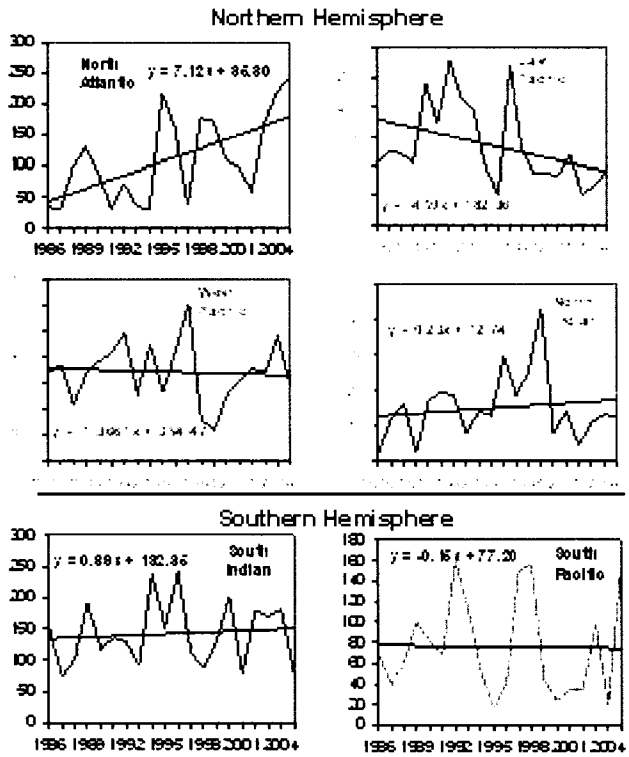

Figure 9.1: Accumulated Cyclone Energy (ACE) index values for individual TC basins from 1986-2005. Figure taken from Klotzbach (2006).

Table 9.1 displays total ACE for the ten-year periods of 1986-1995 and 1996-2005 for each of the individual TC basins as well as for the combination of the North Atlantic and Northeast Pacific, the Northern Hemisphere, the Southern Hemisphere and for all TCs worldwide. Ratios of the second ten-year period to the first ten-year period are calculated. Average tropical SSTs for each ten-year period are provided for reference.

Effectively, when grouped into ten-year periods, there has been virtually no trend in globally-summed ACE. The largest individual-basin trends are evident in the North Atlantic and the Northeast Pacific. There has been a large increase in ACE over the past decade in the North Atlantic, and there has been a large decrease in ACE over the past decade in the Northeast Pacific. When ACE in the North Atlantic and Northeast Pacific are added together, there has been a very small increase in Western Hemisphere TC activity over the past twenty years. A slight negative trend in ACE is noted in the Northwest Pacific, which is in contrast to the large increase in PDI noted by Emanuel (2005) since the mid 1970s. One would expect the increasing trend in PDI over the past thirty years to also show an increase over the past twenty years when sea surface temperatures have warmed by approximately 0.2°-0.4°C.

9.4 Trends in Category 4-5 hurricanes

Webster et al. (2005) report that there has been a large (nearly 50%) increase in Category 4-5 hurricanes since the mid 1970s. Table 9.2 displays the number of Category 4-5 hurricanes by individual TC basin, for the North Atlantic and the Northeast Pacific, for the Northern Hemisphere, the Southern Hemisphere and the globe by ten-year periods since 1986. Northern Hemisphere Category 4-5 hurricanes have remained virtually the same between the two ten-year periods, and a modest increase in Category 4-5 hurricanes has been observed in the Southern Hemisphere. Most of this Southern Hemisphere increase occurred in the first five years of the dataset, and since the early 1990s, as satellite observational technology has continued to improve, there has been no continuation of this trend; even though global SSTs and oceanic heat content have continued to rise (Levitus et al. 2000). This increase in Category 4-5 hurricanes from the

late 1980s to the early 1990s is believed to be largely due to improvements in satellite technology. During the past twenty years, the number of Category 4-5 hurricanes has increased dramatically in the North Atlantic, and there has been a large decrease in the Northeast Pacific, in keeping with the ACE values for these basins. Since 1990, the number of Category 4-5 hurricanes across the globe has remained approximately constant which agrees with the findings of Webster et al. (2005, their Figure 4).

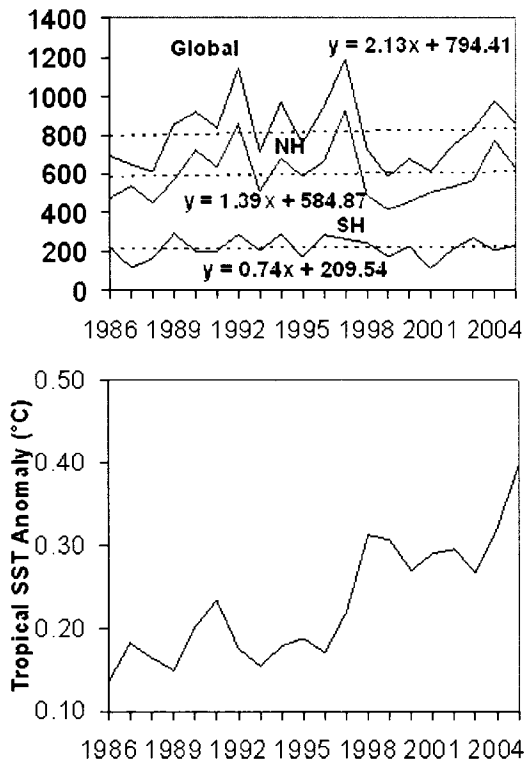

Figure 9.2: Accumulated Cyclone Energy (ACE) index values for 1986-2005 for the Northern Hemisphere (NH), the Southern Hemisphere (SH) and the globe. Linear trends have been fitted to the three curves. Five-year running mean tropical NCEP Reanalysis SST anomalies (23.5°S – 23.5°N, all longitudes) (blue line) are also plotted. The base period for tropical SSTs is 1951-1980. Figure taken from Klotzbach (2006).

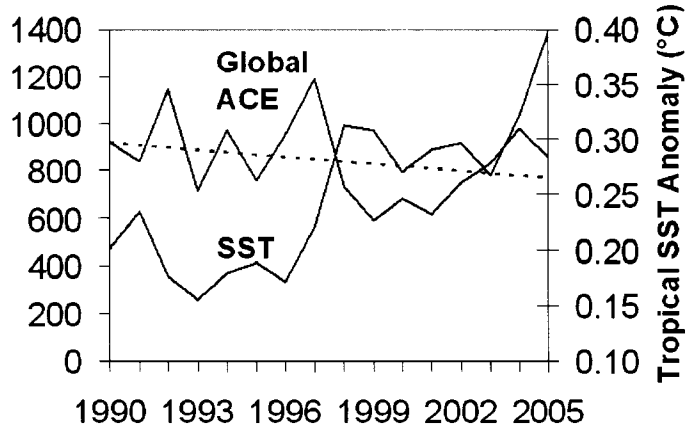

Figure 9.3: Global Accumulated Cyclone Energy (ACE) index values for 1990-2005. A linear trend has been fitted to global ACE. Five-year running mean tropical NCEP Reanalysis SST anomalies (23.5°S – 23.5°N, all longitudes) (blue line) are also plotted. The base period for tropical SSTs is 1951-1980. Figure taken from Klotzbach (2006).

Table 9.1: Accumulated Cyclone Energy (ACE) index values for ten-year periods (1986-1995, 1996-2005) and the ratio of the second ten-year period to the first ten-year period for all TC basins, the North Atlantic and the Northeast Pacific, the Northern Hemisphere, the Southern Hemisphere and the globe. Tropical SSTs for each ten-year period (23.5°S – 23.5°N, all longitudes) derived from the NCEP Reanalysis and the difference between these two periods are provided. The base period for tropical SSTs is 1951-1980.

Basin	1986-1995	1996-2005	Ratio (1996-2005 / 1986-1995) (In Percent)
North Atlantic	762	1438	189%
Northeast Pacific	1646	1037	63%
N. Atl. + NE Pac.	2408	2475	103%
Northwest Pacific	3495	3307	95%
North Indian	123	180	146%
South Indian	1377	1456	106%
South Pacific	757	755	100%
Northern Hemisphere	6026	5962	99%
Southern Hemisphere	2134	2211	104%
Global	8160	8173	100%
Tropical SSTs (23.5°N – 23.5°S, all longitudes)	0.18°C	0.29°C	ΔT = +0.11°C

Table 9.2: Category 4-5 hurricanes by ten-year periods (1986-1995, 1996-2005) for individual TC basins, the North Atlantic and the Northeast Pacific, the Northern Hemisphere, the Southern Hemisphere and the globe.

Basin	1986-1995	1996-2005	Ratio (1996-2005 / 1986-1995)
North Atlantic	10	25	250%
Northeast Pacific	37	23	62%
N. Atl. + NE Pac.	47	48	102%
Northwest Pacific	75	76	101%
North Indian	3	4	133%
South Indian	26	36	138%
South Pacific	13	16	123%
Northern Hemisphere	125	128	102%
Southern Hemisphere	39	52	133%
Global	164	180	110%

9.5 Correlations between ACE and Category 4-5 hurricanes with sea surface temperatures

Table 9.3 shows the correlation between ACE and SSTs along with the correlation between Category 4-5 hurricanes and SSTs for each TC basin over the period 1986-2005 for the Northern Hemisphere and for 1985-1986 through the 2004-2005 hurricane seasons for the Southern Hemisphere. SSTs are taken from the Hadley SST dataset (Rayner et al. 2003). The Hadley SST dataset was correlated from 1986-2005 with the NCEP Reanalysis SST dataset (Kistler et al. 2001) and the Kaplan SST dataset (Kaplan et al. 1998), and both the NCEP Reanalysis and Kaplan SST datasets correlated at greater than 0.90 with Hadley SSTs for each TC basin. Therefore, the correlation would not change much if another SST dataset were selected. TC basins are defined as in Webster et al. (2005).

Based on theoretical research (Emanuel 1987), one would expect there to be a positive correlation between SST in a TC basin and observed TC intensity, and therefore a one-tailed Student's t-test was used to test for statistical significance. Since there are 20

years of data, a correlation of 0.38 is needed to be statistically significant at the 95% level. There is a statistically significant relationship between SSTs and ACE as well as SSTs and Category 4-5 hurricanes for both the North Atlantic and the Northeast Pacific; however, correlations for the other four TC basins are actually slightly negative. Even for the North Atlantic and the Northeast Pacific, these correlations only explain between 25-30% of the variance, and therefore large amounts of variance are unexplained. Clearly, other atmospheric and oceanic features such as vertical wind shear, mid-level instability, etc. (e.g., Gray 1968) are critical for TC development and intensification besides warm SSTs.

Table 9.3: Correlations between ACE and SSTs and Category 4-5 hurricanes and SSTs for all TC basins. TC basins and seasons are defined as in Webster et al. [2005] (North Atlantic Ocean - 5° to 25°N, 20° to 90°W, June-October), (Northeast Pacific Ocean - 5° to 20°N, 90° to 120°W, June-October), (Northwest Pacific Ocean - 5° to 20°N, 120° to 180°E, May-December), (North Indian Ocean - 5° to 20°N, 55° to 90°E, April-May and September-November), (South Indian Ocean - 5° to 20°S, 50° to 115°E, November-April), and the (South Pacific Ocean - 5° to 20°S, 155° to 180°E, December-April). Correlations significant at the 95% level based on a one-tailed Student's t-test are bold-faced.

Basin	Correlation with ACE	Correlation with Cat. 4-5 Hurricanes
North Atlantic	**0.57**	**0.39**
Northeast Pacific	**0.58**	**0.59**
Northwest Pacific	-0.28	-0.11
North Indian	-0.07	-0.29
South Indian	-0.32	-0.18
South Pacific	-0.38	-0.20

9.6 Conclusions

These findings are contradictory to the conclusions drawn by Emanuel (2005) and Webster et al. (2005). They do not support the argument that global TC frequency, intensity and longevity have undergone increases in recent years. Utilizing global "best track" data, there has been no significant increasing trend in ACE and only a small

increase (~10%) in Category 4-5 hurricanes over the past twenty years, despite an increase in the trend of warming sea surface temperatures during this time period. This leads one to believe that most of the increase in TC activity found during the period prior to 1986 is likely due to data quality issues.

The results of this paper are more in line with a prior study from Shapiro and Goldenberg (1998) and a project report from Gray and Klotzbach (2005). Shapiro and Goldenberg (1998) showed only marginally significant correlations between SSTs in the tropical Atlantic and major hurricane development in the basin. Vertical wind shear was shown to be a much more fundamental component for major hurricane development and maintenance. Gray and Klotzbach (2005), while developing seasonal hurricane forecasts for TC activity, found only a modest correlation ($r \sim 0.4$) between seasonal and monthly Atlantic basin SSTs and major (Category 3-4-5) hurricane frequency. This study indicates that, based on data over the last twenty years, no significant increasing trend is evident in global ACE or in Category 4-5 hurricanes.

An independent result from Jim Kossin and colleagues at the Cooperative Institute for Meteorological Satellite Studies using an automated version of the Dvorak technique and satellite imagery since 1983 reached similar conclusions as those reached in this chapter (Kossin et al. 2007). They found an increase in TC activity in the Atlantic, a decrease in TC activity in the East Pacific and small trends elsewhere. Potential relationships between global warming and tropical cyclone activity will likely be an area of considerable debate for the next few years.

Chapter 10
Summary and future work

10.1 Summary

I have discussed in detail some of the latest research being conducted by the author that has translated into the new statistical forecasts that are now being used by the TMP. New statistical seasonal forecasts have been developed for each of the four seasonal predictions issued in early December, early April, early June and early August. In addition, the development of sub-seasonal forecasts for August-only, September-only and October-only activity have been discussed in detail.

The remainder of this manuscript has discussed the latest developments in United States landfall probability forecasts. Landfall probabilities were calculated based upon 20th century landfall frequency and were then adjusted based upon the latest seasonal forecast issued by the TMP. Landfall probabilities are now available for 11 regions, 55 sub-regions and 205 coastal and near-coastal counties from Brownsville, Texas to Eastport, Maine on the United States Landfalling Hurricane Probability Webpage.

Multi-decadal variability in the Atlantic basin has also been investigated in detail. There is considerable variability in Atlantic basin hurricane activity that is likely related to the phase of the AMO and the strength of the THC. In general, a positive phase of the

AMO and a strong THC relate to warm North and tropical Atlantic SSTs, weaker vertical wind shear values, increased instability and low-level convergence and more tropical cyclone activity. In addition, it was shown that many more major hurricanes make landfall along the United States coastline with a positive phase of the AMO.

Finally, trends in global tropical cyclone activity have been analyzed in detail. Using data over the past twenty years (1986-2005) when data quality is considered to be highest, a large increasing trend in TC activity is seen in the Atlantic basin while a large decreasing trend in TC activity is seen in the East Pacific basin. All other basins show insignificant trends, indicating that, as of yet, no detectable trend in global TC activity is evident despite increasing SSTs. The analysis conducted here indicates that other features besides SSTs are critical for TC development and intensification.

10.2 Future work

Seasonal prediction of Atlantic basin hurricane activity continues to be a work in progress. Every hurricane season that occurs provides the TMP with another realization of how the atmosphere and ocean interact to cause an active, normal or inactive season. As more hurricane seasons are added to the database, the skill of seasonal forecasts using statistical techniques is likely to improve.

The European Centre for Medium-Range Weather Forecasts (ECMWF) has recently conducted an independent reanalysis termed the ERA-40 reanalysis for the period from mid-1957 through 2001. In the future, the skill of predictors selected using the NCEP/NCAR reanalysis will be compared to the skill that would be achieved over the same time period using the same predictors obtained from the ECMWF reanalysis. If the

skill is similar in both datasets, it provides increased confidence that the predictors are physically related to Atlantic basin tropical cyclone activity.

As mentioned in some of the previous chapters, I intend to subject the early December, early April and early June statistical seasonal prediction techniques to the same rigorous tests that were applied to the early August seasonal forecast. Namely, the schemes must show similar skill during an earlier independent time period (1900-1949) and a recent independent time period (1990-2004) that they have demonstrated over the developmental period between 1950-1989. If statistical schemes show similar skill over all three periods, it increases the likelihood that the scheme will be useful in real-time forecasts.

Sub-seasonal forecasts for the individual months of August, September and October will also be revised and updated in the next couple of years. These schemes will use two-month average predictors immediately preceding the forecast issue date, and these schemes will also be subjected to the rigorous statistical tests that have been applied to the early August seasonal forecast.

The United States Landfalling Hurricane Probability Webpage will also be upgraded and updated in the next few years. I intend to update the webpage to include gust probabilities, monthly landfall probabilities, user-selected short-term probabilities and future damage values. In addition, climatological average probabilities will be updated to include data for the past several hurricane seasons and will include revisions based upon research by the Atlantic Hurricane Database Re-Analysis Project (Landsea et al. 2004).

Research into the causes of Atlantic basin multi-decadal TC variability will continue for the next few years. Stronger physical links tying down the relationship between

Atlantic SST and sea level pressure fluctuations and the THC are needed, and future work involves better cementing this postulated relationship.

Finally, the relationship between currently warming tropical SSTs and global TC activity will continue to be analyzed in detail. Unfortunately, data sets currently available are of short-period duration and are likely not of sufficiently high quality for climate studies. However, a recent effort by scientists at the Cooperative Institute for Meteorological Satellite Studies (CIMSS) to create a homogeneous database of objective Dvorak estimates for all tropical cyclones occurring since 1983 is an important step in the right direction for allowing better analysis of global tropical cyclone trends (Kossin et al. 2007).

Tropical cyclones continue to be one of the world's most deadly and destructive hazards (e.g., Pielke and Landsea 1998). Seasonal hurricane predictions issued by the TMP since 1984 have helped to raise awareness of the upcoming hurricane season and the potential damage and devastation that these storms can cause. Continued improvements in the quality of the data available and in forecasting techniques will likely lead to increasing levels of skill in the coming years.

References

Allan, R. J., and T. J. Ansell, 2006: A new globally complete monthly historical mean sea level pressure data set (HADSLP2): 1850-2004. *J. Climate,* **19,** 5816-5842.

Basnett, T. and D. Parker, 1997: Development of the global mean sea level pressure data set GMSLP2. *Climate Research Technical Note,* **79**, Hadley Centre Met Office, Exeter, UK.

Bell, G. D., and M. Chelliah, 2006: Leading tropical modes associated with interannual and multidecadal fluctuations in North Atlantic hurricane activity. *J. Climate,* **19,** 590-612.

___, and Coauthors, 2000: Climate assessment for 1999. *Bull. Amer. Meteor. Soc.,* **81,** S1-S50.

Blake, E. S., 2002: Prediction of August Atlantic basin hurricane activity. Dept. of Atmospheric Science Paper 719, Colorado State University, Fort Collins, CO, 80 pp.

___, and W. M. Gray, 2004: Prediction of August Atlantic basin hurricane activity. *Wea. and Forecasting,* **19,** 1044-1060.

Bove, M. C., J. B. Elsner, C. W. Landsea, X. Niu, and J. J. O'Brien, 1998: Effect of El Niño on U.S. landfalling hurricanes, revisited. *Bull. Amer. Meteor. Soc.,* **79,** 2477-2482.

Chelliah, M., and S. Saha, 2004: Dynamical forecasts of atmospheric conditions associated with North Atlantic hurricane activity by the Coupled Forecast System at NCEP. *29th Annual Climate Diagnostics and Prediction Workshop*, Madison, WI, NOAA/Climate Prediction Center. Presentation available online at: http://www.cpc.ncep.noaa.gov/products/outreach/proceedings/cdw29_proceedings/chelliah.ppt

Chiang, J. C. H., and D. J. Vimont, 2004: Analogous Pacific and Atlantic meridional modes of tropical atmosphere-ocean variability. *J. Climate,* **17,** 4143-4158.

Chu, J.-H., C. R. Sampson, A. S. Levin, and E. Fukada, 2002: The Joint Typhoon Warning Center tropical cyclone best tracks 1945-2000. Joint Typhoon Warning Center Report, Joint Typhoon Warning Center, Pearl Harbor, HI.

Cook, K. H., 2000: The South Indian Convergence Zone and interannual rainfall variability over southern Africa. *J. Climate,* **13,** 3789-3804.

Delworth, T. L., and R. J. Greatbatch, 2000: Multidecadal thermohaline circulation variability driven by atmospheric surface flux forcing. *J. Climate,* **13,** 1481-1495.

___, S. Manabe, and R. J. Stouffer, 1993: Interdecadal variations of the thermohaline circulation in a coupled ocean-atmosphere model. *J. Climate,* **6,** 1993-2011.

___, and M. E. Mann, 2000: Observed and simulated multidecadal variability in the Northern Hemisphere. *Climate Dyn.,* **16,** 661-676.

DeMaria, M., J. A. Knaff, and B. H. Connell, 2001: A tropical cyclone genesis parameter for the North Atlantic. *Wea. and Forecasting,* **16,** 219-233.

Dickson, R. R., J. Meincke, S. A. Malmberg, and A. J. Lee, 1988: The "great salinity anomaly" in the North Atlantic 1968-1982, *Proc. Oceanog.,* **20,** 103-151.

Dvorak, V. F., 1975: Tropical cyclone intensity and forecasting from satellite images. *Mon. Weather Rev.*, **103,** 420-430.

___, 1984:, Tropical cyclone intensity analysis using satellite data. NOAA Tech. Report NESDIS 11, NOAA/NESDIS, Washington, DC, 47 pp.

Dunn, G. E., 1940: Cyclogenesis in the tropical Atlantic. *Bull. Amer. Meteor. Soc.,* **21,** 215-229.

Elsner, J. B., 2003: Tracking hurricanes. *Bull. Amer. Meteor. Soc.,* **84,** 353-356.

___, K. B. Liu, and B. Kocher, 2000: Spatial variations in U.S. hurricane activity: Statistics and a physical mechanism. *J. Climate,* **13,** 2293-2305.

___, and C. P. Schmertmann, 1993: Improving extended-range seasonal predictions of intense Atlantic hurricane activity. *Wea. Forecasting,* **8,** 345–351.

___, and ___, 1994: Assessing forecast skill through cross validation. *Wea. Forecasting,* **9,** 619-624.

Emanuel, K. A., 1987: The dependence of hurricane intensity on climate. *Nature,* **326,** 483-485.

___, 2005: Increasing destructiveness of tropical cyclones over the past 30 years, *Nature*, **326,** 686-688.

Fischer, H., and B. Mieding, 2005: A 1000-year ice core record of interannual to multidecadal variations in atmospheric circulation over the North Atlantic. *Climate Dyn.*, **25,** 65-74.

Frank, W. M., and E. A. Ritchie, 2001: Effects of vertical wind shear on the intensity and structure of numerically simulated hurricanes. *Mon. Wea. Rev.*, **129,** 2249-2269.

Goldenberg, S. B., C. W. Landsea, A. M. Mestas-Nuñez, and W. M. Gray, 2001: The recent increase in Atlantic hurricane activity: Causes and implications. *Science,* **293,** 474-479.

___, and L. J. Shapiro, 1996: Physical mechanisms for the association of El Niño and West African rainfall with Atlantic major hurricane activity. *J. Climate,* **9,** 1169-1187.

Gray, W. M., 1968: Global view of the origin of tropical disturbances and storms. *Mon. Wea. Rev.*, **96,** 669-700.

___, 1984a: Atlantic seasonal hurricane frequency. Part I: El Niño and 30 mb quasi-biennial oscillation influences. *Mon. Wea. Rev.*, **112,** 1649-1668.

___, 1984b: Atlantic seasonal hurricane frequency. Part II: Forecasting its variability. *Mon. Wea. Rev.*, **112,** 1669-1683.

___, 1989: Forecast of Atlantic hurricane activity for 1989. Dept. of Atmospheric Science Report, Colorado State University, Fort Collins, CO, 38 pp.

___, 1990: Strong association between West African rainfall and U.S. landfall of intense hurricanes, *Science,* **249**, 1251-1256.

___, 1998: Forecast probability of U.S. hurricane landfall for 1998. Dept. of Atmospheric Science Report, Colorado State University, Fort Collins, CO, 15 pp.

___, C. W. Landsea, E. S. Blake, P. W. Mielke Jr., and K. J. Berry, 2001: Updated early August forecast of Atlantic seasonal hurricane activity and US landfall strike probability for 2001. Dept. of Atmospheric Science Report, Colorado State University, Fort Collins, CO, 30 pp.

___, ___, and P. J. Klotzbach, 2002a: Extended range forecast of Atlantic seasonal hurricane activity and US landfall strike probability for 2003. Dept. of Atmospheric Science Report, Colorado State University, Fort Collins, CO, 17 pp.

___, ___, and ___, 2002b: Updated forecast of Atlantic seasonal hurricane activity and US landfall strike probability for 2002. Dept. of Atmospheric Science Report, Colorado State University, Fort Collins, CO, 28 pp.

___, ___, and ___, 2003a: Extended range forecast of Atlantic seasonal hurricane activity and US landfall strike probability for 2003. Dept. of Atmospheric Science Report, Colorado State University, Fort Collins, CO, 21 pp.

___, ___, and ___, 2003b: Extended range forecast of Atlantic seasonal hurricane activity and US landfall strike probability for 2003. Dept. of Atmospheric Science Report, Colorado State University, Fort Collins, CO, 20 pp.

___, ___, P. W. Mielke Jr., and K. J. Berry, 1992a: Predicting Atlantic seasonal hurricane activity 6–11 months in advance. *Wea. Forecasting,* **7,** 440–455.

___, ___, ___, and ___, 1993: Predicting Atlantic basin seasonal tropical cyclone activity by 1 August. *Wea. Forecasting,* **8,** 73-86.

___, ___, ___, and ___, 1994: Predicting Atlantic basin seasonal tropical cyclone activity by 1 June. *Wea. Forecasting,* **9,** 103-115.

___, ___, ___, and ___, 2000a: Early August updated forecast of Atlantic basin seasonal hurricane activity and landfall probability for 2000. Dept. of Atmospheric Science Report, Colorado State University, Fort Collins, CO, 28 pp.

___, ___, ___, and ___, 2000b: Extended range forecast of Atlantic seasonal hurricane activity and US landfall strike probability for 2001. Dept. of Atmospheric Science Report, Colorado State University, Fort Collins, CO, 22 pp.

___, and P. J. Klotzbach, 2003: Forecast of Atlantic hurricane activity for October 2003 and seasonal update through September. Dept. of Atmospheric Science Report, Colorado State University, Fort Collins, CO, 13 pp.

___, and ___, 2004: Extended range forecast of Atlantic seasonal hurricane activity and US landfall strike probability for 2004. Dept. of Atmospheric Science Report, Colorado State University, Fort Collins, CO, 17 pp.

___, and ___, 2005: Extended range forecast of Atlantic seasonal hurricane activity and US landfall strike probability for 2005. Dept. of Atmospheric Science Report, Colorado State University, Fort Collins, CO, 19 pp.

___, and J. D. Sheaffer, 1991: El Niño and QBO influences on tropical cyclone activity. *Teleconnections Linking Worldwide Climate Anomalies,* M. H. Glantz, R. W. Katz, and N. Nicholls, Eds., Cambridge University Press, 535 pp.

___, ____, and J. A. Knaff, 1992b: Influence of the stratospheric QBO on ENSO variability. *J. Meteor. Soc. Japan,* **70,** 975-995.

___, ___, and C. W. Landsea, 1997: Climate trends associated with multidecadal variability of Atlantic hurricane activity. H*urricanes: Climate and Socioeconomic Impacts,* H. F. Diaz and R. S. Pulwarty, Eds., Springer-Verlag Press, pp. 15-54.

Hastenrath, S., 1990: Tropical climate prediction: A progress report, 1985-1990. *Bull. Amer. Meteor. Soc.,* **71,** 819-825.

Hess, J. C., and J. B. Elsner, 1994: Historical developments leading to current forecast models of annual Atlantic hurricane activity. *Bull. Amer. Meteor. Soc.,* **75,** 1611-1622.

___, ___, and N. E. LaSeur, 1995: Improving seasonal hurricane predictions for the Atlantic basin. *Wea. Forecasting,* **10,** 425–432.

Horel, J. D., and J. M. Wallace, 1981: Planetary-scale atmospheric phenomena associated with the Southern Oscillation. *Mon. Wea. Rev.,* **109,** 813-829.

Hoskins, B. J., and D. J. Karoly, 1981: The steady linear response of a spherical atmosphere to thermal and orographic forcing. *J. Atmos. Sci.,* **38,** 1179-1196.

Jarvinen, B. R., C. J. Neumann, and M. A. S. Davis, 1984: A tropical cyclone data tape for the North Atlantic basin, 1886-1983: Contents, limitations, and uses. NOAA Tech. Memo., NWS NHC 22, Miami, FL, 21 pp.

Kalnay, E., and Coauthors, 1996: The NCEP/NCAR 40-year reanalysis project. *Bull. Amer. Meteor. Soc.,* **77,** 437-471.

Kaplan, A., M. Cane, Y. Kushnir, A. Clement, M. Blumenthal, and B. Rajagopalan, 1998: Analyses of global sea surface temperature 1856-1991. *J. Geophys. Res.,* **103,** 567–589.

Kistler, R., and Coauthors, 2001: The NCEP–NCAR 50–year reanalysis: Monthly means CD–ROM and documentation. *Bull. Amer. Meteor. Soc.,* **82,** 247–267.

Klotzbach, P. J., 2002: Forecasting September Atlantic basin tropical cyclone activity at zero and one month lead times. Dept. of Atmospheric Science Paper 723, Colorado State University, Fort Collins, CO, 91 pp.

___, 2006: Trends in global tropical cyclone activity over the past twenty years. *Geophys. Res. Lett.,* **33,** L10805, doi:10.1029/2006GL025881.

___, 2007a: Recent developments in statistical prediction of seasonal Atlantic basin tropical cyclone activity. *Tellus,* in press.

___, 2007b: Revised prediction of seasonal Atlantic basin tropical cyclone activity from 1 August. *Wea. Forecasting,* in press.

___, and W. M. Gray, 2003: Forecasting September Atlantic basin tropical cyclone activity. *Wea. Forecasting,* **18,** 1109-1128.

___, and ___, 2004: Updated 6-11-month prediction of Atlantic basin seasonal hurricane activity. *Wea. Forecasting,* **19,** 917-934.

___, and ___, 2006a: Causes of the unusually destructive 2004 Atlantic basin hurricane season. *Bull. Amer. Meteor. Soc.,* **87,** 1325-1333.

___, and ___, 2006b: Extended range forecast of Atlantic seasonal hurricane activity and US landfall strike probability for 2006. Dept. of Atmospheric Science Report, Colorado State University, Fort Collins, CO, 31 pp.

___, and ___, 2006c: Extended range forecast of Atlantic seasonal hurricane activity and US landfall strike probability for 2007. Dept. of Atmospheric Science Report, Colorado State University, Fort Collins, CO, 23 pp.

___, and ___, 2006d: Forecast of Atlantic hurricane activity for October-November 2006 and seasonal update through September. Dept. of Atmospheric Science Report, Colorado State University, Fort Collins, CO, 16 pp.

___, and ___, 2007a: Extended range forecast of Atlantic seasonal hurricane activity and US landfall strike probability for 2007. Dept. of Atmospheric Science Report, Colorado State University, Fort Collins, CO, 22 pp.

___, and ___, 2007b: Extended range forecast of Atlantic seasonal hurricane activity and US landfall strike probability for 2007. Dept. of Atmospheric Science Report, Colorado State University, Fort Collins, CO, 22 pp.

Knaff, J. A., 1993: Evidence of a stratospheric QBO modulation of tropical convection. Department of Atmospheric Science Paper 520, Colorado State University, Fort Collins, CO, 91 pp.

___, 1997: Implications of summertime sea level pressure anomalies in the tropical Atlantic region. *J. Climate,* **10,** 789-804.

___, 1998: Predicting summertime Caribbean pressure in early April. *Wea. Forecasting,* **13,** 740–752.

___, and C. W. Landsea, 1997: An El Niño-Southern Oscillation climatology and persistence (CLIPER) forecasting scheme. *Wea. Forecasting,* **12,** 633-652.

___, S. A. Seseske, M. DeMaria, and J. L. Demuth, 2004: On the influences of vertical wind shear on symmetric tropical cyclone structure derived from AMSU. *Mon. Wea. Rev.,* **132,** 2503-2510.

Kossin, J. P., K. R. Knapp, D. J. Vimont, R. J. Murnane, and B. A. Harper, 2007: A globally consistent reanalysis of hurricane variability and trends. *Geophys. Res. Lett.,* **34,** L04815, doi:10.1029/2006GL028836.

Landsea, C. W., 2007: Counting Atlantic tropical cyclones back to 1900. *EOS,* **88,** 197, 202.

___, and W. M. Gray, 1992: The strong association between western Sahel monsoon rainfall and intense Atlantic hurricanes. *J. Climate,* **5,** 435-453.

___, B. A. Harper, K. Hoarau, and J. Knaff, 2006:, Can we detect trends in extreme tropical cyclones, *Science,* **313,** 452-454.

___, and Coauthors, 2004: The Atlantic hurricane database re-analysis project: Documentation for the 1851-1910 alterations and additions to the HURDAT database. *Hurricanes and Typhoons: Past, Present and Future,* R. J. Murnane and K.-B. Liu, Eds., Columbia University Press, 177-221.

Larkin, N. K., and D. E. Harrison, 2002: ENSO warm (El Niño) and cold (La Niña) event life cycles: Ocean surface anomaly patterns, their symmetries, asymmetries and implications. *J. Climate,* **15,** 1118-1140.

Lehmiller, G.S., T. B. Kimberlain, and J. B. Elsner, 1997: Seasonal prediction models for North Atlantic basin hurricane location. *Mon. Wea. Rev.,* **125,** 1780-1791.

Levitus, S., J. I. Antonov, T. P. Boyer, and C. Stephens, 2000: Warming of the world ocean. *Science,* **287,** 2225-2229.

Madden, R. A., and P. R. Julian, 1994: Observations of the 40-50 day tropical oscillation – a review. *Mon. Wea. Rev.,* **122,** 814-837.

Mann, M. E., and K. A. Emanuel, 2006: Atlantic hurricane trends linked to climate change. *EOS,* **87,** 233-244.

Namias, J., 1973: Thermal communication between the sea surface and the lower troposphere. *J. Phys. Oceanogr.,* **3,** 373-378.

Neumann, C. J, 1999: The HURISK model: An adaptation for the Southern Hemisphere (A user's manual). Science Applications International Corporation Report, Monterey, CA, 31 pp.

Pielke Jr., R. A. and C. W. Landsea, 1998: Normalized hurricane damage in the United States: 1925-95. *Wea. Forecasting,* **13,** 621-631.

___, and ___, 1999: La Niña, El Niño, and Atlantic hurricane damages in the United States. *Bull. Amer. Meteor. Soc.,* **80,** 2027-2033.

___, ___, M. Mayfield, J. Laver, R. Pasch, 2005: Hurricanes and global warming. *Bull. Am. Meteorol. Soc.*, **86,** 1571–1575.

Rayner, N. A., D. E. Parker, E. B. Horton, C. K. Folland, L.V. Alexander, D. P. Rowell, E. C. Kent, and A. Kaplan, 2003: Globally complete analyses of sea surface temperature, sea ice and night marine air temperature, 1871-2000. *J. Geophys. Res.,* **108,** 4407, doi: 10.1029/2002JD002670.

Renwick, J. A., and J. M. Wallace, 1996: Relationships between North Pacific wintertime blocking, El Niño, and the PNA pattern. *Mon. Wea. Rev.,* **124,** 1981-1991.

Saha, S., S. Nadiga, C. Thiaw, J. Wang, W. Wang, and co-authors, 2006: The NCEP Climate Forecast System. *J. Climate,* **19,** 3483-3517.

Samelson, R. M., and E. Tziperman, 2001: Instability of the chaotic ENSO: The growth-phase predictability barrier. *J. Atmos. Sci.,* **58,** 3613-3625.

Shapiro, L. J., 1989: The relationship of the quasi-biennial oscillation to Atlantic tropical storm activity. *Mon. Wea. Rev.,* **117,** 1545-1552.

___, and S. B. Goldenberg, 1998: Atlantic sea surface temperatures and tropical cyclone formation. *J. Climate,* **11,** 578-590.

Simpson, R. H., 1974: The hurricane disaster potential scale. *Weatherwise,* **27,** 169, 186.

Thompson, D. W. J., and J. M. Wallace, 1998: The Arctic Oscillation signature in the wintertime geopotential height and temperature fields. *Geophys. Res. Lett.,* **25,** 1297-1300.

van Loon, H., and J. C. Rogers, 1978: The seesaw in winter temperatures between Greenland and northern Europe. Part I: General description. *Mon. Wea. Rev.,* **106,** 296-310.

Vecchi, G. A., and B. J. Soden, 2007: Increased tropical Atlantic wind shear in model projects of global warming. *Geophys. Res. Lett.,* **34,** L08702, doi:10.1029/2006GL028905.

Vitart, F., and T. N. Stockdale, 2001: Seasonal forecasting of tropical storms using coupled GCM integrations. *Mon. Wea. Rev.,* **129,** 2521-2537.

Wallace, J. M., and D. S. Gutzler, 1981: Teleconnections in the geopotential height field during the Northern Hemisphere winter. *Mon. Wea. Rev.*, **109,** 784-812.

Weatherford, C. L., and W. M. Gray, 1988: Typhoon structure as revealed by aircraft reconnaissance. Part II: Structural variability. *Mon. Wea. Rev.*, **116,** 1044-1056.

Webster, P. J., G. J. Holland, J. A. Curry, and H.-R. Chang, 2005:, Changes in tropical cyclone number and intensity in a warming environment, *Science*, **309**, 1844-1846.

Wilks, D. S., 1995: *Statistical Methods in the Atmospheric Sciences: An Introduction.* Academic Press, 464 pp.